



Virginia Commonwealth University
VCU Scholars Compass

Theses and Dissertations


Graduate School

2019

Structure-Activity Relationship Studies of Synthetic Cathinones and Related Agents

Rachel A. Davies

Follow this and additional works at: <https://scholarscompass.vcu.edu/etd>

 Part of the [Medicinal and Pharmaceutical Chemistry Commons](#), [Medicinal Chemistry and Pharmaceutics Commons](#), [Molecular and Cellular Neuroscience Commons](#), [Organic Chemicals Commons](#), [Other Psychiatry and Psychology Commons](#), [Pharmacology Commons](#), and the [Substance Abuse and Addiction Commons](#)

© Rachel A. Davies, 2019 All Rights Reserved

Downloaded from

<https://scholarscompass.vcu.edu/etd/5953>

This Dissertation is brought to you for free and open access by the Graduate School at VCU Scholars Compass. It has been accepted for inclusion in Theses and Dissertations by an authorized administrator of VCU Scholars Compass. For more information, please contact libcompass@vcu.edu.

© Rachel A. Davies, 2019

All Rights Reserved

STRUCTURE ACTIVITY RELATIONSHIP STUDIES OF SYNTHETIC CATHINONES
AND RELATED AGENTS

A dissertation submitted in partial fulfillment of the requirements for the degree of Doctor of
Philosophy in Medicinal Chemistry at Virginia Commonwealth University.

By

RACHEL A. DAVIES

Bachelor of Science, Middle Tennessee State University, United States, 2013

Director: DR. GLENNON

PROFESSOR

DEPARTMENT OF MEDICINAL CHEMISTRY

Virginia Commonwealth University
Richmond, Virginia
July, 2019

Acknowledgements

I begin by acknowledging my mentor Dr. Richard Glennon, as well as Dr. Malgorzata Dukat, for their investments of time and resources in my development as an academic. I most appreciate both of their high standards and expectations, which I believe have helped me grow professionally and become a more resilient person. I look forward to joining the ranks of the distinguished alumni of the Glennon/Dukat group.

When it comes to technical training, I first acknowledge Dr. Umberto Battisti for the training in organic synthesis. I hope to emulate in my future endeavors the leadership he exemplified as a post-doctoral researcher and laboratory manager. Dr. Glen Kellogg, Dr. Philip Mosier, and Claudio Catalano provided considerable assistance in computational modeling. Claudio in particular spent considerable time assisting me. Dr. Jose Eltit trained me in cell culture and calcium imaging, supported me in developing the pharmacology aspect of my project, and taught me how to effectively manage time to complete experimental investigations. My committee members present and former, including Dr. Katherine Nicholson, Dr. Richard Young, and Dr. Javier Gonzales-Maeso, are to be thanked for their investment of time and expertise in my education. Dr. Chris Kelly provided provocative counsel on organic reaction mechanisms. Suggestions from these faculty to improve this work have been essential.

I was very fortunate to join the synthetic cathinone project and Glennon/Dukat laboratory at an exciting time, in the midst of a collaboration between physiology, pharmacology, and medicinal chemistry. Everyone involved in this project enhanced the development of my work. Our weekly meetings were enriching and I am grateful to have participated. Firstly, I would like to thank Dr. Louis J. De Felice, and may he rest in peace. I will never forget his warm nature or his creative mind. Dr. Jose Eltit's group, particularly Vy Nguyen, and also Brian Ruiz,

contributed immensely to this work. Dr. Steve Negus and his laboratory, as well as Dr. Michelle Peace and her forensics team, especially Tyson Baird, should also be acknowledged for their contributions to this project. Additionally, the animals used in the course of these investigations are hereby acknowledged for their sacrifices.

I have shared the Glennon/Dukat lab with many scholars over the years, including Dr. Osama I. Alwassil, Dr. Farhana T. Sakloth, Dr. Supriya A. Gaitonde, Dr. Kavita Iyer, Dr. Abdelrahman E. S. Shalabi, Ahmed S. Abdel Khalek, Dr. Malaika D. Argade, Dr. Urjita H. Shah, Alessandro Magueri, and Preeth Hemanth. I must specially recognize Pallavi Nistala and Dr. Barkha Yadav, both of whom went above and beyond what is expected of any lab mate or friend.

On a personal note, I would like to acknowledge the contribution of my friends and community in Richmond, VA. These individuals include Celia Pringle, Thomas Bannard, Dr. Linda Hancock, Dr. Jessica Bourdon, Daniel Roh, and Dr. Kenny Kane. My closest friends in Richmond, Mike Shea and Stephen Flores, helped care for my dog as I completed this work. Erin Fowler also deserves special recognition, not only for providing close friendship, but for helping me get to the lab on time.

Finally I must acknowledge those who have inspired and supported me all along: my family. Amber Burgstahler and Shane Faulkner must be credited with inspiring me by their personal triumphs. My mother, Ellen Mast, supported me in pursuing my passion, without which this work would not have been possible. To select other family and family friends, including Mattie and Jordan Watkins, Annie and Frank Dufay and Peg Justice, thank you for your love and support along this journey. Finally, I would like to thank and dedicate this dissertation to the memory of my late father, Dr. Jack Davies, who instilled in me the value of fidelity to science and truth above all else.

Table of Contents

Acknowledgements	iii
List of Tables	viii
List of Figures.....	ix
List of Schemes	xi
List of Abbreviations.....	xii
<i>Abstract</i>	<i>xiv</i>
<i>I. Introduction</i>	<i>1</i>
<i>II. Background</i>	<i>5</i>
A. The Phenylalkylaminome	5
1. Overview	5
2. Psychoactive Classes of Phenylalkylamines	7
B. Amphetamine-Type Stimulants	10
1. The State of ATS Use and Misuse	10
2. Definitions of ATS	12
3. History of ATS	14
a. ATS Natural Products: Pharmacognosy of Khat and Ephedrine.....	14
b. Amphetamine and Early Synthetic ATS: Clinical Use and Misuse.....	19
c. Illicit ATS and Designer Drugs: Methamphetamine, MDA, MDMA, and Methcathinone	22
d. ATS NPS: Synthetic Cathinones (2010-Present)	23
i. Bath Salts	23
ii. α -Pyrrolidinophenones and Second-Generation “Bath Salts”	24
C. Monoamines and their Transporters	25
1. Monoaminergic Neurotransmission.....	25
a. Overview	25
b. Biosynthesis	26
c. Monoamine Receptors	26
d. Monoamine Degradation and Signal Termination	27
e. Discovery of DA Pathways	28
2. Monoamine Transporters: Discovery.....	28
3. Structure of MATs – from Cloning to Crystals and Beyond.....	30
4. Evolution of MATs.....	34
5. Mechanism of Neurotransmitter Transport.....	35
6. Monoamines and ATS in Substance Use Disorders	36
D. Pharmacology	40
1. Overview	40
2. ATS as MAT Blockers.....	40
3. ATS as MAT Substrates.....	43
a. Mechanism of Substrates as Releasing Agents	43
b. Potency and Selectivity of ATS Substrates.....	45
4. Behavioral Pharmacology of Synthetic Cathinones.....	46
E. SAR of ATS	47

III. Specific Aims.....	60
Aim 1: To elucidate the role of stereochemistry of the MCAT α-carbon atom.....	61
Aim 2: To establish the SAR of α-pyrrolidinophenones at DAT.	63
2.1: To assess the nature of stereoselectivity observed for α -pyrrolidinophenones by synthesizing and evaluating an achiral α -pyrrolidinophenone analog.	63
2.2: To establish QSAR for aryl-substituted α -pyrrolidinophenones, and determine similarity with MCAT activity via parallel SAR.	63
Aim 3: To synthesize analogs to progress the SAR of synthetic cathinone-related amphetamines at the α-carbon atom.....	65
Aim 4: To construct homology models of NET and use them to gain insight into MAT substrate selectivity.....	67
IV. Results and Discussion	68
A. Aim 1: To elucidate the role of stereochemistry of the MCAT α-carbon atom.....	68
1. Synthesis.....	68
2. Pharmacology.....	72
3. Modeling	76
B. Aim 2: To further establish SAR of α-pyrrolidinophenones.	79
a. Synthesis Aim 2.1.....	79
b. Pharmacology Aim 2.1.....	80
c. Modeling Aim 2.1	80
a. Synthesis Aim 2.2.....	81
b. Pharmacology Aim 2.2.....	85
c. Correlational Studies Aim 2.2	88
C. Aim 3: To synthesize analogs for progress in SAR of synthetic cathinone-related amphetamines at the α-carbon.....	93
1. Aim 3.1: To synthesize analogs for the investigation of the impact of α -carbon alkyl chain extension on 4-methylamphetamines.....	93
2. Aim 3.2: To stereoselectively synthesize <i>N</i> -ethylamphetamine isomers for future evaluation of ATS stereochemistry on DAT/NET/SERT selectivity.....	95
D. Aim 4: To construct homology models of NET to inform MAT substrate studies.....	96
1. Template.....	96
2. Model Generation and Evaluation.....	102
3. Docking endogenous substrates.....	107
4. Insights to MCAT selectivity	111
V. Conclusions	116
VI. Experimentals.....	122
A. Synthesis	122
α -Methylaminoisobutyrophenone Hydrochloride (26).....	122
2-Methylamino-1-phenylethan-1-one Hydrochloride (27).....	123
α - <i>gem</i> -Dimethyl- α -pyrrolidinopropiophenone Hydrochloride (28).....	124
4-Methyl- α -pyrrolidinohexanophenone Hydrochloride (30).....	126
4-Methoxy- α -pyrrolidinohexanophenone Hydrochloride (31)	127
4-Ethyl- α -pyrrolidinohexanophenone Hydrochloride (32)	128
4-Chloro- α -pyrrolidinohexanophenone Hydrochloride (33).....	128
4-Bromo- α -pyrrolidinohexanophenone Hydrochloride (34).....	129
4-Trifluoromethyl- α -pyrrolidinohexanophenone Hydrochloride (35).....	130
α -Ethyl-4-methylmethamphetamine Hydrochloride (36).....	131

Method A	131
Method B	132
<i>N</i> -Methyl-1-(<i>p</i> -tolyl)pentan-2-amine Hydrochloride (37).....	133
<i>R</i> (-) <i>N</i> -Ethylamphetamine Hydrochloride (<i>R</i> (-) 38).....	133
<i>S</i> (+) <i>N</i> -Ethylamphetamine Hydrochloride (<i>S</i> (+) 38).....	134
α -Bromoisobutyrophenone (40)	135
3-(Benzyl(methyl)amino)-2-methyl-1-phenylpropan-1-one Oxalate (41).....	136
<i>N</i> -Trifluoroacetyl Sarcosine (47).....	137
<i>N</i> -Trifluoroacetyl Sarcosinyl Chloride (48).....	137
α -Bromohexanophenone (50).....	137
1-(<i>p</i> -Tolyl)-2-nitrobut-1-ene (52)	138
1-(<i>p</i> -Tolyl)butan-2-one (53)	138
1-(<i>p</i> -Tolyl)hexan-1-ol (54).....	139
2-(Benzyl(methyl)amino)-1-(<i>p</i> -tolyl)pentan-1-one (55)	139
<i>R</i> (-)-1-Phenylpropan-2-ol (<i>R</i> (-) 57).....	140
<i>S</i> (+)-1-Phenylpropan-2-ol (<i>S</i> (+) 57)	141
<i>R</i> (-)-1-Phenylpropan-2-yl Methanesulfonate (<i>R</i> (-) 58).....	142
<i>S</i> (+)-1-Phenylpropan-2-yl Methanesulfonate (<i>S</i> (+) 58).....	142
4-Methoxyhexanophenone (59).....	143
4-Ethylhexanophenone (60).....	143
4-Bromohexanophenone (61)	144
4-Methoxy- α -bromohexanophenone (62).....	145
4-Ethyl- α -bromohexanophenone (63).....	145
4-Bromo- α -bromohexanophenone (64).....	146
1-(<i>p</i> -Tolyl)hexan-1-ol (65)	146
1-(4-Chlorophenyl)hexan-1-ol (66)	147
1-(4-(Trifluoromethyl)phenyl)hexan-1-ol (67)	148
2-(Methylamino)-1-(<i>p</i> -tolyl)-pentan-1-one Hydrochloride (68).....	149
B. Computational Modeling	149
1. Homology Modeling.....	149
a. hDAT and hSERT	149
b. hNET	149
2. Docking.....	150
C. Cell Culture and expression of MATs.....	150
D. Ca²⁺ Imaging for evaluation of test compounds.....	151
1. Substrate activity using Ca ²⁺ imaging	152
2. Blocker activity using Ca ²⁺ imaging.....	152
E. APP+ Imaging for assessing blocker activity	152
VII. Bibliography	154
VITA	181

List of Tables

Table 1. Prevalence of use of various ATS among United States 12th graders, in percent. Brackets indicate significant change from previous year. Adapted from NIDA’s Monitoring the Future Study.	11
Table 2. Potencies of ephedrine isomers and related compounds as synaptosomal releasing agents. Modified from Rothman et al., 2003.	18
Table 3. Diagnostic Criteria of Substance Use Disorders. Adapted from DSM-5.	37
Table 4. Inhibition of [³ H]Neurotransmitter reuptake at MATs for cocaine (19), methylphenidate (17), bupropion (20), MDPV (21), and α -PVP (11). While not all rat brain synaptosome assay results were gathered from the same paper, they were all performed in the same laboratory.	42
Table 5. Effect of <i>S</i> (+)amphetamine or <i>S</i> (+)methamphetamine on [³ H]neurotransmitter release from rat brain synaptosomes. Adapted from Rothman et al. 2003. ⁶⁷	49
Table 6. Potency of α -alkyl chain-extended α -pyrrolidinophenones as inhibitors of [³ H]neurotransmitter uptake at MATs.	53
Table 7. Potency to release or inhibit uptake of [³ H]neurotransmitter in rat brain synaptosomes.	57
Table 8. Potency of <i>para</i> -substituted MCAT analogs to release [³ H]Neurotransmitter from rat brain synaptosomes. Reproduced from Bonano et al. 2015, ⁶⁸ and Shalabi et al. 2019. ¹⁸¹	58
Table 9. Potency of MCAT isomers and achiral analogs as substrates of hDAT in a calcium flux assay.	73
Table 10. Potency of MCAT isomers and achiral analogs as substrates of hSERT, and their selectivity for hDAT, in a calcium flux assay.	75
Table 11. Inhibition of APP+ transport by α -PHP analogs in HEK cells, or release of [³ H]MPP+ by MCAT analogs from rat brain synaptosomes. MCAT data reproduced from Bonano et al. 2015. ⁶⁸	87
Table 12. Model evaluation using molpdf, DOPE, and GA341 scores, generated using Modeller v9.14. Conditional formatting was added using Microsoft Excel, using green to indicate relatively superior models on the basis of the scoring function for that column.....	102
Table 13. Alignment of binding site residues between hDAT, hNET, and hSERT. Conserved alanine residue between hNET and hSERT highlighted in red. All those residues that are not conserved between hNET and hSERT are highlighted in green.	112
Table 14. HINT Scores for 4-MCATs at MATs.	115
Table 15. Pearson correlation between HINT scores and potency at individual transporters....	115

List of Figures

Figure 1. Chemical structures of selected phenylalkylamines, with their common scaffold emphasized in purple.	6
Figure 2. Selected subgroups of the phenylalkylamines displayed as concentric circles.	7
Figure 3. The monoamines, which share an arylalkylamine chemical scaffold. A common phenylalkylamine structure highlighted in purple where it exists.	8
Figure 4. Selected ATS, with their similarity to amphetamine (9) highlighted in blue.	13
Figure 5. Illustration from Vaughan's report on khat use in Aden. ⁵⁶	14
Figure 6. The hormone epinephrine, displayed alongside ephedrine isomers and similar compounds extracted from ma-huang and khat, and the structurally related compound (+)norephedrine.	17
Figure 7. Amphetamine and selected synthetic ATS developed for clinical use in the mid-1900s.	21
Figure 8. Pacholczyk's proposed structure of hNET based on cloning. Conserved residues with GAT are indicated by darkened circles. Reproduced from Pacholczyk et al., 1991. ¹⁰⁴	31
Figure 9. <i>S</i> (+)Amphetamine (green) co-crystallized with dDAT (blue), PDB ID: 4XP9. Generated in PyMOL Version 2.1.1.	32
Figure 10. Evolutionary origin of the MATs. Highlights the evolutionary distance between dDAT and hDAT. Generated in ChemDraw Professional 17.1.	35
Figure 11. PET scan of DAT radioligand [¹¹ C]d- <i>threo</i> -methylphenidate bound to 33-year-old male human brains. The methamphetamine user was imaged 80 days after detoxification. [Reproduced from Volkow et al. 2001.	39
Figure 12. Known psychostimulant MAT blockers, with ATS structural features highlighted in blue where applicable, including known drugs of abuse (all) and drugs approved for medical use (17, 20, under rare circumstances 19).	41
Figure 13. Pyrovalerone, an NDRI.	43
Figure 14. Primary amine amphetamines with their secondary amine counterparts.	48
Figure 15. Bupropion, its analogs, and MCAT for comparison.	56
Figure 16. Methcathinone, its isomers, and proposed achiral analogs.	62
Figure 17. An achiral α -PPP analog.	63
Figure 18. α -PHP and <i>para</i> -substituted analogs proposed in Aim 2.2.	65
Figure 19. Synthetic targets of Aim 3.1: 4-MMA analogs.	66
Figure 20. Synthetic targets of Aim 3.2: <i>N</i> -Ethylamphetamine optical isomers.	67
Figure 21. A potential mechanism via Michael addition for the transformation of 40 to 41	71
Figure 22. Epoxy intermediate 45	71
Figure 23. Dose-response curves for: (A) MCAT racemate and optical isomers; (B) MCAT racemate and MCAT achiral analogs 26 and 27	73
Figure 24. Common binding modes for Aim 1 compounds at hDAT (top), hNET (middle), and hSERT (bottom).	78
Figure 25. (A) <i>S</i> (+)Amphetamine (green) co-crystallized with dDAT (yellow, PDB ID:4XP9) ⁶⁹ overlaid with <i>S</i> (-) 5a (blue) docked at an hDAT homology model (yellow); (B) same as A, but overlaid with <i>S</i> (-) 5a docked once to an hNET homology model (salmon).	79
Figure 26. α -PHP analogs.	81
Figure 27. Concentration-response curves for inhibition of APP+ transport by 4-substituted α -PHP analogs.	86

Figure 28. Correlation between potencies of α -PHP compounds and corresponding methcathinone analogs.	88
Figure 29. Correlation between α -PHPs and methcathinone analogs when 4-trifluoromethyl is removed.	89
Figure 30. Linear regression of α -PHPs and MCATs with outlier test applied.	90
Figure 31. Linear regression analysis between α -PHP series and methcathinone series with 4-methoxy compounds excluded.	91
Figure 32. Linear regression of potency to inhibit DAT and Taft's steric E for α -PHP series.	92
Figure 33. Alignment of dDAT/methamphetamine (beige/green, PDB ID: 4XP6) and dDAT/nortriptyline (red/pink, PDB ID: 4M48). Phe325 shift emphasized by grey arrow. Generated in PyMOL and Microsoft PowerPoint.	98
Figure 34. Sequence alignments of dDAT, hDAT, hNET, and hSERT for comparison. Asterisks (*) indicate fully conserved amino acid residues, colons (:) indicate moderately conserved residues, and periods (.) indicate weakly conserved residues. Generated using Clustal Omega.	100
Figure 35. Percent identity matrix (PIN) for MATs of interest. Percent identity between hNET and hSERT or hNET and dDAT highlighted in blue or red, respectively. Generated based on alignment shown in Figure 34 using Clustal Omega.	101
Figure 36. Alignment of dDAT/methamphetamine crystal structures (beige/green, PDB ID:4XP6), with hSERT/paroxetine (blue/dark salmon, PDB ID:5I6X) and hSERT/citalopram (blue/salmon, PDB ID:5I71). Generated in PyMOL. Shows a different angle than Figure 33... ..	101
Figure 37. Model evaluation using PyMOL and PROCHECK. (A) Homology model #66 of hNET, generated in PyMOL; (B) Ramachandran plot of homology model #66, generated in PROCHECK; (C) Visualization of Asp493 and surrounding residues, generated in PyMOL. ...	106
Figure 38. Induced-fit docking pose for DA at hNET. (A) DA-1 with predicted distances from potential residues of interaction emphasized. (B) DA-1 (red), DA as co-crystallized with dDAT (salmon, PDB ID: 4XP1), and methamphetamine as co-crystallized with dDAT (lavender, 4XP6).	108
Figure 39. Induced-fit docking poses for NE at hNET. (A) NE-1; (B) NE-2; (C) NE-1 and DA-4 overlaid; (D) NE-2 and DA-1 overlaid. Image generated in PyMOL and Microsoft PowerPoint.	110
Figure 40. Side-by-side comparison of the docked 4-substituted MCATs at hDAT, hNET, and hSERT, with the alignment of their binding-site residues displayed below. In the hNET model, magenta and blue have been used to indicate residues conserved with hDAT and hSERT, respectively. The only residues that were conserved between hDAT and hNET (A81 and A77, respectively), but smaller in hSERT (G100) are circled in white.	113
Figure 41. Docked poses of 4-methoxyMCAT at hDAT, hNET, and hSERT. Highlighted is a residue conserved between hNET and hSERT, but not hDAT. Image generated in Sybyl-X 2.1.	114
Figure 42. Clinically available achiral phenylalkylamines phentermine (73) and phenylephrine (74), alongside structurally similar achiral MCAT analogs from these studies 26 and 27	117

List of Schemes

Scheme 1. ^a Synthesis of Compounds 26 and 41	69
Scheme 2. ^a Synthesis of Compound 27	72
Scheme 3. ^a Synthesis of Compound 28	80
Scheme 4. ^a Synthesis of Compound 29	81
Scheme 5. ^a Synthesis of Compounds 30—32 and 34	82
Scheme 6. ^a Extended Grignard approach that was considered for making α -PHPs, as it had been used previously for related compounds.....	83
Scheme 7. ^a Synthesis of Compound 30 , 33 , and 35	85
Scheme 8. ^a Synthesis of Compound 36	94
Scheme 9. ^a Synthesis of Compound 37	95
Scheme 10. Synthesis of Compounds <i>S</i> (+) 38 and <i>R</i> (-) 38	96

List of Abbreviations

[¹ H]NMR	Proton nuclear magnetic resonance
4-MA	4-Methylamphetamine
4-MMA	4-Methylmethamphetamine
5-HT	5-Hydroxytryptamine, serotonin
α	Alpha
β	Beta
ATS	Amphetamine Type Stimulant
BNDD	Bureau of Narcotics and Dangerous Drugs
COMT	Catecholamine O-methyltransferase
CHN	Carbon, hydrogen, and nitrogen elemental analysis
DA	Dopamine
DAT	Dopamine transporter
dDAT	Drosophila dopamine transporter
DDC	DOPA decarboxylase
DEA	Drug Enforcement Administration
DMEM	Dulbecco's modified eagle medium
DOB	2,5-Dimethoxy-4-bromoamphetamine
DOM	2,5-Dimethoxy-4-methylamphetamine
FBS	Fetal Bovine Serum
GABA	γ-Aminobutyric acid
GAT	γ-Aminobutyric acid transporter
hDAT	Human dopamine transporter
hNET	Human norepinephrine transporter
hSERT	Human serotonin transporter
ICD	International Statistical Classification of Diseases and Related Health Problems
iDAT	Invertebrate DAT
IR	Infrared spectroscopy
IS	Imaging solution
KDa	Kilodalton
LeuT	Leucine transporter
MAO	Monoamine Oxidase

MCAT	Methcathinone
MDA	3,4-Methylenedioxyamphetamine
MDMA	3,4-Methylenedioxymethamphetamine
MS	Mass spectrometry
NA	Numerical Aperture
NCBI	National Center for Biotechnology Information
NDRI	Norepinephrine and Dopamine Reuptake Inhibitor
NE	Norepinephrine
NET	Norepinephrine transporter
NPS	New Psychoactive Substance
PEA	β -Phenylethylamine
PIN	Percent identity matrix
qSAR	Quantitative structure-activity relationship
RMSD	Root Mean Squared Deviation
SAR	Structure-activity Relationship
SKF	Smith, Kline, and French Pharmaceuticals
SLC6	Solute carrier 6
SNRI	Serotonin and Norepinephrine Reuptake Inhibitor
SSRI	Selective Serotonin Reuptake Inhibitor
StUD	Stimulant Use Disorder
SUD	Substance Use disorder
VMAT	Vesicular monoamine transporter

Abstract

STRUCTURE ACTIVITY RELATIONSHIP STUDIES OF SYNTHETIC CATHINONES AND RELATED AGENTS

A dissertation submitted in partial fulfillment of the requirements for the degree of Doctor of Philosophy in Medicinal Chemistry at Virginia Commonwealth University.

By

RACHEL A. DAVIES

Bachelor of Science, Middle Tennessee State University, United States, 2013

Director: DR. GLENNON

PROFESSOR

DEPARTMENT OF MEDICINAL CHEMISTRY

Synthetic cathinones and related agents represent an international drug abuse problem, and at the same time an important class of clinically useful compounds. Structure-activity relationship studies are needed to elucidate molecular features underlying the pharmacology of these agents. Illicit methcathinone (i.e., MCAT), the prototype of the synthetic cathinone class, exists as a racemic mixture. Though the differences in potency and target selectivity between the positional and optical isomers of synthetic cathinones and related agents have been demonstrated to have important implications for abuse and therapeutic potential, the two MCAT isomers have never been directly compared at their molecular targets: the monoamine transporters (MATs). Additionally, previous studies have found that the carbonyl oxygen atom can be replaced with a

methoxy group, but this results in two chiral centers (i.e., four possible optical isomers for synthesis and evaluation). Here, the individual isomers of MCAT, their racemate, and achiral MCAT analogs were prepared where necessary, and examined *in vitro* and *in silico* at the MATs. All agents were active as substrates, with a rank order of potency suggesting that α -position chirality, in either configuration, is favored but not required, with the *S*(-) configuration slightly preferred. Either chiral center removal approach resulted in a reduction in potency, suggesting both favorable interactions with the α -methyl, and limited bulk tolerance. To further investigate this possibility, docking studies were conducted using homology models of the MATs. Common binding modes were identified that were similar to the binding mode of *S*(+)amphetamine co-crystallized at drosophila DAT. Taken together, these studies supported our conclusions, as steric hindrance was observed in the α -methyl region of the proposed binding site for the *R*(+)MCAT isomer.

Inclusion of the original synthetic cathinones among Schedule I controlled substances has driven the clandestine development of a second generation of agents, resulting in an array of new synthetic cathinones diverse in structure and effect. Pyrrolidinophenones are a major constituent of second-generation bath salts. Little is known about their structure-activity relationships. Here, we have synthesized and examined a series of aryl-substituted pyrrolidinophenone analogs, as well as an achiral pyrrolidinophenone analog, utilizing novel synthetic chemistry and an innovative cell-based epifluorescence Ca^{2+} imaging technique. Herein, we evaluated the neurochemical properties of these novel compounds at the dopamine transporter (DAT), considered to exert a major role in actions of drugs of abuse.

For future structure-activity relationship studies, additional analogs of synthetic cathinone-related agents were produced using novel synthetic approaches, including analogs and

isomers of known amphetamine drugs of abuse.

Finally, though much has been learned about the role of the dopamine and serotonin transporters in the mechanisms of action of synthetic cathinones, the role of the norepinephrine transporter is poorly understood. Homology models of the human norepinephrine transporter were built and docking studies conducted to inform the study of MAT ligand selectivity, activity, and binding.

In conclusion, these studies represent progress towards the establishment of comprehensive structure-activity relationships for synthetic cathinones and related agents. Particular emphasis was placed on the SAR of the phenylalkylamine α -carbon in the synthetic cathinone context, and the role of the norepinephrine transporter in their activity.

I. Introduction

The drug abuse problem has received increasing attention in recent years as overdose deaths have risen to surpass automobile accidents as the leading cause of accidental death in the United States.¹ Yearly economic costs of illicit drug use in the United States were estimated at \$193 billion overall for 2007, the last year comprehensive data were available.² However, that number is expected to have risen substantially in the intervening years; the White House Council of Economic Advisers estimated a cost of \$504 billion dollars for 2015, or 2.8 percent of GDP, due to changes in drug misuse and their associated social and healthcare costs.³ This problem includes the current “opioid crisis,” and it has been associated with increased potency, purity, availability, and marketing of both illicit and prescription opioids.⁴

In the study of the opioid crisis thus far, three distinct phases can be identified. First, high-potency prescription opioids (i.e., OxyContin®) became widely available and clinically accessible. Although they were marketed as abuse-deterrent based on an extended-release formulation, abuse became a major problem. Recognizing this, new regulations were put in place to stop prescription opioid misuse, but these policies drove users towards illicit heroin, which was increasingly available in a high-purity formulation (i.e., “black tar”).⁵ Heroin overdose defined the second phase. Most recently, new psychoactive substances (NPS) in the form of highly potent fentanyl analogs have emerged, followed by a rapid acceleration in already rising overdose rates to define the third phase.⁶ However, and unfortunately, the story of the drug abuse crisis does not end with opioids.

Global supply-driven increases in markets for non-opioid drugs of abuse, including cocaine, benzodiazepines, and amphetamine-type stimulants,⁶ have coincided with increased contributions of non-opioids to overdose deaths in the US.¹ Meanwhile, molecular and

pharmacological diversity of abused drugs has expanded, with 803 distinct NPS reported between 2009 and 2017. Stimulants are the primary psychoactive effect group amongst NPS (36%), and prominent among these are synthetic cathinones, a chemical group defined by their phenylisopropylamine scaffold and β -keto moiety.⁶

Beginning in 2008, synthetic cathinones started to garner significant attention, as they were detected in emerging mixtures of NPS known as “bath salts,” which became known for the bizarre behavior with which their intoxication was associated; many synthetic cathinones are β -keto analogs of abused amphetamines. Synthetic cathinones were often sold legally in these mixtures under the protection of facetious labeling such as “not for human consumption” or “bath salts,” earning them their colloquial name. Use of bath salts often led to unpredictable, severe adverse effects,^{7,8} leading to the scheduling of many synthetic cathinones in the United States and Europe.^{9,10} Despite the ban, however, new synthetic cathinones and related agents continued to emerge in the NPS marketplace; these largely consisted of analogs of the newly scheduled compounds and were termed “second-generation” bath salts.^{10–15} These compounds produced adverse behavioral and physiological effects that were sometimes life-threatening.^{16,17} Today, bath salts have gone “generic” and the name is employed for many different agents that contain at least one synthetic cathinone. The term “bath salts” no longer represents a specific combination of agents.¹⁸

Much like the opioid crisis, with one phase leading directly into the next, for stimulants, many of the same trends and problems have emerged. Diverted extended-release stimulants prescribed for neuropsychiatric conditions are a considerable drug abuse problem, especially among youth.⁵ Deaths attributable to high-purity imported illicit methamphetamine are on the rise, especially in rural communities, where their rise outpaces the rise in opioid overdose.

Synthetic cathinones and related agents likely have a fentanyl-like role to play in the developing global drug abuse problem with respect to stimulants.

The parallels between the opioid and stimulant abuse trends don't end with classes of substances. A clear trend emerges from the observation of both classes of drugs: despite decades of attempts to deter abuse through scheduling and otherwise banning these substances, the drug abuse problem has only become more widespread and deadly. The increasing variable in both classes is potency. NPS synthetic opioids range from 15- to 10,000-fold the potency of morphine.¹⁹ Some NPS synthetic cathinones are 50- to 100-fold more potent than cocaine.¹⁵ Prohibition incentivizes the invention and manufacture of agents with increased potency, as first described and termed the “iron law of prohibition” by economist Richard Cowan in 1986.²⁰ Like many current strategies to prevent and deter drug abuse, this strategy is increasingly demonstrated to be counterproductive.

Moving forward, new strategies will be necessary to reduce drug-related harm, treat individuals with substance use disorders, and effectively regulate psychoactive drugs. Fundamental to effective clinical treatment and public policy will be a strong foundation in science of drug action and effects. In the case of synthetic cathinones, our group pioneered the study of their structure-activity relationships beginning in the 1987 with the prototype methcathinone.²¹ Since then, we have learned a great deal about their mechanisms of action and abuse-related effects. However, much remains to be elucidated, including additional structural features of the synthetic cathinones, and the details of the complex interplay between neurochemistry and abuse-related pharmacological effects in animals and humans.

Structure-activity relationship studies of cathinones might be useful in developing both antidotes to their poisoning and pharmacotherapy to treat addiction. Additionally, some synthetic

cathinones might have clinical utility in the treatment of various psychiatric and neurological disorders. For example, bupropion (Wellbutrin®) is currently approved for the treatment of major depressive disorder, and is unmistakably, from a structural perspective, a cathinone. *N,N*-Diethylpropion (Tenuate®), another synthetic cathinone, is used clinically as an appetite suppressant. Furthermore, cathinones share molecular scaffolds and molecular targets with drugs used in the management of attention-deficit hyperactivity disorder, sleep-related disorders, mood disorders, Parkinson's disease, and substance-use disorders. Many of these conditions lack adequate options for treatment. Studies of synthetic cathinones may inform future drug development in this area, resulting in improved patient health.

In these studies, progress was made towards the establishment of comprehensive structure activity relationship data for synthetic cathinones and related agents. This included the utilization of design concepts, novel synthetic approaches, innovative pharmacological evaluation, and molecular modeling for several series of compounds, each aimed at elucidating a particular feature of a specific cathinone or related amphetamine structure. Together, the insight gleaned from these studies will strengthen and inform the science of drug abuse, an essential starting point for an effective global response, and might lead to novel therapeutic agents for the treatment of various neuropsychiatric disorders.

II. Background

A. The Phenylalkylamine

1. Overview

Synthetic cathinones, the subject of this dissertation, belong to the greater phenylalkylamine chemical class of centrally-acting agents, that belong to an even greater arylalkylamine class. The phenylalkylamine moiety is common amongst centrally-acting agents,¹⁸ from endogenous neurotransmitters to psychoactive drugs (Figure 1), including those of clinical, recreational, and illicit use. A prominent group of molecular targets for phenylalkylamines are those proteins involved, both directly and indirectly, with monoaminergic neurotransmission. Modifications to the general phenylalkylamine scaffold can confer selectivity, and even specificity, for individual targets in the monoamine signaling pathways, exerting corresponding quantitative changes in the pharmacological effects of a compound.¹⁸ Selectivity for specific targets has been linked to distinct psychoactive effects, that are associated with names of the classes of drugs producing them, such as psychostimulants, empathogens, hallucinogens, or antidepressants, all of which feature phenylalkylamines as prominent members.¹⁸ Some effects of phenylalkylamines are clinically useful in treating psychiatric disorders and neurological diseases, whereas others confer potential for abuse, though considerable overlap exists between these two outcomes. Thus, structure-activity relationship (SAR) studies of phenylalkylamines are critical for distinguishing between: 1) feasible pathways for pharmaceutical development, and 2) scaffolds, pharmacophores, and lead compounds of likely high abuse potential.

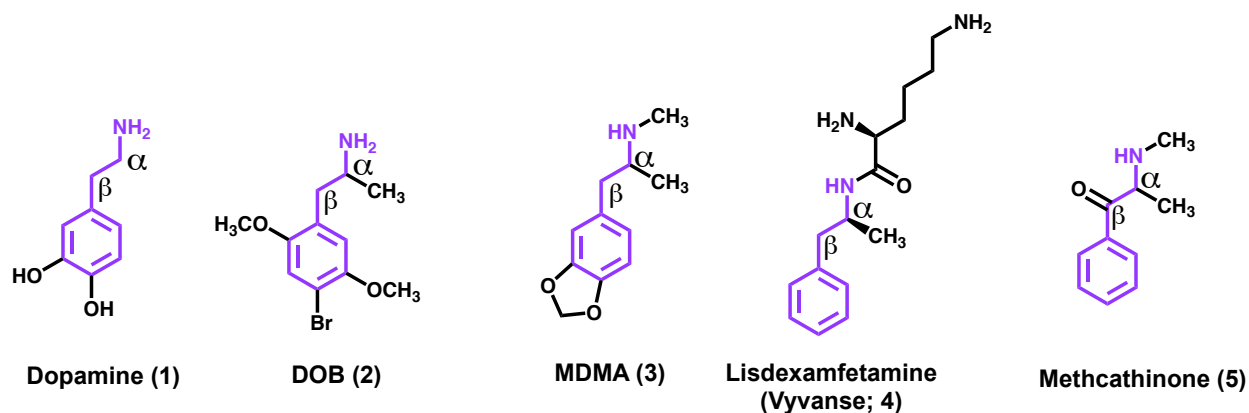


Figure 1. Chemical structures of selected phenylalkylamines, with their common scaffold emphasized in purple.

The phenylalkylamine scaffold is defined as a phenyl ring connected to a basic amine, most commonly by a two-carbon linker, but sometimes by a three-carbon linker. Because of the typical two-carbon distance in phenylalkylamines, they are also commonly referred to as phenylethylamines or phenethylamines.^{18,22} However, the alkyl chain is frequently extended at the alpha (α) position; commonly, it is extended by one carbon atom, and compounds meeting the latter description are also referred to as phenylisopropylamines.²³ This extension by one carbon atom at the α position is ideal for stimulant effects of amphetamine.²⁴ However, as is the case for the pyrrolidinophenones investigated herein, the alkyl chain can sometimes be extended further than one carbon with activity retained; sometimes, this extension results in an increase in potency.²⁵ Additional subcategorization is possible (Figure 2): ephedrine and related compounds are grouped into the subcategory of phenylpropanolamines. Cathinones contain a keto group at the beta (β) position. Recognizing the disparate pharmacological effects scattered throughout the phenylalkylamine subgroups, it is useful to discuss psychoactive effects, mechanisms of action, and SAR of synthetic cathinones in the context of the greater “phenylalkylaminome.” The latter term was coined by Glennon to refer to the entire known set of compounds fitting the phenylalkylamine chemical description,¹⁸ a survey of which will be henceforth presented.

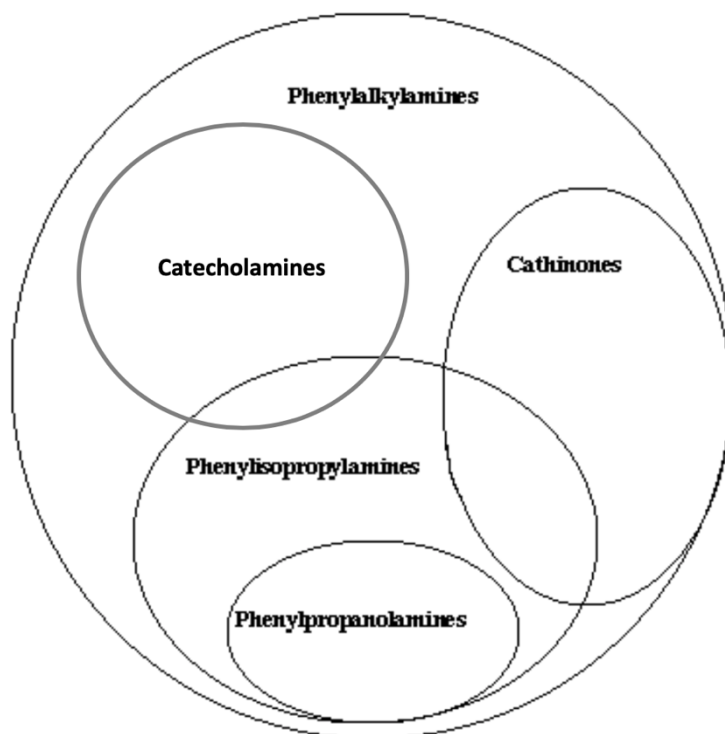


Figure 2. Selected subgroups of the phenylalkylamines displayed as concentric circles.

2. Psychoactive Classes of Phenylalkylamines

Endogenous phenylalkylamines include two of the monoamine neurotransmitters: dopamine (DA, **1**) and *R*(-)-norepinephrine (NE, *R*(-)**6**),^{26–28} and the related hormone epinephrine (*R*(-)**7**, Figure 3).^{29,30} These compounds, while phenylalkylamines, are commonly called catecholamines in acknowledgement of their catechol moiety. The third monoaminergic neurotransmitter, serotonin (5-HT, **8**), belongs to the structurally related but distinct tryptamine chemical class, and is not strictly a phenylalkylamine.³¹ 5-HT is an indolealkylamine. Collectively, phenylalkylamines and indolealkylamines belong to a larger class of agents referred to as arylalkylamines.¹⁸

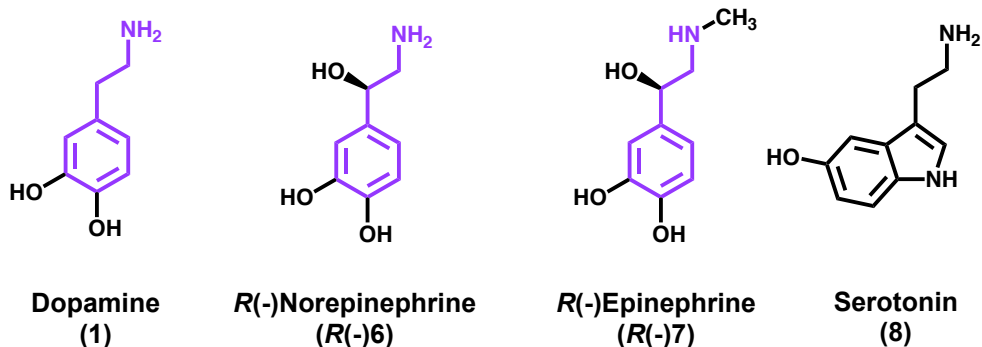


Figure 3. Monoamines that share an arylalkylamine chemical scaffold. A common phenylalkylamine structure is highlighted in purple where it exists.

Exogenous centrally-active phenylalkylamines include those used for medicinal purposes and those used recreationally.¹⁸ Psychoactive effects that confer these applications may be distinct or overlapping. Included among the top 100 pharmaceutical products by prescription are many phenylalkylamines acting at monoaminergic targets,^{18,32} including venlafaxine, an antidepressant with no known abuse potential, bupropion, an antidepressant with moderate abuse potential,^{33,34} and amphetamine, a stimulant with high abuse potential,³⁵ but which is used commonly in the treatment of attention-deficit hyperactivity disorder (ADHD) and narcolepsy.^{36,37} In the study of phenylalkylamines that are commonly abused, three predominant psychoactive effect groups emerge: psychostimulants, classical hallucinogens, and empathogens.¹⁸

Psychostimulants of prevalent use in the phenylalkylamine class include amphetamine (**9**), methamphetamine (**10**), and the synthetic cathinones (e.g., **5**).⁶ As psychostimulant phenylalkylamines (also known as amphetamine-type stimulants, or ATS) are a major focus of this dissertation, they will be reviewed in detail in the following section.

Another principal psychoactive effect class of phenylalkylamines is the “classical hallucinogens,” so called for their ability to produce visual, tactile, and auditory hallucinations. They are defined by this quality, and their corresponding agonist activity at 5-HT₂ receptors.³⁸ Also referred to as “psychedelics,” meaning “mind-manifesting,” for the psychological and spiritual utilities for which they are sometimes employed, they are capable of producing transcendent states otherwise associated with dreams or spiritual experiences.^{39,40} The use of these agents is prehistoric, playing important roles in ancient cultures of Asia, North and South America, and Europe.⁴⁰ Phenylalkylamines are well represented among the hallucinogens, including plant-derived agents such as mescaline, and synthetic substances such as 2,5-dimethoxy-4-bromoamphetamine (DOB; **2**).

The term “empathogen” was coined to describe 3,4-methylenedioxyamphetamine (MDA, **23**), 3,4-methylenedioxymethamphetamine (MDMA, **3**), and related agents, which were distinct from other phenylalkylamines based on their purported ability to produce empathy-related states such as “emotional oneness and connectedness,” as described by Ralph Metzner, in human users.⁴¹ MDMA (**3**), which is often considered the prototypical empathogen, is a phenylisopropylamine structurally derived from methamphetamine by the addition of a 3,4-methylenedioxy moiety. MDMA (**3**) has been found to exert its empathogenic class-defining psychoactive effects by 5-HT- and oxytocin-mediated processes.⁴² Advancements in neuropsychological understanding of empathy combined with decades of sophisticated pharmacological analysis of MDMA (**3**) have confirmed that it does promote emotional empathy, but not cognitive empathy, with which it may interfere. The empathogens have alternatively been called sympathogens, or entactogens, for their ability to enhance introspection in MDMA-assisted psychotherapy.⁴¹ The effective labeling and definition of this psychoactive class of

compounds has been the subject of some controversy,⁴¹ and complicated by the mixed activity and subjective effects of its constituents.¹⁸

B. Amphetamine-Type Stimulants

1. The State of ATS Use and Misuse

Overdose deaths for ATS are on the rise. In the year 2017 (the last year data were available), 10,333 overdose deaths in the United States were attributed to ATS.¹ This represents an 8-fold rise in rate of death since 2007, the second-greatest increase in any drug class after fentanyl-type opioids.¹ In rural areas, the rate increased by 10-fold, the highest for any drug class in those areas.¹ In the state of Virginia, 88 deaths were reported for methamphetamine alone in 2017, representing a 69.8% increase from the previous year. An additional increase, for a total of 106, is estimated for 2018.⁴³

Despite the increase in overdose deaths, use of ATS has remained relatively stable in the United States among young people (Table 1).⁴⁴ Worldwide, ATS are considered a major concern, with 34.2 million estimated users in 2016, and increases in use reported in West Asia, Western and Central Europe, and Latin America.⁴⁵ In many East Asian countries, ATS are considered the highest priority illicit drug concern,⁴⁵ as countries including Japan, Korea, and the Philippines have reported rates of ATS use 5- to 7-fold higher than rates of cocaine and heroin use combined.⁴⁶

Table 1. Prevalence of use of various ATS among United States 12th graders, in percent. Brackets indicate significant change from previous year. Adapted from NIDA’s Monitoring the Future Study.⁴⁴

Drug	2015	2016	2017	2018
Methylphenidate (16)	2	[1.20]	1.3	0.9
Amphetamine (9)	10.8	10	9.2	8.6
Adderall® (Salts of 9)	7.5	6.2	5.5	[4.60]
Methamphetamine (10)	1	1.2	1.1	0.7
MDMA (3)	[5.90]	[4.90]	4.9	4.1
“Bath salts” (Synthetic cathinones)	1	0.8	0.6	0.6

The cause of the ATS burden on public health is likely multi-faceted. Sharp increases in ATS-related overdose deaths might be related to the widespread emergence of imported, high-purity illicit formulations, as was the case for a significant portion of opioid-related deaths (i.e., high-purity heroin).^{47,48} Also implicated in high rates of ATS misuse is the diversion of those agents prescribed for clinical treatment of ADHD, narcolepsy, and binge eating disorder (e.g., Adderall®, see Table 1).³⁷ Finally, the emergence of high-potency new/novel psychoactive substances (NPS) with diverse structural modifications contribute to the overall health burden of NPS.⁴⁴

2. Definitions of ATS

It is necessary, before discussing the history, pharmacology, and SAR of ATS, to describe the scope of their amorphous, sometimes controversial, label. Multiple definitions exist for ATS. Some prominent definitions include the following:

“[A] group of substances composed of synthetic stimulants controlled under the Convention on Psychotropic Substances of 1971 and from the group of substances called amphetamines, which includes amphetamine, methamphetamine, methcathinone and the “ecstasy”-group substances (3,4-methylenedioxymethamphetamine (MDMA) and its analogues).” – United Nations Office on Drugs and Crime⁶

“[A] group of drugs whose principal members include amphetamine and methamphetamine. However, a range of other substances also fall into this group, such as methcathinone, fenetylline, ephedrine, pseudoephedrine, methylphenidate and MDMA or ‘Ecstasy’ – an amphetamine-type derivative with hallucinogenic properties.” – World Health Organization⁴⁶

These definitions are not strictly in alignment, with the former specifying that ATS are controlled under a specific act, while the latter includes ephedrine and pseudoephedrine, which are not federally scheduled, and are unscheduled in many states.^{49,50} Additionally, ephedrine and pseudoephedrine are natural products, whereas the former definition specifies a synthetic origin for ATS.

In general, it can be said that all ATS share three main points in common: 1) an amphetamine (**9**) core structure; 2) psychostimulant pharmacological effects; and 3) indirect augmentation of catecholamine signaling. While the reinforcing effects of ATS are thought to be

mediated by DA, most ATS increase NE signaling to a degree greater than or equal to that of DA, and ATS active doses more closely correlate with noradrenergic potency.⁵¹ Therefore, adrenergic signaling is thought to be more important for ATS subjective effects than dopamine signaling. However, an agent that selectively increases either catecholamine might still be considered a psychostimulant. Additionally, a compound falling under the ATS umbrella could interact with other neurotransmitter signaling pathways, including the serotonergic system, although, as in such a case, this can result in additional subjective effects (e.g. *S*(+)MDA, MDMA).¹⁸

The structure of the eponymous amphetamine (9) was defined as “(1) an unsubstituted phenyl ring, (2) a two-carbon side chain between the phenyl ring and nitrogen atom, (3) an α -methyl group, and (4) a primary amino group” by Biel and Bopp,⁵² and Sulzer and colleagues.⁵³ ATS may diverge from this definition, containing substituted phenyl rings, and/or secondary or tertiary amines.¹⁸ Contained within their structures, however, the amphetamine (9) scaffold is almost universally present (Figure 4). The α -carbon substituent distinguishes this scaffold from that of the general phenylalkylamines, and is the reason for the name amphetamine (9), a contracted form of **α -methyl-phenethyl-amine**.

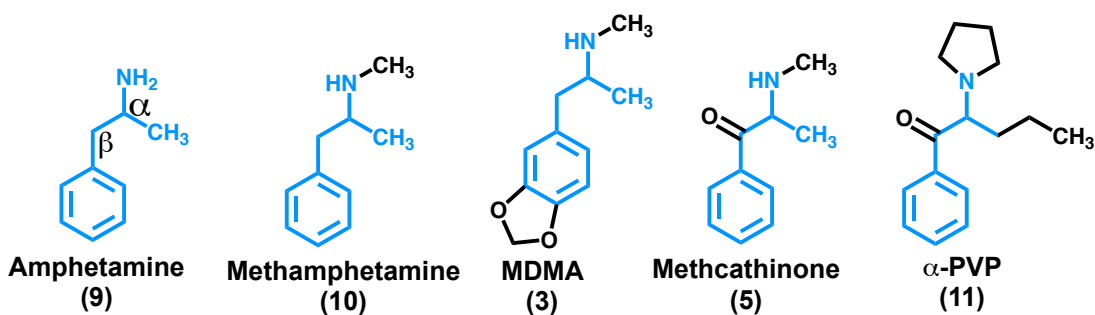


Figure 4. Selected ATS, with their similarity to amphetamine (9) highlighted in blue.

3. History of ATS

The first known synthesis of amphetamine (9) itself was reported by Romanian chemist Lazar Edeleano, who had been working on methodology of liquid-liquid extraction,⁵⁴ in 1887,⁵⁵ but it was not pharmacologically evaluated at that time. It was not until 1927, in the course of early investigations of sympathomimetic pharmacology, that its stimulant properties were first explored. These studies arose, like much early pharmacology, from the discovery of pharmaceutically-active natural products.



a. ATS Natural Products: Pharmacognosy of Khat and Ephedrine

The story of ATS begins with two plants: ephedra (i.e., ma-huang; *ephedra sinica*), and khat (i.e., “qat;” *catha edulis*). Estimates of the early history of these plants date back at least 5,000 years when ephedra was described in a catalog of herbs by Chinese emperor Shen Nung.⁵⁶ Ephedra was used in traditional Chinese medicine for millennia, with written records of its clinical applications emerging in the sixteenth century. These applications included use as a circulatory stimulant, diaphoretic, antipyretic, and antitussive.⁵⁶

In the Arabian peninsula, the khat plant has been cultivated for clinical use, specifically depression treatment,

Figure 5. Illustration from Vaughan's report on khat use in Aden.⁵⁶

dating back to the 11th century.⁵⁷ Cultivation for other purposes in Yemen and Ethiopia is thought to date back further, preceding that of coffee.⁵⁶ The plant was introduced to Western literature by Swedish botanist P. Forskal, who characterized it on a trip to northern Africa in 1762.^{56,58} He did not survive the return home to witness publication of his findings, but a colleague edited and submitted Forskal's manuscript, calling the plant in Forskal's honor "*catha edulis* Forskal," a name still used today.^{57,58}

Western interest in the pharmacology of khat began with the writings of Vaughan, a physician in Yemen's port city, Aden, who published on the plant in 1852 (Figure 5). He described the cultural value of the plant, and how its stimulant properties interacted with local Islamic tradition forbidding intoxication.^{56,59} Khat use was common in that time, as it still is today, throughout much of the Arabian peninsula and East Africa, most notably Yemen, where its leaves were often chewed for their stimulant effects and as part of social activities.^{54,60}

Thirty years later, in the 1890s, back in East Asia, but following the birth of modern pharmacology,⁶¹ ephedra became the project of interest for Japanese chemist Nagayoshi Nagai.⁶² Nagai had recently completed 12 years of post-doctoral training in Berlin, and would eventually found the Pharmaceutical Society of Japan.^{54,62} In collaboration with the pharmacologist Miura, he isolated, identified, and profiled the active constituents of ephedra. They identified two active compounds: diastereomers, which would be called l-ephedrine (i.e. (-)ephedrine, 1*R*,2*S*(-)**12**) and d-pseudoephedrine (i.e., (+)pseudoephedrine, 1*S*,2*S*(-)**13**).⁶² Miura evaluated "ephedrinum muriaticum" (the hydrochloride salt of the ephedra alkaloid base), a slightly yellow salt that crystallized in needles, and considered the results of such high interest as to justify a rapid communication of his findings.⁶³ He had evaluated the compound in frogs, dogs, and mice, finding it fatal via cardiac and respiratory effects. However, in all species, he noticed dilation of

the pupil, and this effect was recapitulated upon application directly to the conjunctival sac. He moved into clinical experiments with the assistance of Drs. Scriba and Kono at the Surgical Ophthalmological University Hospital in Tokyo, in which ephedrinum muriaticum appeared to be a potent, well-tolerated mydriatic of significant advantage to homatropine, an anti-cholinergic in common use at the time.⁶³

Despite Miura's enthusiasm, interest in ephedra and its active constituents waned until the early 1900s,⁶² when interest was growing in adrenergic pharmacology.³⁰ The pressor effect of a suprarenal extract had been discovered, and epinephrine (i.e., "adrenalin") identified as its active constituent.^{29,30,64} Japanese pharmacologists Kubota and Amatsu revisited 1*R*,2*S*(-)**12** in 1913, in the wake of these new discoveries. Testing its sympathetic modulatory properties, they found it similar to adrenaline and tyramine, both of which had recently been described as sympathomimetics.⁶² They found that 1*R*,2*S*(-)**12** raised blood pressure, accelerated heart rate, and relaxed smooth bronchial muscle. As a result of the latter property, an anti-asthmatic formulation of **12** was prepared and introduced into clinical usage in Manchuria, but this pharmaceutical product was not particularly successful. Ephedra was forgotten for another decade.⁶²

In 1923, Chen and Schmidt, who were stationed at Peking Union Medical College, but trained in physiology in the United States, began an investigation of the indigenous pharmacopoeia in the area. Ignorant of the previous work of Nagai and Miura, as those papers were written in German, Chen and Schmidt conducted dose-response studies in dogs and cats, describing many aspects of the sympathomimetic response in more detail than was possible with the resources of the earlier Japanese investigations. Their results aligned with those of Kubota and Amatsu: **12** was similar to epinephrine and tyramine in pharmacological effect, and therefore

belonged in the sympathomimetic amine category defined by Barger and Dale.^{30,65} They concluded that **12** was similar to **7** in structure (Figure 6), but importantly, its actions were more prolonged. Publication of these findings in English received much attention, as pharmacologists were searching for a superior anti-asthmatic to the recently developed pharmaceutical preparation of **7** itself, which was effective, but had many drawbacks, including poor oral bioavailability and stability/shelf life.³⁰ Clinical testing showed that **12** was superior across many therapeutic dimensions, and it became first-line therapy for asthma by the 1930s, with its use peaking in the 1940s and 1950s.⁶²

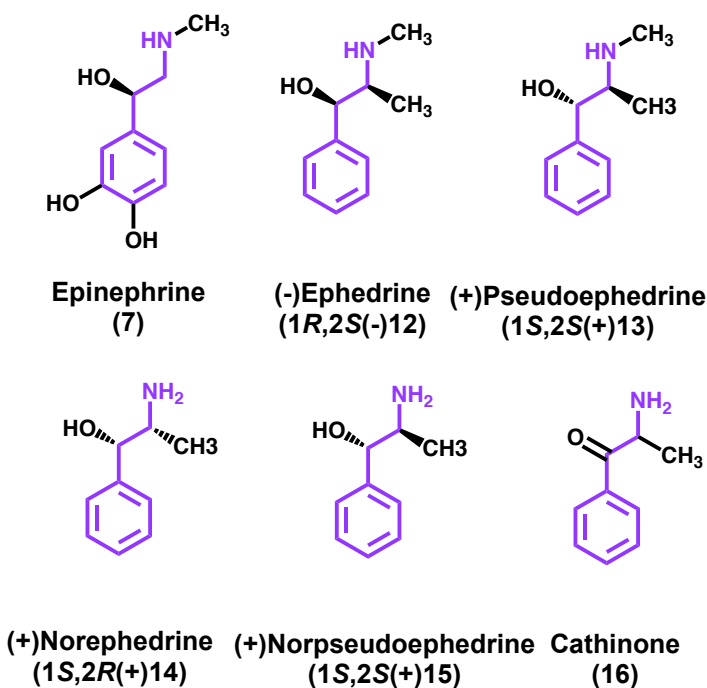


Figure 6. The hormone epinephrine, displayed alongside ephedrine isomers and similar compounds extracted from ma-huang and khat, and the structurally related compound (+)norephedrine.

Pharmacologic investigations of khat had also begun by the early 1900s.⁵⁶ After decades of attempts to identify the active constituents of khat, in the 1930's, (+)norpseudoephedrine (1S,2S(+))**15**, Figure 6) was extracted from the plant and named “cathine” in respect of its

incipient designation as such.^{60,66} However, these extraction studies had been performed on old dry plant material,⁶⁷ in which the later-extracted β -keto counterpart of 1*S*,2*S*(+)15 (i.e., cathinone, 16, Figure 6) was likely degraded, therefore going undetected at the time. Rothman and coworkers⁶⁷ would later investigate all four stereoisomers each of ephedrine and norephedrine alongside *S*(-)16, finding that *S*(-)16 and 1*S*,2*S*(+)15 were similar in noradrenergic potency, but *S*(-)16 was >3-fold higher in dopaminergic potency as compared to 1*S*,2*S*(+)15. Later behavioral studies found correlations between dopaminergic potency and reward-related effects for synthetic cathinones,^{68,69} supporting the assertion that cathinone is the constituent of khat more responsible for its widespread abuse. However, the impact of noradrenergic potency on abuse-related effects was yet to be determined. To date, 1*S*,2*R*(+)12 and 1*S*,2*R*(+)14 are the most selective known noradrenergic releasing agents in this series (9.7- and 10-fold selectivity, respectively, as compared to DA; Table 2).

Table 2. Potencies of ephedrine isomers and related compounds as synaptosomal releasing agents. Modified from Rothman et al., 2003.⁶⁷

Compound	EC ₅₀ , nM	
	NE	DA
(-)Ephedrine (1 <i>R</i> ,2 <i>S</i> (-)12)	43.1	236
(+)Pseudoephedrine (1 <i>S</i> ,2 <i>S</i> (+)13)	223	1988
(+)Ephedrine (1 <i>S</i> ,2 <i>R</i> (+)12)	218	2104
(-)Pseudoephedrine (1 <i>R</i> ,2 <i>R</i> (+)13)	4092	9125

(-)Cathinone (<i>S</i> (-) 16)	12.4	18.5
(-)Norephedrine (<i>1R,2S</i> (-) 14)	42.1	302
(+)Norpseudoephedrine (<i>1S,2S</i> (+) 15)	15.0	68.3
(+)Norephedrine (<i>1S,2R</i> (+) 14)	137	1371
(-)Norpseudoephedrine (<i>1R,2R</i> (-) 15)	30.1	294

Pseudoephedrine (**13**) was later found to be effective as a decongestant.⁷⁰ Being orally active, its use became widespread in over-the-counter pharmaceutical products for colds and other sinus conditions. In the early 2000's, it became the most common precursor for illicit methamphetamine synthesis in home labs, which led many states to regulate it more carefully.^{49,54} Various formulations of **12** have been popular as appetite suppressant and performance-enhancing drugs.⁵⁴ For the latter reason, **12** was banned by the FDA for use in unregulated supplements in 2004.⁵⁴

b. Amphetamine and Early Synthetic ATS: Clinical Use and Misuse

Just as they were inspired by the endogenous phenylalkylamine epinephrine (**7**), medicinal chemists were intrigued by the pharmacognosy of khat and ma huang. Analogs and homologs of the natural products discussed above were produced and evaluated using new physiological techniques.⁷¹⁻⁷³ Various ATS, and amphetamine (**9**) itself, were produced in the course of these investigations. Methcathinone (MCAT, **5**), the term being coined by Glennon and coworkers,²¹ which would later be described as a psychostimulant, was first produced during this

time. Its clinical utilization was limited, and it eventually became a controlled substance due to reports of its abuse, which was particularly widespread in the former Soviet Union.⁶⁰

Of particular interest in the late 1920s was an improved bronchodilator.^{37,74} Ephedrine (12) was prized for its oral bioavailability, but its supplies were limited,⁶² and it was difficult and expensive to make with the synthetic tools available at the time. Medicinal chemistry studies in search of a new bronchodilator, originally focused on phenylethanolamine, which was disappointing, led to the discovery of amphetamine (9) by Gordon Alles. Observing positive results in animals, he tested the compound on himself. He noted its stimulatory, euphoriant properties, but considered these side effects unwanted in an anti-asthmatic.^{75,76} In the mid-1930s, he offered samples of 9 to clinicians for testing in various applications, having struggled to optimize a bronchodilator. Coincident to these studies, Smith, Kline and French (SKF) Pharmaceuticals introduced to the market their product “Benzedrine” – the free base form of 9. Alles had only patented the salts, as the free base was volatile, and he had likely lost some initiative following a research presentation in 1929.³⁷ SKF capitalized on the volatility of the free base, delivering the drug via an inhaler for decongestant purposes.³⁷

In 1934, Alles resolved his dispute and partnered with SKF to further develop and market 9. Together, they sought to reposition their drug in the developing field of neuropsychiatry. Results of early trials were intriguing for the treatment of Parkinson’s disease,⁷⁶ alcoholism,⁷⁷ narcolepsy,⁷⁸ and most prominently: mood-related conditions that were likely synonymous with depressive disorders of today.⁷⁶ Amphetamine (9), in tablet formulation, was adopted for the treatment of “neurotic depressions,” and its use expanded dramatically during the 1940s. Annual sales of amphetamine (9) tablets were \$500,000 in 1941, or 4% of SKF revenue, and \$2,000,000

in 1945.³⁷ Reports of amphetamine (**9**) abuse had begun to emerge by this time, with some patients taking the drug *ad libitum* rather than as prescribed.

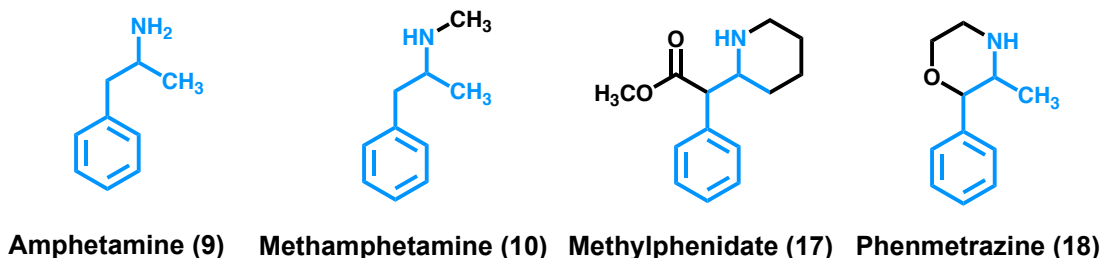


Figure 7. Amphetamine and selected synthetic ATS developed for clinical use in the mid-1900s.

Over the next several decades, use of prescription amphetamine and similar ATS continued to rise as new formulations, derivatives, and indications (e.g., weight loss) were introduced.³⁷ Methamphetamine (**10**), first synthesized by Ogata in Japan in 1919, was marketed as an anorectic under the brand name “Methedrine.”⁷⁹ By 1971, reviewers had estimated, based on manufacturing data, approximately 5% of Americans had used amphetamine or methamphetamine within the past year. Widespread diversion, along with misuse of legitimately obtained prescriptions, led to public scrutiny.³⁷ For years, some psychiatrists had raised the alarm that the abuse potential of ATS were not worth the benefits. In response, the United States Bureau of Narcotics and Dangerous Drugs (BNDD) moved amphetamine and its ATS derivatives methylphenidate (**17**) and phenmetrazine (**18**) to Schedule II, increasing regulatory control, in 1971. In coordination, the United States Food and Drug Administration (FDA) revised the approved indications for these agents, limiting them for the treatment of narcolepsy and “hyperkinetic disorder of childhood,” while removing depression and obesity on the basis of poor evidence of effectiveness.³⁷ This same year, President Richard Nixon declared the “War on

Drugs,” dissolved the BNDD, and established the modern Drug Enforcement Administration (DEA). These combined actions precipitated an estimated 60% decline in amphetamine prescription sales.³⁷ However, in the intervening years, the numbers of prescription ATS use has steadily climbed such that in 2005 they surpassed their 1969 peak. This increase might be related to expanded scope and increased diagnosis of the modern clinical conception of “hyperkinetic disorder of childhood:” ADHD, which now includes adults.⁸⁰

c. Illicit ATS and Designer Drugs: Methamphetamine, MDA, MDMA, and Methcathinone

Following increased regulations on clinical amphetamine prescriptions, demand-driven illicit methamphetamine supply increased. As measured by rates of treatment-seeking patients, methamphetamine use and abuse specifically increased alongside trends in supply.³⁷ Various “designer drugs,” or uncontrolled analogs, based on amphetamine, were observed on the market in the coming decades.⁸¹ Designer drugs are now more commonly referred to as new psychoactive substances (NPS), and are generally intended to recapitulate the subjective effects of a controlled substance while subverting regulation, both of which are often achieved by slight structural modifications to a known drug of abuse.

Illicit MDA (**23**) and MDMA (**3**), empathogens, emerged in the 1960s and 1970s, respectively, following diversion from research settings, where they were considered promising agents for use in assisted psychotherapy. They became prominent fixtures in electronic music “rave” culture.⁸² Concerns about abuse and neurotoxicity, although this has since been challenged,⁸³ led to their controlled substance designations (Schedule I). At the time of this writing, following renewed interest, **3** is again under investigation in clinical trials for the

treatment of post-traumatic stress disorder, social anxiety, and anxiety associated with life-threatening illness.⁸⁴

MCAT (5a), which had not previously been scheduled despite the discovery of its stimulant properties decades earlier, emerged as a “designer drug” (i.e., NPS) in the 1990s. It was named “methcathinone” by Glennon and coworkers in acknowledgement of its structural similarity to cathinone (**16**). Users had called it “cat” or “jeff.” It saw some abuse at this time and was included in an emergency scheduling action that also included other ATS designer drugs, such as 4-methylaminorex. MCAT is currently prohibited in Europe, the US, and at the level of the United Nations since its addition to Schedule I in the 1990s.⁸⁵

d. ATS NPS: Synthetic Cathinones (2010-Present)

i. Bath Salts

In the late 2000s to early 2010s, a group of ATS NPS emerged consisting primarily of mephedrone (**5f**), MDPV (**21**), and methylone. These substances, and related cathinone derivatives, together became known as a distinct class, collectively referred to as synthetic cathinones, although they are closely related to other ATS in pharmacology and SAR.⁸⁶ As a group, they received special attention following recognition of an upsurge in related poisonings and emergency room admissions.⁸⁷ These compounds were colloquially referred to as “bath salts,” as being NPS, they were available for purchase legally, and were sold at many retail locations in the United States in packages facetiously labeled “not for human consumption,” “plant food,” or “bath salts,” among others; hence, their name. Other synthetic cathinones were available for purchase through online retailers, and were known as “legal highs.” This was quite

common in the United Kingdom.¹¹ Accessibility of purchase, and perceptions of superior purity to street drugs led some drug users to choose bath salts.⁸⁸

Bath salts mixtures contained compounds that our lab, and later others, found to act via two distinct mechanisms of action, resulting in synergistic effects when mixed.⁸⁹ Being sold in inconsistent ratios, and often consumed alongside other substances, bath salts often led to unpredictable effects for users and clinicians treating them. Adverse effects, both acute and chronic, were sometimes severe, including agitation, tachycardia, psychosis, addiction, and multi-organ failure.^{7,8} In response, the cathinones found in “bath salts” were rapidly banned in the United States and many European countries.^{9,10}

ii. α -Pyrrolidinophenones and Second-Generation “Bath Salts”

Following the prohibition of the original bath salts compounds in the United States and much of Europe, a second generation of synthetic cathinones emerged,^{90,91} populating the psychoactive drug space with an array of synthetic cathinones diverse in structure and effect.^{10,14,91,92} Like their progenitors, second-generation bath salts acted differentially at the monoamine transporters in terms of potency, selectivity, and mechanisms of action.^{10,93} They also produced adverse behavioral and physiological effects that were sometimes life-threatening.^{16,17}

The “second-generation” moniker was first employed in reference to NPS by Brandt and coworkers in 2010.¹¹ This publication followed the 2010 general ban on synthetic cathinones in the United Kingdom, which precipitated a shift in marketing of NPS towards purportedly legal alternatives to mephedrone (**5f**), MDPV (**21**), and butylone.¹¹ Using gas chromatography ion-trap mass spectrometry in combination with nuclear magnetic resonance (NMR) spectrometry,

Brandt and coworkers analyzed 24 samples of NPS obtained via internet drug retailers, 22 of which were labeled “NRG-1” or “NRG-2,” a code for 1-(naphthalen-2-yl)-2-(pyrrolidin-1-yl)propan-1-one, also known as naphyrone or naphthylpyrovalerone.¹¹ Only one of these samples contained the expected compound; instead detected in the other samples were caffeine, local anesthetics procaine and benzocaine, then recently scheduled mephedrone and butylone, and other synthetic cathinones, including flephedrone (i.e., 4-fluoromethcathinone), and the entirely novel compound 4-methyl-*N*-ethylcathinone.^{11,18} The ban on cathinones seemed ineffective at promoting public safety, as the diversity of NPS was increasing, and banned products were consistently mislabeled, both seemingly to subvert said ban.⁸⁸ This occurred despite the fact that users of NPS reported harm reduction-related reasons, such as perceived increased purity, among their primary motivation for their choice of substance.⁸⁸

Pyrrrolidinophenones were prominent amongst second-generation bath salts in the United States (i.e., α -PVP, α -PHP). Like most ATS and synthetic cathinones, their pharmacological effects have been linked to activity at the monoamine transporters (MATs).^{18,89}

C. Monoamines and their Transporters

1. Monoaminergic Neurotransmission

a. Overview

Monoamines, including DA (**1**), NE (**6**), and 5-HT (**8**), are important neurotransmitters responsible for chemical signaling between their respective neurons. They are each synthesized in their presynaptic neurons, where they are stored in vesicles, and upon upstream electrical stimulation in the form of an action potential, they are released into the synapse via fusion of the vesicle with the plasma membrane of the presynaptic neuron. Following release, the monoamine

meets with its receptors (i.e., transmembrane proteins found both pre- and post-synaptically), to propagate its signal.

b. Biosynthesis

The major biosynthetic pathway of DA is via hydroxylation of dietary L-tyrosine by tyrosine hydroxylase, followed by decarboxylation of L-DOPA by DOPA decarboxylase (DDC).⁹⁴ These processes occur in the cytosol of dopaminergic neurons.⁹⁴ Analogously, 5-HT (**8**) is produced following decarboxylation of L-5-hydroxytryptophan, which is synthesized by hydroxylation of dietary tryptophan by tryptophan hydroxylase.⁹⁵ NE (**6**) is made from DA (**1**) by dopamine β -hydroxylase.⁹⁶ The latter process takes place primarily within storage vesicles.⁹⁷

c. Monoamine Receptors

Multiple subtypes of receptor exist for each individual neurotransmitter. Five types of DA receptor are known (D₁-D₅), each G-protein coupled. D₁ and D₅ are considered D₁-like, and coupled to G_s, stimulating cyclic AMP (cAMP) production. The remaining DA receptors (D₂-D₄), called D₂-like, are G_i-coupled, inhibiting cAMP in contrast to their D₁-like counterparts. For 5-HT (**8**), there are seven populations of receptors (5-HT₁-5-HT₇), some of which are subdivided into subpopulations for a total of at least 14 distinct 5-HT receptors in humans.⁹⁸ All are G-protein coupled with the exception of 5-HT₃, a ligand-gated ion channel. Like the DA receptor family, they include G_i-coupled (5-HT₁ and 5-HT₅) and G_s-coupled 5-HT₄, 5-HT₆, and 5-HT₇ receptors, as well as G_q-coupled 5-HT₂, which stimulates protein kinase C. NE (**6**) binds to adrenergic receptors, which are divided into two types: α and β , which are each subdivided into multiple subtypes, and all of which are G-protein coupled, including G_s, G_i, and G_q among them.

ATS are indirect agonists, and as such activate these receptors indiscriminately, with selectivity between dopaminergic, noradrenergic, and serotonergic (where applicable) potency. There are some exceptions to this rule, as in the case of MDA, which acts directly at 5-HT₂ receptors.⁹⁹

d. Monoamine Degradation and Signal Termination

Early understanding of monoaminergic signal termination focused exclusively on enzymatic degradation.¹⁰⁰ Their metabolism has been reviewed in detail elsewhere,⁹⁵ but can be summarized as follows. The catecholamines (**1**, **6**) are degraded primarily by catechol-*O*-methyltransferase (COMT), which abstracts a methyl group from *S*-adenosylmethionine and places it at the 3-*O* position of its substrate.⁹⁵ The methylated metabolites are then oxidized to aldehydes by monoamine oxidase (MAO), followed by dehydrogenation or reduction before excretion.⁹⁵ Alternatively, they may be oxidized by MAO first, and methylated by COMT later.⁹⁵ While methylation of 5-HT (**8**) is possible by hydroxyindole-*O*-methyltransferase, this pathway is of little metabolic importance *in vivo*.⁹⁵ The primary metabolic degradation of 5-HT (**8**) is analogous to that of the catecholamines, via oxidation by MAO.⁹⁵ While metabolism is an important component of monoaminergic signal termination, there is another critically important contributor (i.e., reuptake), but this remained unknown for decades after the discovery of monoaminergic degradative enzymes.¹⁰¹ The transporters responsible for monoamine reuptake (i.e., MATs) are also the primary molecular target for ATS, and their discovery be discussed in greater detail in a following section.

e. Discovery of DA Pathways

Monoaminergic circuits differ in their projections, localization, and the neuropsychiatric processes under their control. Their mapping has been extensively reviewed,¹⁰² but its genesis can be summarized briefly as follows. Carlsson and coworkers first identified the catecholamines (**1, 6**) in the brain, followed by the description of 12 distinct groups of catecholamine cells (A1-A12) by Dahlestrom and Fuxe in 1964. DA projections were mapped in the 1970s by immunohistochemistry and tyrosine hydroxylase staining.¹⁰² The accumulation of decades of mapping has revealed multiple pathways in which DA is involved.¹⁰³ The mesolimbic DA pathway, one of these pathways, is central to current theories of drug addiction, as will be discussed in the final subsection herein (**C.6**).

2. Monoamine Transporters: Discovery

The existence of MATs was a surprise. As reviewed by Iversen,¹⁰¹ and described above, termination of monoamine signaling was thought to be exclusively mediated by enzymatic degradation. The enzymatic model was revised following experiments with tritium-labelled catecholamines, which became available in the late 1950s.¹⁰⁰ Hertting and Axelrod observed that [³H]NE, *in vivo*, was not all degraded; 30-40% of it was absorbed and stored in tissue.¹⁰⁰ Furthermore, they found that denervation of sympathetic nerves prevented the observed uptake of [³H]NE.¹⁰⁰ Therefore, they proposed the mechanism of re-uptake into the presynaptic neuron.¹⁰⁰ Similar mechanisms were eventually discovered for the other monoamines, as well as for other neurotransmitters, including γ -aminobutyric acid (GABA), glycine, and L-glutamate, among others.¹⁰⁰ Additionally, vesicular transporters, including those specifically for

monoamines (i.e., VMAT) were discovered in the membranes of synaptic vesicles, and included two subtypes (VMAT-1 and VMAT-2).¹⁰⁰

3. Structure of MATs – from Cloning to Crystals and Beyond

In 1991, Tadeus Pocholczyk and coworkers at Yale reported the first cloning of a human monoamine transporter: the human NE transporter (hNET).¹⁰⁴ Using an expression cloning strategy, they elucidated the DNA sequence, amino acid sequence, and topology of hNET.¹⁰⁴ Their findings suggested a 69 kilodalton (KDa) protein of 617 amino acid residues, with 12-13 hydrophobic regions of 18-23 amino acid residues each that were proposed to form transmembrane domains (Figure 8).¹⁰⁴ Similarly to the γ -aminobutyric acid transporter (GAT), which had been cloned just a year earlier,¹⁰⁵ the hNET cloning suggested that the hNET N and C termini were located intracellularly, with an extracellular loop containing three glycosylation sites.¹⁰⁴

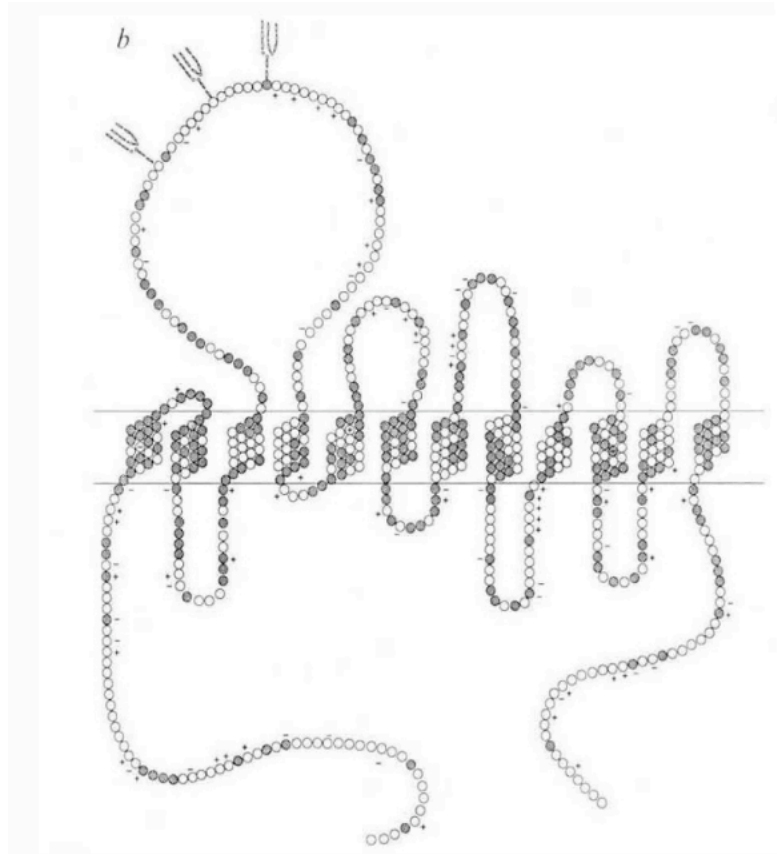


Figure 8. Pacholczyk's proposed structure of hNET based on cloning. Conserved residues with GAT are indicated by darkened circles. Reproduced from Pacholczyk et al., 1991.¹⁰⁴

The cloning of a DA transporter (DAT), in this case the rat DAT, was first reported in *Science* in 1991 by John Kilty and colleagues.¹⁰⁶ They used PCR, degenerate oligonucleotides, and stringent screening to identify a full-length clone containing 12 hydrophobic regions corresponding to 12 transmembrane helices, similarly again to GAT, as well as to the just reported hNET. *In situ* hybridization and pharmacological inhibition by cocaine, mazindol, and desipramine supported the identification of DAT.¹⁰⁶ In the same issue of *Science*, Beth Hoffman reported the cloning of rat SERT, and its homology to GAT, NET, and DAT.¹⁰⁷ Ramamoorthy cloned the first human SERT (hSERT) several years later.¹⁰⁸

The first crystal structure of a solute carrier 6 (SLC6) transporter was published in 2005 by Yamashita and coworkers.¹⁰⁹ This would become the basis for many homology modeling studies of MATs.¹⁰⁹

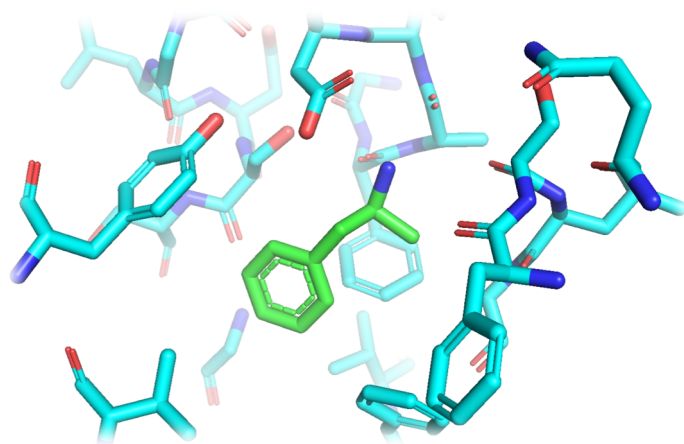


Figure 9. *S*(+)Amphetamine (green) co-crystallized with dDAT (blue), PDB ID: 4XP9. Generated in PyMOL Version 2.1.1.

In 2013, the first MAT was crystallized by Penmatsa, Wang, and Gouaux, working at the Vollum Institute of Oregon Health and Science University.¹¹⁰ The DA transporter of *drosophila melanogaster* (i.e., the fruit fly; dDAT) was cocrystallized with nortriptyline. The same team published a series of new dDAT crystal structures

in 2015, which were cocrystallized with a range of other ligands, including amphetamine (**9**; Figure 9).¹¹¹ Coleman and Green, also working with Gouaux, released the first and, at the time of writing, only human MAT crystal structure: that of hSERT, cocrystallized with antidepressants (*S*)-citalopram and paroxetine.¹¹²

In each of the crystal structures, cocrystallized ligands were found in a common binding site defined by conserved residues, including an aspartate residue that likely forms hydrogen bond interactions with the basic amine of ATS.^{110–112} This site is commonly referred to as the S1 site. An additional S2 site has been proposed on the basis of previous crystallography studies with the related protein LeuT, the leucine transporter.¹¹³ In hSERT, an additional molecule of (*S*)-citalopram was cocrystallized in what was proposed as a potential allosteric site just above the common MAT binding site.¹¹²

No crystal structure has been produced for NET, and no crystal structure has been produced for the human form of DAT (hDAT). However, homology modeling studies have been used to simulate the structures of all three human MATs. Koldsø and colleagues created homology models of hDAT, hNET, and hSERT even before the release of the first dDAT crystal structure, basing their models on LeuT.¹¹⁴ They conducted induced-fit docking studies of the endogenous substrates using the leucine binding site of LeuT as the pre-defined binding site.¹¹⁴ This site was the same as that later identified for ligands in the crystal structures of dDAT and hSERT.^{111,112,114} Koldsø and colleagues found at least two common binding modes for each substrate.¹¹⁴ In our studies described in later chapters, we were able to identify similar common binding modes for the endogenous substrates of hNET using a different template for hNET models.

Models of the human MATs have also been used to dock synthetic cathinones. Sakloth and coworkers docked a series of previously synthesized and biologically evaluated *para*-substituted MCAT analogs at models of hDAT and hSERT.⁶⁹ Through qSAR analysis, they described a correlation between the volume and maximum width of the *para*-substituent and selectivity for hSERT activity over hDAT activity.⁶⁹ Modeling revealed a non-conserved residue in the direct vicinity of the *para* substituent.⁶⁹ The same residue by alignment was a serine in hDAT and an alanine in hSERT, potentially explaining why larger substituents were favored by hSERT.⁶⁹ This residue was proposed to control the selectivity of MCAT (5a) analogs between hSERT and hNET.⁶⁹ The studies described herein describe developments in this explanation.

4. Evolution of MATs

Systems of monoaminergic neurotransmission are widespread in the animal kingdom. Evidence suggests that 5-HT and DA neurons emerged at least 600,000,000 years ago, based on their presence in an ancient flatworm (i.e., the stem metazoan) thought to be the shared common ancestor of all animals, including bilateria (i.e., bilaterally symmetrical animals) and cnidaria (i.e., radially symmetrical animals).¹¹⁵ Following this flatworm, the bilaterian common ancestor possessed genes for the full suite of monoaminergic neurotransmission, including reuptake.¹¹⁵ The genes for these MATs were derived from the greater solute carrier 6 (SLC6) transporter family, which also includes amino acid and GABA transporters.¹¹⁶

The basal bilaterian is thought to be a common ancestor for all protostomes and deuterostomes, which are two clades distinguished predominantly by embryonic developmental factors.¹¹⁵ The MATs, however, did not descend from the basal bilaterian unmodified.¹¹⁵ Its gene for SERT persisted into protostomes and deuterostomes, and its gene for DAT, termed invertebrate DAT (iDAT), persisted in many protostomes.¹¹⁵ Among the deuterostomes, iDAT was lost in the common ancestor of chordata.¹¹⁵ Instead, the genes for both DAT and NET in chordata evolved from a general catecholamine transporter (Figure 10).¹¹⁵ Therefore, hNET and hDAT are both derived from this common catecholamine transporter, and are evolutionarily divorced from dDAT, which descended from iDAT.¹¹⁵ Therefore, similarity in structure and function of hDAT and dDAT are a consequence of convergent evolution. In protostomes, the catecholamine transporter became the octopamine transporter in those cases where it remained.¹¹⁵

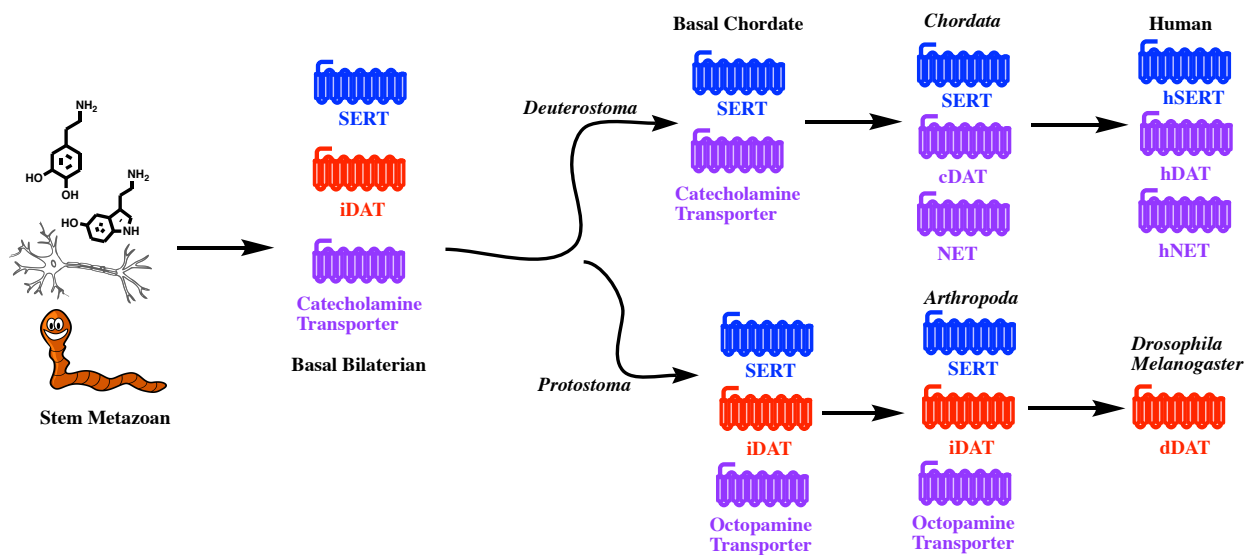


Figure 10. Evolutionary origin of the MATs. Highlights the evolutionary distance between dDAT and hDAT. Generated in ChemDraw Professional 17.1.

5. Mechanism of Neurotransmitter Transport

Transport of monoamines against their concentration gradient, from the extracellular space to the cytosol, is entropically unfavorable when considering the transport of substrate itself. Therefore, substrate transport is dependent on another source of energy.¹¹⁷ This energy comes from coupling substrate transport to that of Na^+ ions along their concentration gradient. The extracellular monoamine substrate is thought to bind to the MAT along with Na^+ and Cl^- ions, and they are all transported together into the cytosol.¹⁰⁹

Physically, the MATs are thought to cycle through discrete conformations to facilitate substrate transport, as described by the alternating access model. As reviewed by Kristensen,¹¹⁶ this model originated from the work of Mitchell and Wilbrandt in the late 1950s, who proposed that transporters are allosteric proteins, and that they alternate conformation between cytosolic and extracellular accessibility.¹¹⁶ Jardetzky refined this model in the 1960s. The model states that transporters undergo conformational changes that allow sequestration of the substrate and its

binding site from the extracellular or cytosolic medium.¹¹⁶ These discrete conformations are known as outward-facing open, occluded, and inward-facing open states.¹⁰⁹

Though the alternating access model can be supported by observations of each of the proposed states in crystal structures of LeuT and detailed kinetic analyses, there are observations that it cannot totally explain.¹⁰⁹ For example, the stoichiometry of ion transport is out of step with what would be predicted based on the cotransport of substrate, Na⁺, and Cl⁻ ions alone.¹⁰⁹ Alternatives, such as a channel mode, in which the transporter is open to both cytosol and the extracellular medium, have also been proposed.¹¹⁸⁻¹²⁰

6. Monoamines and ATS in Substance Use Disorders

There are various models in biology, psychology, and sociology that attempt to explain how drugs of abuse exert complex behavioral effects in humans, and how this behavior can sometimes lead to consistent symptoms of behavioral dysfunction that define a distinctive psychiatric disorder.¹²¹ At the time of writing, a widely accepted definition and labeling of this disorder is that of the Diagnostic and Statistical Manual of Mental Disorders Fifth Edition (DSM-5), which calls it substance use disorder (SUD).¹²² SUD is diagnosed on the basis of symptoms of impaired control over substance use, social impairment, risky use, and/or pharmacological criteria (Table 3). SUD involving ATS are defined more specifically as stimulant use disorders (StUD), which are subdivided into StUD involving amphetamine-type substances or cocaine. Out of 11 possible symptoms, diagnosis of most SUD, regardless of substance, requires 2-3 symptoms for mild, 4-5 for moderate, and 6 or more for severe SUD, the latter severity which is associated with the pathological drug-taking pattern traditionally defined

as addiction.¹²³ The common symptoms, regardless of substance, are reflective of the unified theories of addiction neurobiology that are prevalent in current literature.

Table 3. Diagnostic Criteria of Substance Use Disorders. Adapted from DSM-5.¹²²

Category	Criterion
Impaired control over substance use	1. Substance taken in greater amount/time than originally intended
	2. Unsuccessful efforts to decrease/discontinue use
	3. Great deal of time using, recovering from substance
	4. Craving
	5. Failure to fulfill major role obligations at work, school, or home
Social Impairment	6. Continue use despite persistent interpersonal problems
	7. Activities given up or reduced because of use
Risky Use	8. Recurrent physically hazardous use
	9. Continued substance use despite persistent health problem
Pharmacological Criteria	10. Tolerance
	11. Withdrawal

Unified theories of addiction emphasize the similarities in SUD across drug classes.^{121,124} Major current theories include hedonic allostasis, incentive sensitization, aberrant learning, and frontostriatal dysfunction.¹²⁴ The role of DA-mediated activation of reward circuitry, particularly via the mesolimbic system, at least in the initial phases of drug taking, is a common theme in many of these theories.^{124,125} The mesolimbic DA system extends through several brain regions implicated in rewarding and reinforcing effects of drugs, and those mediating incentive salience,

including the basal ganglia, which includes the nucleus accumbens, and the ventral tegmental area (VTA).^{126,127} An important role for DA has also been implicated in the withdrawal/negative affect stage of addiction central to the allostasis model.¹²⁶ Unified theories are not without controversy, as differences have been identified between individual substances and their associated behavioral and molecular pharmacological profiles.¹²¹ Additionally, while many people will use drugs of abuse, including ATS, most will never develop SUD;¹²⁸ this and additional behavioral evidence clearly suggest that the individual is a variable in the developmental process of SUD.¹²⁹ The environment can also play an important role, and its effects vary on the basis of substance.¹²⁴

For StUD as opposed to other SUD, the evidence for DA as a central mediator of addiction may be strongest, as psychostimulants directly increase DA by their molecular interaction with the DAT.^{111,126} Intracranial injection studies in the 1990s led to the identification of DA neurons in the nucleus accumbens and VTA as those primarily responsible for psychostimulant reward-related properties.¹³⁰ Animal study evidence of ATS neurotoxicity via dopaminergic mechanisms had also accumulated by this time.^{131–136} Imaging of human brains by N. Volkow and coworkers in the early 2000s revealed severe disruptions in dopaminergic systems of methamphetamine (**10**) users, even after detoxification.¹³⁷ These disruptions were associated with motor and cognitive impairment, and specifically indicated DA transporters as the site of the dysfunction. This work produced famous images (Figure 8) that served as supporting evidence for the brain disease model of addiction, which in development at the time,¹²⁵ and has since been strongly promoted by the National Institutes of Drug Abuse (NIDA).^{137,138}

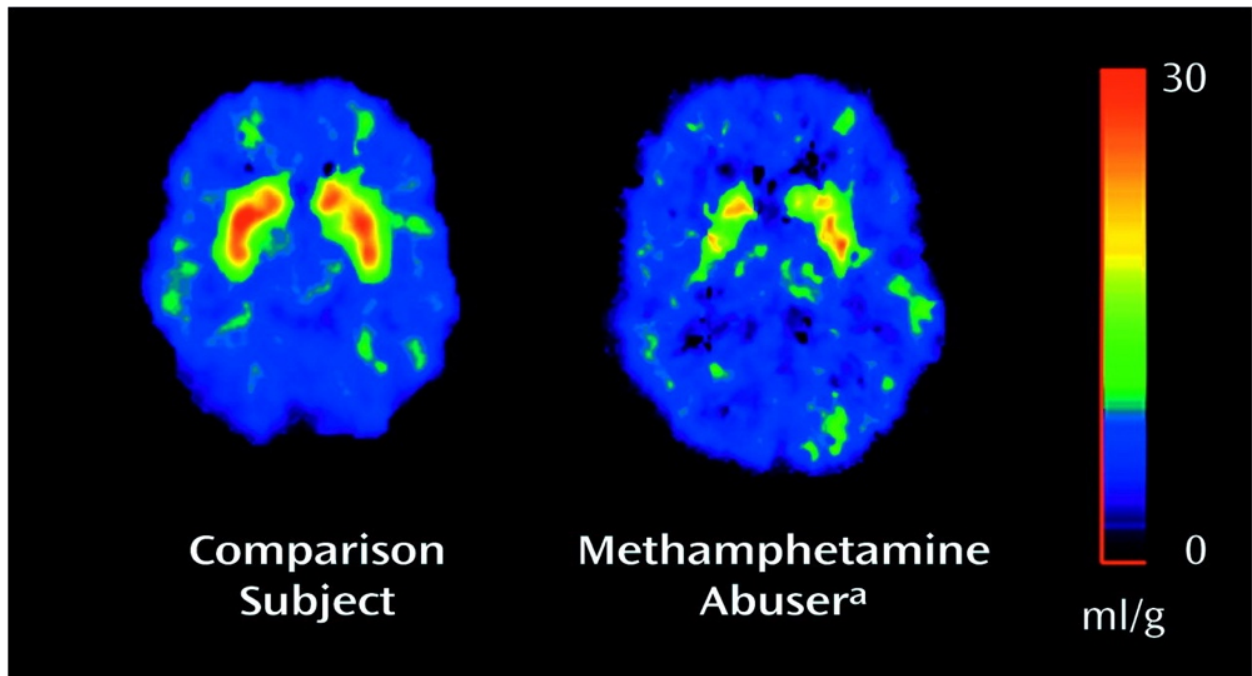


Figure 11. PET scan of DAT radioligand $[^{11}\text{C}]d\text{-threo-methylphenidate}$ bound to 33-year-old male human brains. The methamphetamine user was imaged 80 days after detoxification. [Reproduced from Volkow et al. 2001.

Though SUD is often a chronic, progressive, and potentially fatal disorder, sustained remission and recovery are possible.¹³⁹ However, StUD patients face particular barriers to recovery and treatment. These can include, based on direct activation of DA by ATS, psychosis, and neurotoxicity-based cognitive and behavioral impairment, which preclude engagement with treatment and recovery processes.¹⁴⁰ Sociodemographic trends of users may pose additional barriers.¹⁴⁰ Though many have been evaluated at the pre-clinical and clinical level, no pharmacotherapies are currently FDA-approved for use in treating StUD. Considering the rising contribution of ATS to the overdose crisis and global drug abuse problem,⁶ and unique features of StUD,¹⁴¹ it may be in need of targeted intervention.

D. Pharmacology

1. Overview

As discussed in a prior section, some important features of ATS are their ability to augment catecholamine signaling indirectly and produce psychostimulant effects. As argued convincingly by Sitte and Freissmuth in their thorough review,¹⁰⁹ evidence suggests that this augmentation is dependent first and foremost on interaction as ligands at MATs. Besides ATS, other phenylalkylamines also act at MATs, include monoaminergic neurotransmitters, the endogenous substrates. MATs serve as important drug targets for a broader molecular scope as well; notably, most antidepressants are MAT ligands, though most antidepressants are neither ATS nor traditional phenylalkylamines. In addition to differences in selectivity between DAT, SERT, and NET, ligands for these transporters differ in mechanism of action. In general, they act via one of two general mechanisms of action: as blockers (i.e., reuptake inhibitors) or substrates (i.e., releasing agents). Additionally, some evidence suggests the existence of intermediate mechanisms of action between the two prior categories (i.e., partial releasers),¹⁴² and additional molecular targets that modulate substrate activity.¹⁰⁹ Subtle differences in target selectivity and mechanism of action at MATs have important implications for pharmacology, giving rise to behavioral effects, psychoactivity, and therapeutic class where applicable.

2. ATS as MAT Blockers

The most seemingly straightforward mechanism by which ATS may augment catecholamine signaling is by reuptake inhibition. Many therapeutic drugs and drugs of abuse act at the MATs in this way. They bind to the S1 site of the outward-facing open conformation of

DAT, NET, and/or SERT, competing with the substrate and stabilizing the outward-facing open conformation.¹¹⁶

The primary pharmacological class utilizing reuptake inhibition is that of antidepressant drugs. Antidepressants may inhibit all three MATs, though modern antidepressants are more selective for SERT, and sometimes NET (SSRIs and SNRIs), over DAT. Bupropion (**20**), Figure 12) is an exception. An ATS synthetic cathinone, **20** is an approved antidepressant and is more

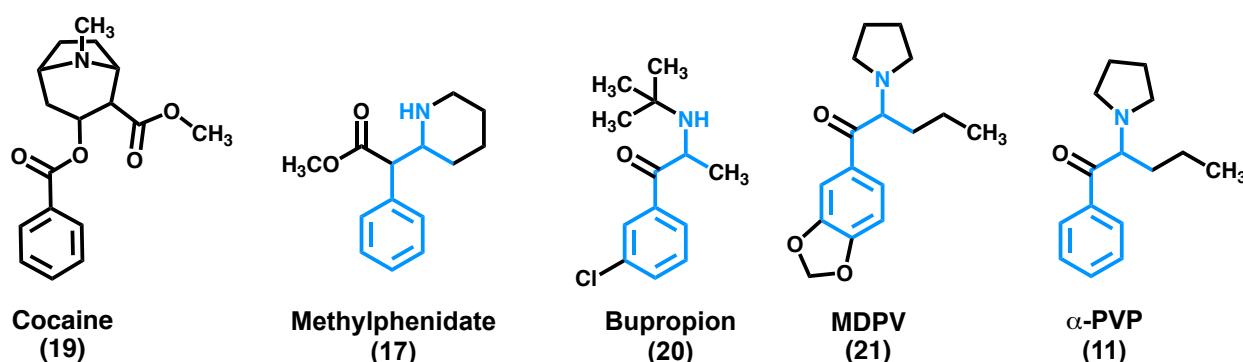


Figure 12. Known psychostimulant MAT blockers, with ATS structural features highlighted in blue where applicable, including known drugs of abuse (all) and drugs approved for medical use (17, 20, under rare circumstances 19).

selective for DAT and NET (an NDRI) than for SERT.

The prototypical psychostimulant drug of abuse acting as a reuptake inhibitor is cocaine (**19**, Figure 12). Cocaine is relatively nonselective between the three MATs, and not particularly potent. It is not an ATS, as it has a distinct molecular structure from that of phenylalkylamines. However, it has been cocrystallized in the same S1 binding site as ATS and antidepressants alike at dDAT.¹¹¹

Comparing potency and selectivity of psychostimulant MAT reuptake inhibitors yields surprising results (Table 4). Though cocaine is considered a drug of high abuse potential in humans, it is not considerably more potent at DAT than the antidepressant bupropion, which is

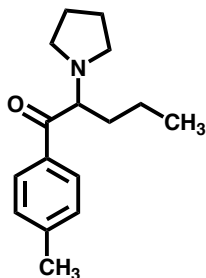
considered to have lower abuse potential. This, despite the fact that dopaminergic activity is thought to be determinative of abuse potential.¹⁰⁹ Cocaine is also nonselective between DAT and SERT, and much less selective than bupropion or methylphenidate, which are both approved psychiatric medications. Therefore, neither can DAT/SERT selectivity explain its history of abuse in humans, despite observed correlations between these pharmacological properties for other compounds (vide infra).^{68,143}

Table 4. Inhibition of [³H]neurotransmitter reuptake at MATs for cocaine (**19**), methylphenidate (**17**), bupropion (**20**), MDPV (**21**), and α -PVP (**11**). While not all rat brain synaptosome assay results were gathered from the same paper, they were all performed in the same laboratory.

Compound	IC ₅₀ (μ M)			Assay	Reference
	DAT	NET	SERT		
Cocaine (19)	0.211	0.292	0.313	Rat brain synaptosome	^a Baumann et al. 2013 ¹⁴⁴
	0.90	0.48	1.5	HEK 293 cells	Luethi et al. 2017 ¹⁴⁵
Methylphenidate (17)	0.13	0.12	274	HEK 293 cells	Luethi et al. 2017 ¹⁴⁵
Bupropion (20)	0.305	3.715	>10000	Rat brain synaptosome	^a Shalabi et al. 2017 ¹⁴⁶
MDPV (21)	0.004	0.026	3.305	Rat brain synaptosome	^a Baumann et al. 2013 ¹⁴⁴
α -PVP (11)	0.01	0.01	>10	Rat brain synaptosome	^a Marusich et al. 2014 ¹⁵

^a Experiments performed in the same laboratory under the same or similar conditions.

MDPV (**21**) and α -PVP (**11**) are the prototypical synthetic cathinones in the MAT blocker mechanistic class. Both emerged as NPS as part of the synthetic cathinone “bath salts” phenomenon (see section **B.3.d.** above), though they had both been investigated and patented in the mid-1900s (see Glennon and Young for a thorough review).⁹¹



Pyrovalerone (22)

Figure 13.
Pyrovalerone, an NDRI.

Pyrovalerone (**22**; Figure 13), the 4-methyl counterpart of α -PVP, was also investigated in the mid-1900s, and used clinically as an anti-obesity and wakefulness agent in France, alongside amphetamine and its analogs as described in section **B.3.b.** However, it was withdrawn from the market in France in 1979 due to problems with its abuse.¹⁴⁷ In general, the α -pyrrolidinophenones act as MAT blockers, most often as NDRIs, based on their inactivity or negligible activity as blockers of SERT.

3. ATS as MAT Substrates

a. Mechanism of Substrates as Releasing Agents

Though ATS MAT blocker activity is the more straightforward mechanism, ATS substrate activity is by far more common. Amphetamine (**9**), methamphetamine (**10**), cathinone (**16**), MCAT (5a), ephedrine (**13**), MDMA (**3**), and mephedrone together represent many of the most well-known ATS. Though they differ in pharmacological effects, they all act as substrates for the MATs, eventually triggering augmentation of monoaminergic signaling through various processes. The details of how this augmentation takes place in the case of substrates remains to be fully elucidated, but several components of the mechanism have garnered significant evidence in their support. These hypotheses were reviewed by Sitte in 2015 with application specifically to ATS NPS.¹⁰⁹

In the “weak base hypothesis,” described first by Sulzer in 1993,¹⁴⁸ the concerted actions of ATS on multiple targets give rise to their substrate-releasing properties.¹⁰⁹ As substrates for MATs, ATS enter presynaptic neurons.¹⁰⁹ As substrates for VMATs, they enter the vesicle.¹⁰⁹ As weak bases, they bring protons with them, dissipating the physiological baseline proton gradient, and precluding the transport of endogenous substrate into the vesicle.¹⁰⁹ This, in concert with ATS inhibition of degradative enzyme COMT, elevates cytosolic monoamine concentration to unnatural levels; under normal circumstances, little endogenous substrate remains in the cytosol thanks to spatial proximity of vesicles and high turnover number of VMATs.¹⁰⁹ The concentration of neurotransmitter in the cytosol near the MATs it thought to be high enough for neurotransmitter to occupy the inward-facing binding site of the MAT and drive transport in reverse.¹⁰⁹

Alternative targets, including trace amine associated receptor 1 (TAR1), ligand gated channel-55 (LGC-55), and the glutamate receptor (EAAT3), have also been proposed as responsible for ATS substrate releasing effects.¹⁰⁹ These additional targets have been linked to ATS activity, and even the weak base hypothesis implicates multiple targets (MATs, VMATs, and COMT).¹⁰⁹ This plethora of targets for substrate ATS raises a question as to which target is most directly responsible for substrate release. Considerable evidence calls into question the possibility of targets other than MATs as the primary mediators of release. VMAT blockade fails to induce DA release in DAT-deficient neurons, not all substrates are active at TAR1, amphetamine is weakly potent at LGC-55, and EAAT3 internalization may explain long-term effects of ATS, but would fail to explain their rapid psychoactivity.¹⁰⁹ On the other hand, substrate potency at MATs expressed in HEK 293 cells has been correlated with releasing

activity at rat brain synaptosomes, supporting the primacy of MAT activity in determining substrate release.¹⁴⁹

b. Potency and Selectivity of ATS Substrates

Crystal structures in concert with mutagenesis studies have suggested that substrates (e.g. amphetamine, **9**) and blockers (e.g. cocaine, **19**) bind at the same S1 site in DAT.¹¹¹ By definition, substrates have low affinities for the MATs. Higher affinities would be predicted to convert these substances into blockers, as remaining bound to the transporter would increase competition for the substrate binding site. Instead, substrates have low affinities, as they ostensibly must detach easily from the binding site to be transported. Therefore, functional data is more reliable for evaluating molecular pharmacology of substrate ATS.

Potency of substrate ATS can be evaluated using various assays. One can evaluate the degree of transport into the cell, or the degree of substrate release. The studies described in these works utilize calcium imaging as a biosensor process to detect substrate activity. In this assay, voltage-gated calcium channels are co-expressed with DAT, NET, or SERT in HEK-293 cells. The cells are pre-loaded with Fura2 dye, which fluoresces when exposed to Ca^{2+} . The substrate of interest (e.g. **9**) is perfused on the cell, and substrate transport increases the permeability of the cell membrane to Na^+ ions. This results in a substrate-induced but uncoupled Na^+ current that depolarizes the membrane, opening the co-expressed voltage-gated Ca^{2+} channels. This allows the influx of Ca^{2+} ions along their concentration gradient, which corresponds to a fluorescence that can be visualized and quantified using epifluorescence microscopy.¹⁵⁰ This assay has been validated as a measure of substrate-induced release by correlating measured substrate potency with release potency in rat brain synaptosome assays.^{149,150}

4. Behavioral Pharmacology of Synthetic Cathinones

Synthetic cathinones produce reliable results in various behavioral animal models. Psychostimulants, including cocaine and ATS, typically produce locomotor stimulation, which can be measured using rodents in an open field chamber. Synthetic cathinones including MCAT, mephedrone, MDPV, and bupropion, among others, produce locomotor stimulation, as reviewed in detail by Glennon.⁸⁶ ATS are readily self-administered in an operant paradigm, and produce conditioned place preference. Cocaine (**19**), amphetamine (**9**), and MCAT (5a) readily substitute for one another in drug discrimination trials.⁸⁶

Of particular interest in measuring abuse-related effects of ATS, considering their mechanism of action at the MATs, is the intracranial self-stimulation (ICSS) paradigm. This assay allows differentiation of DA- and 5-HT- mediated effects by measuring facilitation and depression of baseline responding rates,¹⁵¹ which have been connected to distinctive dopaminergic and serotonergic effects in synthetic cathinones.^{68,152} In the ICSS protocol used in these studies, rats are implanted with an electrode in their left medial forebrain bundle, an area of the brain directly connected to rewarding effects of drugs of abuse.¹⁵¹ They are able to press a lever to receive an electrical stimulation of a variable frequency; the amplitude of this stimulation is tuned to stimulate the proper neurons.¹⁵¹ At a high frequency, the rats will reliably press the lever to receive the stimulation. When the frequency is reduced, however, the rats will no longer press the lever. Lever-pressing at a low frequency is facilitated, however, when a rewarding substance is administered before the trial.¹⁵¹ This phenomenon is clearly observed in a dose-dependent manner for DAT blockers and substrates, including MDPV (**21**), methamphetamine (**10**), and MCAT (5a). SERT releasers, on the other hand, produce depression

of ICSS (e.g. fenfluramine).¹⁵¹ For ATS with serotonergic activity, ICSS allows for the observation of facilitation and depression, teasing out DAT-mediated and SERT-mediated effects.¹⁵¹

E. SAR of ATS

Simple variations to the amphetamine (**9**) structure confer drastic changes in pharmacology in terms of molecular target and pharmacological effect, with various psychoactive states on offer from the shared phenylalkylamine scaffold (hallucinogens, empathogens, stimulants, etc., *vide supra*). Alterations to the structure can be divided into five categories: 1) to the amine nitrogen, 2) to the α -carbon atom, 3) to the β -carbon atom, 4) to the two-carbon side-chain connecting the phenyl ring to the nitrogen atom, and 5) to the phenyl ring.

Though Biel and Bopp defined amphetamines as primary amines, the *N*-methyl counterparts of amphetamine (**9**; i.e., methamphetamine, **10**) and MDA (**23**; i.e., MDMA, **3**) are well-known drugs of abuse whose reputations precede even those of their primary amine counterparts (Figure 14). The degree to which *N*-methylation of amphetamine (**9**) to methamphetamine (**10**) produces changes in pharmacology has been a subject of some debate in the literature for many years. Methamphetamine (**10**) is often reported to be more potent and dangerous, but this observation may be biased in light of its status as the more widely abused substance obtained via illicit production.¹⁵³ Often cited as a possible explanation for its decrease in polarity as giving rise to greater blood-brain barrier penetrability.¹⁵⁴ An alternative explanation for the widespread illicit production of methamphetamine, as opposed to amphetamine, has been its facile synthesis via reduction of pseudoephedrine (**13**),⁷⁹ which until recently was widely available over the counter (i.e., purchase limits or prescriptions are now required in many states). Pharmacological investigations have yielded mixed results.

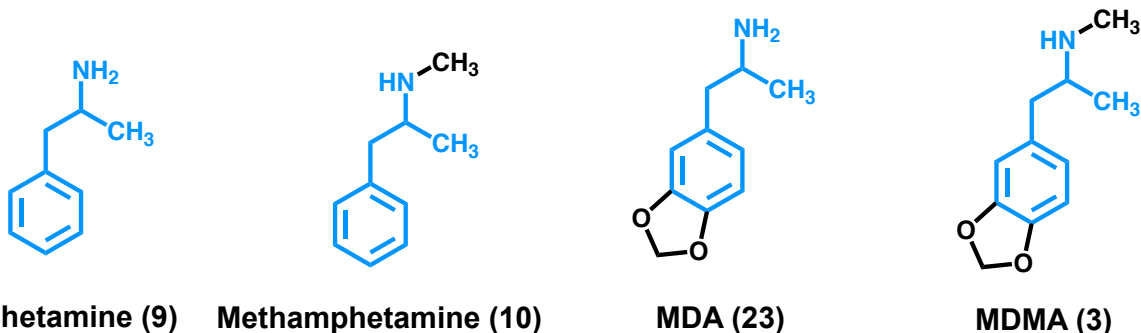


Figure 14. Primary amine amphetamines with their secondary amine counterparts.

In studies of tritiated neurotransmitter release from rat brain synaptosomes, (+)-amphetamine and (+)-methamphetamine were similar in potency (Table 5).⁶⁷ The two were virtually identical in terms of dopaminergic releasing potency,⁶⁷ and counterintuitively, (+)-amphetamine was both more potent as a NE releaser, and less potent as a serotonergic releaser.⁶⁷ If methamphetamine was the more potent drug of abuse, one might expect it to be the more potent NET releaser and less potent SERT releaser, as noradrenergic potency has been associated with the active dose of psychostimulants,⁵¹ and 5-HT release has abuse-limiting effects.¹⁵⁵

Table 5. Effect of *S*(+)amphetamine or *S*(+)methamphetamine on [³H]neurotransmitter release from rat brain synaptosomes. Adapted from Rothman et al. 2003.⁶⁷

Compound	EC ₅₀ , nM		
	DA	NE	5-HT
<i>S</i> (+)Amphetamine <i>S</i> (+)(9)	24.8	7.07	1765
<i>S</i> (+)Methamphetamine <i>S</i> (+)(10)	24.5	12.3	736

In vivo, differences in molecular pharmacology between the (+)-isomers of amphetamine and methamphetamine have been observed across various dimensions of activity. In microdialysis studies, methamphetamine was less effective at raising DA levels in the prefrontal cortex, and amphetamine, but not methamphetamine, raised glutamate levels in the nucleus accumbens.¹⁵⁶ However, methamphetamine but not amphetamine raised glutamate levels in the prefrontal cortex.¹⁵⁶ More recent electrophysiological studies found that methamphetamine generated greater whole-cell DAT-mediated currents than amphetamine *in vitro*, released five times the levels of DA *in vitro*, and was more effective to inhibit clearance of DA in the nucleus accumbens *in vivo*.¹⁵⁷

Behavioral studies have also yielded mixed results in the comparison of amphetamine (**9**) and methamphetamine (**10**). Depending on the study and the behavioral assay employed, **10** may appear similar,^{156,158–161} less potent,^{162–164} or more potent than **9**.^{165–168} Some of the mixed results may be due to differential pharmacological behavior of individual optical isomers. Some earlier behavioral studies directly compared (+)**9** to (±)**10**. In one study directly comparing the (+)**9** to (+)**10** and (-)**9** to (-)**10** in rat self-administration studies, there was no difference between (+)**9**

and (+)**10**, but rats self-administered 1.75 times greater quantities of (-)**10** than (-)**9** at the same dose.¹⁶² Though **10** is thought to be primarily abused as a racemic mixture, various formulations at a range of optical purities are available clinically for **9**; as such, stereochemistry may be of nuanced importance to abuse in humans. A potential criticism of previous experiments has been the high doses used, which may not be etiologically relevant.¹⁶⁹ In a low-dose study argued to be more constructively valid, which compared the effects of methamphetamine (**10**) and amphetamine (**9**) on locomotor activity in rats, methamphetamine (**10**) was more potent than amphetamine (**9**) at low doses of 0.5 mg/kg or 1.0 mg/kg in the presence of cues, but not in the absence of cues.¹⁶⁹ This subtle difference was proposed to partially explain the fact that methamphetamine (**10**) is more likely to be abused via smoking and injection routes of administration, which offer the opportunity for cue association with drug-taking, even in a real-world setting.¹⁶⁹ This is in contrast to amphetamine, which is more likely to be taken orally, a route of administration without cues.¹⁶⁹ However, an alternative explanation for the discrepancy is that amphetamine is much more widely available via prescription in oral formulation, and it is this diverted supply that constitutes the bulk of amphetamine-specific abuse.³⁷

For the 3,4-methylenedioxy counterparts of amphetamine (**9**) and methamphetamine (**10**; MDA, **23**, and MDMA, **3**, respectively), the transition from primary amine to secondary amine confers changes not only in potency, but in subjective effects and mechanism of action. MDA (**23**) is both a stimulant and hallucinogen, based on its actions at 5-HT₂ receptors, whereas MDMA (**3**) is a mixed stimulant and empathogen, based on activity at SERT.¹⁸

Further extension of the *N*-alkyl substituent of methamphetamine to *N*-ethyl, *N*-propyl, or *N*-butyl causes a progressive loss of activity for amphetamine in behavioral assays.¹⁷⁰ These *N*-alkylations in the presence of a 4-methyl substituent at the phenyl ring (the impact of which is

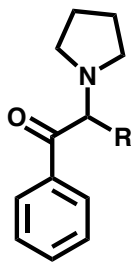
described later in this section) were examined in greater detail at the individual MATs using uptake and release assays in rat brain synaptosomes, voltage-clamp measurements, and the calcium flux assay described above, as well as ICSS *in vivo*.¹⁴⁹ All analogs were active as inhibitors of substrate transport at all MATs, and as substrates at SERT. *N*-ethyl- and *N*-methyl-4-methylamphetamine were also substrates at NET, and *N*-methyl-4-methylamphetamine was also a substrate at DAT. The extension of the *N*-alkyl substituent caused a decrease in reuptake inhibition potency, and appeared to cause a progressive loss of substrate activity, with DAT, followed by NET, most sensitive to these effects. This activity was also associated with a decrease in abuse-related effects in ICSS.¹⁴⁹

The α -carbon atom is a chiral center in most ATS. For the strict psychostimulants amphetamine (**9**), cathinone (**15**), and MCAT (5a), the *S* isomer (*S*(+) in amphetamines, but *S*(-) in cathinones) is typically more potent by 2- to 5-fold in behavioral studies including drug discrimination and locomotor activity.^{60,171} An important caveat is the α -pyrrolidinophenones, in which the *R* isomer is dramatically less active or inactive.¹⁷² For MDA (**23**), the two isomers are not only different in potency, but also different in mechanism of action and pharmacological effect. Glennon and Young determined, utilizing an innovative 3-lever drug discrimination paradigm in which rats were trained to discriminate between the isomers and vehicle, that the *S*-isomer was largely responsible for MDA stimulant effects, whereas the *R*-isomer was responsible for hallucinogenic effects.⁹⁹

Extension of the alkyl substituent at the α -carbon atom for the pyrrolidinophenones results, rather than in a loss of reuptake inhibition potency as observed for 4-methylamphetamine *N*-alkyl extension, in an increase in potency up to at least a five-carbon substituent length (i.e., PV-8, Table 6).²⁵ Several studies have confirmed the same trends, with α -carbon alkyl chain

length increasing potency at DAT, NET, and even SERT, where the pyrrolidinophenones are relatively much less potent (Table 5).^{15,25,173} In these studies, we progress in our investigation of whether the α -substituent extension will increase potency for other ATS scaffolds, such as 4-methylmethamphetamine (4-MMA). For pyrrolidinophenones with extended α -carbon alkyl chains, stereochemical effects are also much more dramatic. Rather than the 2- to 5-fold decrease in potency observed for cathinone and amphetamine, the difference is closer to two orders of magnitude for reuptake inhibition potency at DAT and NET.¹⁷² These studies also seek to investigate the nature of that selectivity.

Table 6. Potency of α -alkyl chain-extended α -pyrrolidinophenones as inhibitors of [3 H]neurotransmitter uptake at MATs.



11, 29, 70-72

Compound	R	IC ₅₀ , nM			Reference
		DAT	NET	SERT	
α -PPP (70)	-CH ₃	196.7	444.7	>10000	^a Marusich et al. 2014 ¹⁵
		540	305	188000	^b Eshleman et al. 2017 ¹⁷³
α -PBP (71)	-CH ₂ CH ₃	63.3	91.5	>10000	^a Marusich et al. 2014 ¹⁵
		78	143	67000	^b Eshleman et al. 2017 ¹⁷³
α -PVP (11)	-(CH ₂) ₂ CH ₃	12.8	14.2	>10000	^a Marusich et al. 2014 ¹⁵
		17.5	ND	>10000	^a Kolanos et al. 2015 ²⁵
		19.7	46	57000	^b Eshleman et al. 2017 ¹⁷³
α -PHP (29)	-(CH ₂) ₃ CH ₃	11.6	ND	>10000	^a Kolanos et al. 2015 ²⁵
		21.6	36.3	40000	^b Eshleman et al. 2017 ¹⁷³
PV-8 (72)	-(CH ₂) ₄ CH ₃	14.5	55.2	26800	^b Eshleman et al. 2017 ¹⁷³

^aData were obtained in the same laboratory under the same or similar conditions in rat brain synaptosomes; ^bData were obtained using HEK-293 cells.

The carbonyl oxygen atom of the cathinones appears to be of more importance for the pyrrolidinophenones as DAT reuptake inhibitors than for the smaller releasing agents (i.e., MCAT) Though MCAT is similar in potency to its *des*-keto counterpart methamphetamine, the *des*-keto analog of MDPV generated in deconstruction studies was 10-fold less potent as a reuptake inhibitor at DAT.¹⁷⁴

Introductions of oxygen atoms via other sp³-hybridized carbon-oxygen bonds may result in active compounds that are clinically useful (i.e., aminorex). In ephedrine (**12**), its isomers, and norephedrine (**14**) and its isomers, the β-carbon substituent is an alcohol, conferring a 10-fold degree of selectivity for noradrenergic releasing potency, as described above (Table 2). but little is known about their SAR. The addition of the sp³-hybridized atom also creates a second stereocenter, which complicates the SAR.

Aryl substitution confers a range of new mechanisms of action and subjective effects to ATS, as in the example of MDA (**23**) and MDMA (**3**) above. Patterns of aryl substitution on amphetamine (**9**) have been established to confer hallucinogenic activity via 5-HT_{2A} receptor agonism. Specifically, 2,5-dimethoxy, 4-substitution, or 3,5-dimethoxy, 4-substitution, often gives rise to these effects. 3,4-dimethoxy substitution produces hallucinogenic or empathogenic effects, as in MDA (**23**) and MDMA (**3**). 4-substituted amphetamines and cathinones may remain strictly psychostimulants, or gain other activity via other targets, depending on context.

In the late 1960s, some early SAR studies investigated the effects of aryl substitution on amphetamine. Observing that amphetamine use sometimes triggered psychotic states, and that ATS with methoxy substitutions to the aryl ring caused hallucinations,¹⁷⁵ they sought to elucidate the connection between the two. Today, the psychosis sometimes elicited by ATS use is called stimulant-induced psychotic disorder (ICD-11),¹⁷⁶ and is thought to arise via a distinct

mechanism (i.e., DA, glutamate, and GABA) from that of classical hallucinogens (i.e., 5-HT_{2A} receptor agonism).^{38,177} These mechanisms were unknown in 1967, when Smythies and coworkers developed their aryl-substituted amphetamine SAR using a novel behavioral test in rats that was predictive of psychotomimetic activity in humans.¹⁷⁸ In a series of mono, di, and tri-methoxy substituted amphetamine analogs, the para-methoxy analog was the most potent in the behavioral assay for hallucinogenic effects.¹⁷⁹ Following up on this work, Smythies joined Beaton and coworkers to test additional groups at the 4-position, including methyl, fluoro, and chloro. The assay allowed for the observation of a hallucinogenic profile for 4-methoxy-amphetamine, and a high- and low-dose stimulant profile for the other three compounds. 4-methyl-amphetamine was the least potent as a stimulant, and showed no signs of hallucinogenic activity. This led the team to conclude that, though they had previously observed the hallucinogenic effects of 2,5-dimethoxy-4-methylamphetamine (i.e. DOM), the 4-methyl group alone could not confer hallucinogenic activity as a 4-methoxy group could.¹⁸⁰

Decades later, in 1990, following reports of abuse of ring-methylated amphetamines, Higgs and Glennon undertook an SAR study of 2-, 3-, and 4-methylamphetamine.⁸¹ Discriminative stimulus effects in rats with respect to (+)-amphetamine were assessed at various doses. Only 2-methylamphetamine substituted fully for (+)-amphetamine, and it was less potent by an order of magnitude ($ED_{50} = 4.1$ mg/kg, $ED_{50} = 0.42$ mg/kg, respectively).⁸¹ 3- and 4-methylamphetamine only partially substituted for (+)-amphetamine, and produced disruption of behavior in the subjects.⁸¹ Higgs and Glennon concluded that the aryl-methylated amphetamines were less potent as stimulants, and that drug discrimination with amphetamine was not the best way to assess their pharmacology.⁸¹ Thus, SAR studies led to the differentiation between structural features of ATS giving rise to psychostimulant effects and those giving rise to

hallucinogenic effects, facilitating efficient development of ATS agents to treat neuropsychiatric disorders (i.e., bupropion, **20**).

Bupropion is an aryl-substituted (3-chloro) clinically available cathinone analog, and provides a basis for investigation of aryl substitution effects of the cathinone scaffold, particularly in the context of *N*-substitution with a *tert*-butyl group (Figure 15). In a deconstruction study by Shalabi et al.,¹⁴⁶ the *N*-methyl (i.e., **22**) and primary amine (i.e., **23**) counterparts to bupropion were synthesized and evaluated. They retained potency at DAT, but lost selectivity, gaining reuptake inhibition and releasing activity at all three transporters (Table 7). Comparing the *N*-methyl bupropion analog (**22**) to its *des*-chloro counterpart MCAT suggests that 3-chloro substitution may slightly reduce potency at DAT and NET (approximately 2-fold), but substantially increase SERT potency (10 to 20-fold). Together, these observations suggest that aryl modification is highly context-dependent, varying on the basis of other structural modifications present in the molecule. Systematic SAR studies are needed to draw conclusive assessments of aryl-substitution effects.

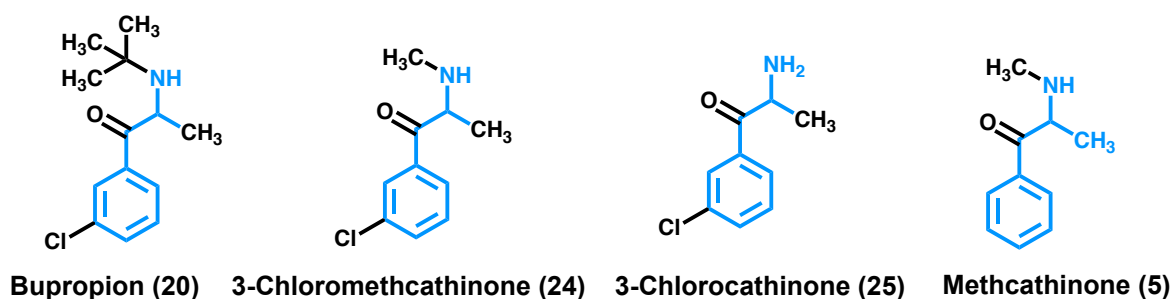


Figure 15. Bupropion, its analogs, and MCAT for comparison.

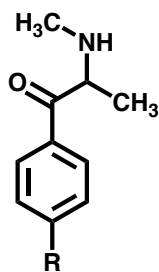
Table 7. Potency to release or inhibit uptake of [³H]neurotransmitter in rat brain synaptosomes.

Compound	Uptake Inhibition			Release			Reference
	IC ₅₀ , nM			EC ₅₀ , nM			
	DAT	NET	SERT	DAT	NET	SERT	
Bupropion (20)	305	3715	>10000	Inactive	Inactive	Inactive	^a Shalabi 2017 ¹⁴⁶
22	342	290	1104	29	40	212	^a Shalabi 2017 ¹⁴⁶
23	399	551	2779	64	105	567	^a Shalabi 2017 ¹⁴⁶
MCAT (5a)				12.5	22	3860	^{a,b} Bonano 2015 ⁶⁸ ^{a,c} Shalabi 2019 ¹⁸¹

^aThese data were obtained in the same laboratory under the same or similar conditions; ^bOriginal publication of DAT and SERT data for MCAT (5a); ^cOriginal publication of NET data for **5**

Systematic studies of 2-,3-, and 4-substituted MCAT analogs have since been conducted by our laboratory.¹⁸¹ A wide range of substituents are tolerated, but variation in substituent identity shifts potency and selectivity between MATs. For the 4-substituted compounds, DAT/SERT selectivity was found to correlate strongly with abuse-related effects.⁶⁸ Selectivity and abuse-related effects correlated additionally with steric bulk of the substituent.⁶⁸ This structural feature was further dissected via quantitative structure activity relationship studies to show that maximum width and volume of the substituent were the controlling features of the relationship between pharmacology and steric bulk.⁶⁹

Table 8. Potency of *para*-substituted MCAT analogs to release [³H]Neurotransmitter from rat brain synaptosomes. Reproduced from Bonano et al. 2015,⁶⁸ and Shalabi et al. 2019.¹⁸¹



R	EC ₅₀		
	DAT	NET	SERT
H (5a)	13	22 ± 4	3860
MeO (5b)	506	111 ± 24	120
F (5c)	83	62 ± 10	1290
Cl (5d)	42	44 ± 9	144
Br (5e)	59	100 ± 16	60
CH ₃ (5f)	49	63 ± 17	118
CF ₃ (5g)	2700	900 ± 300	190

Parallel series of 2- and 3-substituted MCATs were similarly evaluated. These investigations revealed a robust correlation between DAT and NET potency. The 2-substituted compounds were the least potent, whereas the 3-substituted analogs were found to be similar in potency to their 4-substituted counterparts.¹⁸¹

For α -pyrrolidinophenones, little is known about aryl substitution. The 3,4-methylenedioxy group of MDPV appears to confer the small degree of SERT activity present is

that compound. The 4-methyl substituted pyrovalerone remains active as a psychostimulant, as described above (pyrovalerone, **22**).

III. Specific Aims

The goal of these works is to progress the establishment of comprehensive SAR for synthetic cathinones and related agents (i.e., certain ATS), a distinct aspect of the drug abuse problem which will require further scientific understanding in order to most effectively respond. Currently, these compounds represent a unique threat within the drug problem landscape. Mixed, synergistic mechanisms,⁸⁹ in concert with substance novelty, give rise to unpredicted adverse effects including agitation, tachycardia, psychosis, addiction, and multi-organ failure.⁷ The original “bath salts” components were added to Schedule I in the United States and many other countries, but this only drove the clandestine development of a second generation of agents,^{9,10,90} resulting in an array of new synthetic cathinones diverse in structure and effect.^{10,14,91,92}

Despite their toxicity, no antidote for synthetic cathinone poisoning exists. Additionally, no pharmacotherapy for addiction to cathinones or any central stimulant is currently FDA-approved. SAR studies of cathinones might be useful in developing such treatments. Some synthetic cathinones also have clinical utility in the treatment of various psychiatric disorders. For example, bupropion (Wellbutrin®, Figure 2), which might be considered as a synthetic cathinone, is an FDA-approved antidepressant. Our laboratory has previously investigated its mechanism of action,^{146,181} prepared bupropion metabolites¹⁸² and analogs,¹⁴⁶ and investigated their mechanism of action.^{146,182} In summary, some effects of phenylalkylamines are clinically useful or promising for the treatment of psychiatric and neurological disorders, whereas others confer potential for abuse, though considerable overlap exists between these two outcomes. Thus, SAR studies of synthetic cathinones are critical for distinguishing between: 1) feasible pathways for pharmaceutical development, and 2) scaffolds, pharmacophores, and lead compounds of likely high abuse potential.

In these investigations, our goal is to progress towards the establishment of comprehensive SAR for synthetic cathinones and related agents, utilizing design, synthesis, pharmacological evaluation, and molecular modeling, aimed at elucidating particular structural features. Particular emphasis in the present studies will be placed on the role of the α -carbon atom, its substituents, and other structural modifications in the context of α -carbon atom changes. Thus, the specific aims of the following work are as follows.

Aim 1: To elucidate the role of stereochemistry of the MCAT α -carbon atom.

The α -carbon atom is a chiral center for most synthetic cathinones, as is the case for MCAT (**5**; Figure 16). In these studies, we will attempt to further elucidate MCAT stereochemistry in terms of pharmacology at the monoamine transporters, and eventually abuse-related effects as measured by ICSS. The latter goal, however, is not a specific aim of this dissertation. Though racemic MCAT ((\pm)**5a**) is the prototypical synthetic cathinone, its two isomers (*S*(-)**5a**, *R*(+)**5a**) have never been directly compared in terms of activity at MATs or behavioral reward magnitude. Therefore, we seek in the first component of this aim to pharmacologically evaluate the optical isomers of **5a**. We aim to evaluate efficacy and potency of these isomers at hDAT and hSERT using a calcium flux assay described above. In the second portion of this aim, we seek to determine the feasibility of removing the MCAT chiral center. It is known that the β -carbonyl oxygen atom can be replaced with an alcohol, but this results in two stereocenters (i.e., ephedrine, norephedrine, and their isomers **12-15**). We have also found that the carbonyl oxygen atom of MCAT can be replaced with a methoxy group (unpublished data). But, this results in a diastereoisomeric mixture of four isomers. That is, both the α - and β -carbon atom are now optically active. In order to progress further in synthetic cathinone SAR at the β -

position, it would be preferable to remove the α -carbon chiral center in a manner that results in only a single chiral center if the β -keto group becomes a chiral center. This can be accomplished a) by adding a second methyl group (i.e., **26**), or b) by eliminating the α -methyl group (i.e., **27**). We will synthesize **26** and **27** and evaluate them along with the MCAT optical isomers (+)**5** and (-)**5**, and the MCAT racemate (\pm)**5**.

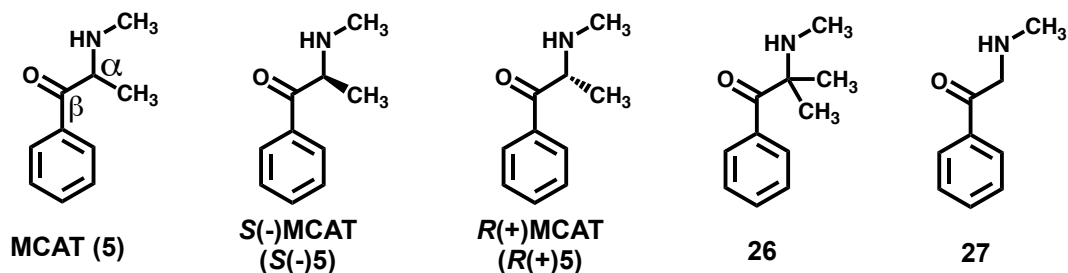


Figure 16. Methcathinone, its isomers, and proposed achiral analogs.

The *hypothesis* here is that because there is little difference in the potency of methcathinone analogs in behavioral studies,^{60,183} there will be little difference in their potencies for DAT release. Consequently, S(+)**5** and R(-)**5** should not differ much in this regard.

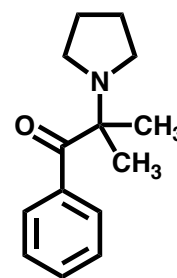
Removal of the α -methyl group of cathinone or amphetamine generally results in decreased potency in behavioral assays.^{24,171,184,185} This is likely the result of decreased blood-brain barrier permeability (due to decreased lipophilicity) or to decreased potency at the dopamine transporter. Two α -*des*-methyl ATS have been investigated in vitro using rat brain synaptosome-based assays to detect DA releasing activity: the *N-des*-methyl counterpart of **27** (i.e., α -*des*-methylcathinone), and β -phenylethylamine (i.e., α -*des*-methylamphetamine, or PEA). Both were less potent than their respective α -methyl parent compounds by 3- and 4-fold, respectively.^{186,187} Those findings suggest that α -*des*-methylation decreases potency at MATs, rather than simply on the basis of decreased lipophilicity and corresponding blood-brain barrier permeability. These studies will further test that finding by applying the same concept to MCAT.

Aim 2: To establish the SAR of α -pyrrolidinophenones at DAT.

2.1: To assess the nature of stereoselectivity observed for α -pyrrolidinophenones by synthesizing and evaluating an achiral α -pyrrolidinophenone analog.

Our laboratory has shown a higher degree of stereoselectivity for MDPV than for most synthetic cathinone substrates.¹⁷² The nature of this stereoselectivity is not well understood. To determine the nature of α -pyrrolidinophenone stereoselectivity, we propose to synthesize and evaluate an achiral analog of α -PPP (**28**, Figure 17). As it is expected to be a blocker rather than a substrate, it will be evaluated using the calcium flux assay described previously,¹⁵⁰ but with a modified protocol to evaluate blocker activity (vide infra, VI.D.2.).

The actions of MDPV (**21**) are nearly stereospecific.¹⁷² The *S*-isomer is nearly 200-fold more potent than its enantiomer as an hDAT reuptake inhibitor.¹⁷² Hence, the α -gem-dimethyl counterpart of simplified α -pyrrolidinophenone α -PPP (**70**), that is, **28**, might be expected to be substantially less potent than **70** at hDAT as a reuptake inhibitor.



28

Figure 17. An achiral α -PPP analog.

2.2: To establish QSAR for aryl-substituted α -pyrrolidinophenones, and determine similarity with MCAT activity via parallel SAR.

Aryl substitution modulates activity of MCAT at DAT and SERT, and correlations with QSAR parameters have been established for MCAT analogs.^{68,69} Little is known about the effects of aryl substitution on α -pyrrolidinophenones. α -PHP is among the most potent of the α -pyrrolidinophenones, and is a known drug of abuse of the second generation of synthetic

cathinone “bath salts.”^{17,25} Its SAR has, hitherto, never been investigated. In these studies, we address the lack of α -pyrrolidinophenone SAR information, conducting a systematic investigation of aryl substitution to the α -pyrrolidinone 4-position, as performed for the MCAT series.

We propose to synthesize a series of *para*-substituted α -PHP analogs (Figure 18) that are systematically designed to evaluate contributions of physicochemical QSAR parameters to activity upon evaluation. Each analog has a different substituent at the 4-position of the phenyl ring, and each substituent varies in size, shape, lipophilicity, and electron-withdrawing character. *para*-Substituted analogs were selected, as opposed to *ortho*- or *meta*-substituted analogs, to avoid problems with rotameric binding. To evaluate this series, we will utilize a cell-based epifluorescence assay that will test the ability of each compound to block uptake of the fluorescent DAT substrate APP⁺. Considering the established blocking mechanism of action of the pyrrolidinophenone class of synthetic cathinones, it is of interest to determine whether these compounds act in a similar manner to substrates. Though cocaine and its analog RTI-55 have been co-crystallized with dDAT (PDB ID 4XP4 and 4XP5, respectively),¹¹¹ no synthetic cathinone or other ATS MAT blocker has been co-crystallized. Little is known about the mechanism of binding for α -pyrrolidinophenones. Having previously synthesized and functionally examined a parallel series of MCAT analogs,^{68,69} we might be able to compare the two series to ascertain similarity using Portoghese’s parallel SAR concept.¹⁸⁸ In other words, do releasing agents and reuptake inhibitors bind at the same transporter site?

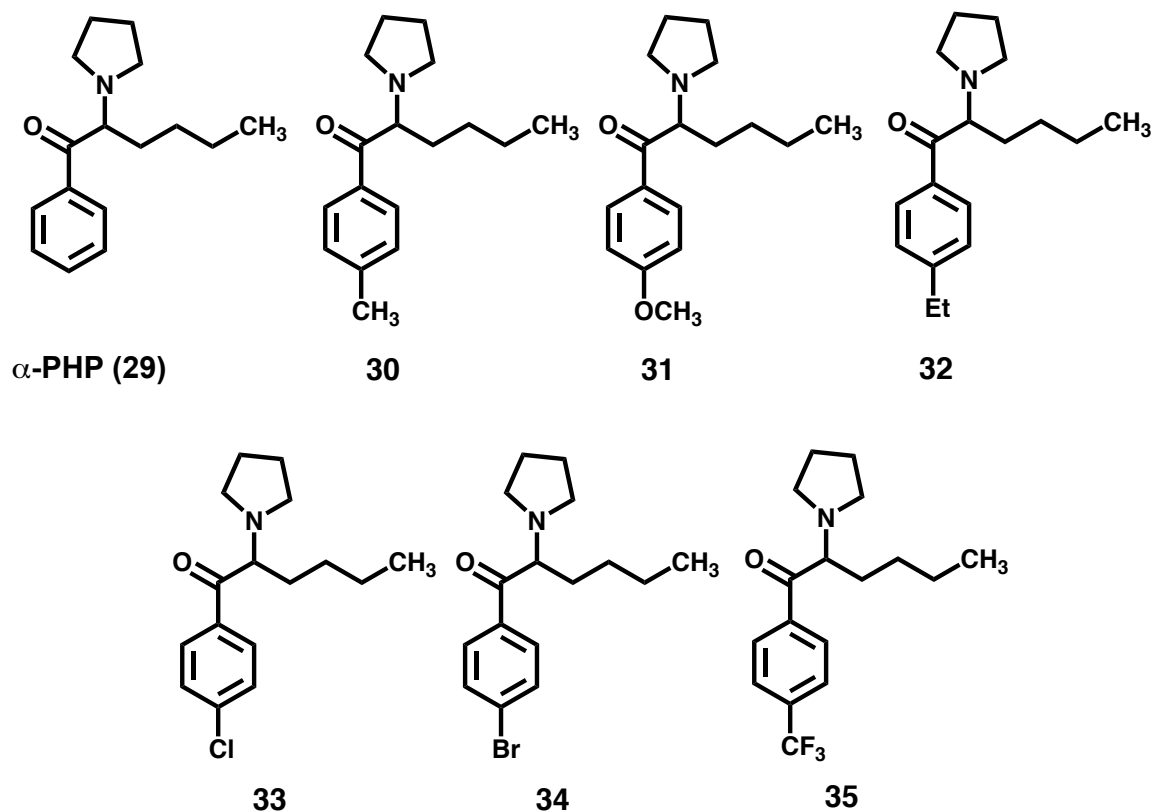


Figure 18. α -PHP and *para*-substituted analogs proposed in Aim 2.2.

Aim 3: To synthesize analogs to progress the SAR of synthetic cathinone-related amphetamines at the α -carbon atom.

3.1 To synthesize analogs for the investigation of the impact of α -carbon alkyl chain extension on 4-methylamphetamines.

Synthetic cathinones are closely related to ATS, differing only in the presence or absence of a β -keto group, respectively. Ring-methylated amphetamines have seen some abuse as NPS in previous decades,⁸¹ and 4-methylmethamphetamine (4-MMA) in particular has emerged in recent years as part of the newest wave of ATS NPS with which synthetic cathinones are

associated.¹⁸⁹ Earlier SAR studies had not conclusively determined the basis for aryl-methylated amphetamine analog abuse potential.^{81,179} More recent studies in our laboratory have examined a

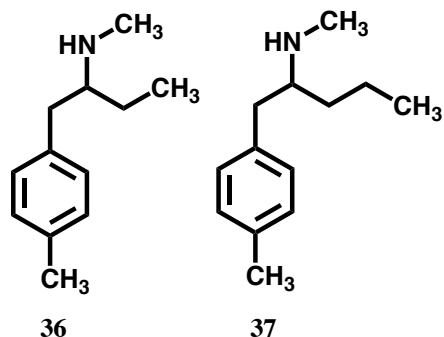


Figure 19. Synthetic targets of Aim 3.1: 4-MMA analogs.

methylamphetamines (4-MAs) is unknown.

The hypothesis for this study is that, for 4-methylamphetamines, alkyl chain extension at the α -carbon atom will reduce substrate activity, as it did for N-alkyl chain extension. Rather than reducing potency with further chain extension, however, it might increase blocker potency, as observed in the pyrrolidinophenone series.²⁵ We propose to prepare two α -alkyl extended analogs of 4-MMA (Figure 19) for future comparison with 4-MMA in pharmacological effect.

3.2 Stereoselective synthesis of *N*-ethylamphetamine for evaluation of ATS stereochemistry on DAT/NET/SERT selectivity.

Currently, few substrates with high selectivity between transporters exist, and while we have learned a great deal about the relative importance of DAT and SERT to abuse potential, the contribution of NET is still unknown. The relative contribution of NET to abuse-related effects in ICSS has yet to be determined. Currently, the most selective noradrenergic releasing agents in ICSS has yet to be determined. Currently, the most selective noradrenergic releasing agents are no more than 10-fold selective for NE as opposed to DA release.⁶⁷ SAR studies suggest the

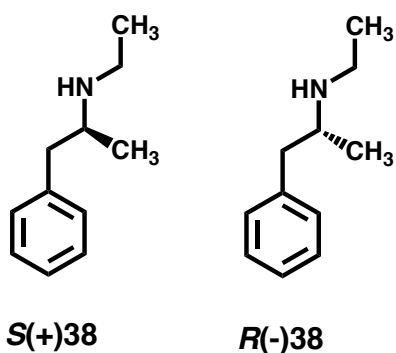


Figure 20. Synthetic targets of Aim 3.2: *N*-Ethylamphetamine optical isomers.

behavioral effects. For this study, the *R*-isomer of *N*-ethylamphetamine will be synthesized stereoselectively, along with its *S*-isomer for comparison (Figure 20).

Aim 4: To construct homology models of NET and use them to gain insight into MAT substrate selectivity.

hNET is also the only one of the three MATs for which a crystal structure is currently unavailable. As such, this study aims to prepare a population of hNET models and conduct docking studies using the endogenous transporters, as well as novel synthetic cathinones. Previously in our laboratory, homology models of hDAT and hSERT were constructed using the crystal structure of dDAT co-crystallized with nortriptyline.²⁵

following: *R-N*-ethyl-4-methyl-amphetamine is a more potent releaser at NET than at DAT, but is also a releaser at SERT,¹⁹⁰ removal of the 4-methyl in MCAT analogs decreases SERT activity.^{68,69} It is of interest to determine the relative MAT releasing activity of *R-N*-ethylamphetamine, with the hypothesis that it might be a

selective NET releaser. Such a compound would be of use for the investigation of NET effects in abuse-related

IV. Results and Discussion

A. Aim 1: To elucidate the role of stereochemistry of the MCAT α -carbon atom.

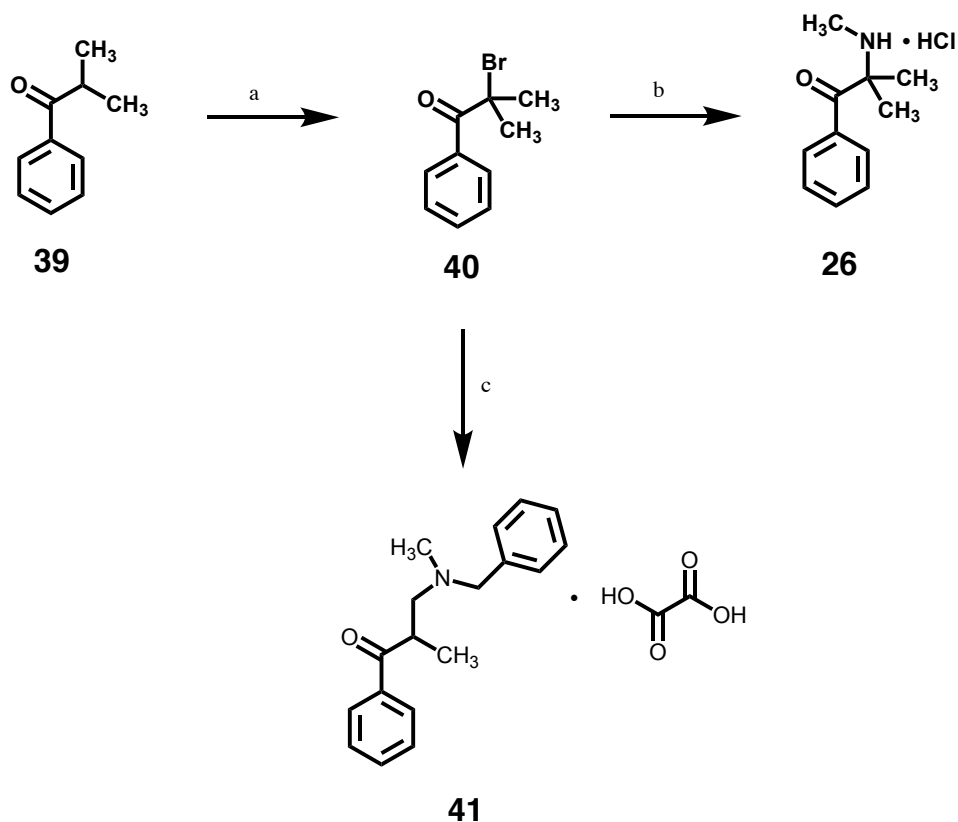
These studies involved the synthesis where necessary (MCAT isomers were already on hand as their HCl salts), pharmacological evaluation, and molecular modeling of (\pm)**5a**, *S*(-)**5a**, *R*(+)**5a** and achiral analogs **26** and **27** (Figure 16). The following section details the findings of this investigation.

1. Synthesis

Compounds (\pm)**5a**, *S*(-)**5a**, and *R*(+)**5a** were available as their HCl salts following previous investigations in the Glennon laboratory.^{60,183} Though **26** is a known compound in the literature, it was synthesized for the first time in our group in the course of these investigations. Compound **27** had been previously synthesized by F. Sakloth (unpublished data), a prior student in the Glennon laboratory, but was synthesized *de novo* for these investigations.

Retrosynthetic analysis of **26** resulted in a simple scheme in which the desired product would be synthesized from α -bromoisobutyrophenone (**40**), which would in turn be synthesized from isobutyrophenone (**39**), which was readily commercially available. Such methods had been

Scheme 1.^a Synthesis of Compounds **26** and **41**.



^aReagents and conditions: (a) Br_2 , CHCl_3 , 24 h, rt; (b) 1. K_2CO_3 , MeOH , 3 h, rt; 2. MeNH_2 (g), 14 h, 70°C ; (c) HCl , $\text{EtOH}/\text{Et}_2\text{O}$

used many times to success in our laboratory in the production of similar compounds. Indeed, α -bromoisobutyrophenone (**40**) was synthesized in quantitative yield from **38** using liquid bromine (Scheme 1). The procedure for bromination was adapted from one published by Layer and MacGregor, using chloroform as the solvent rather than the markedly more carcinogenic carbon tetrachloride of the published synthesis.¹⁹¹

In an attempt to utilize the adapted procedure of Blough et al. that had been used with success by another student in the laboratory (A. Shalabi) for similar compound,¹⁹² the synthesis of **26** from **40** was attempted by the substitution of *N*-benzylmethylamine for the α -bromine atom. Had the reaction been successful, it was to be followed with debenylation to afford **26**, the target compound. However, analysis of the product (i.e., **41**) revealed that *N*-benzylmethylamine had substituted for a hydrogen atom at what had been a terminal CH₃ on the isobutyrophenone substrate. This was surprising, as the pattern of substitution was not observed for analogous syntheses using substrates lacking a *gem*-dimethyl moiety (e.g., propiophenone). Consideration of **41** and the unique structural features of substrate **40** led to the proposal of a mechanism for the observed transformation (Figure 21). It is possible that the phenyl ring of **40** allows for elimination via anchimeric assistance, with the pi system donating into the antibonding orbital of the carbon-bromine bond. The tertiary carbocation would be more stable as compared to a secondary carbocation, explaining why this mechanism does not predominate in other analogous syntheses in our laboratory using non-geminal starting materials. The resulting α,β -unsaturated carbonyl intermediate **44** would serve as a Michael addition donor, allowing for the formation of observed product **41**.

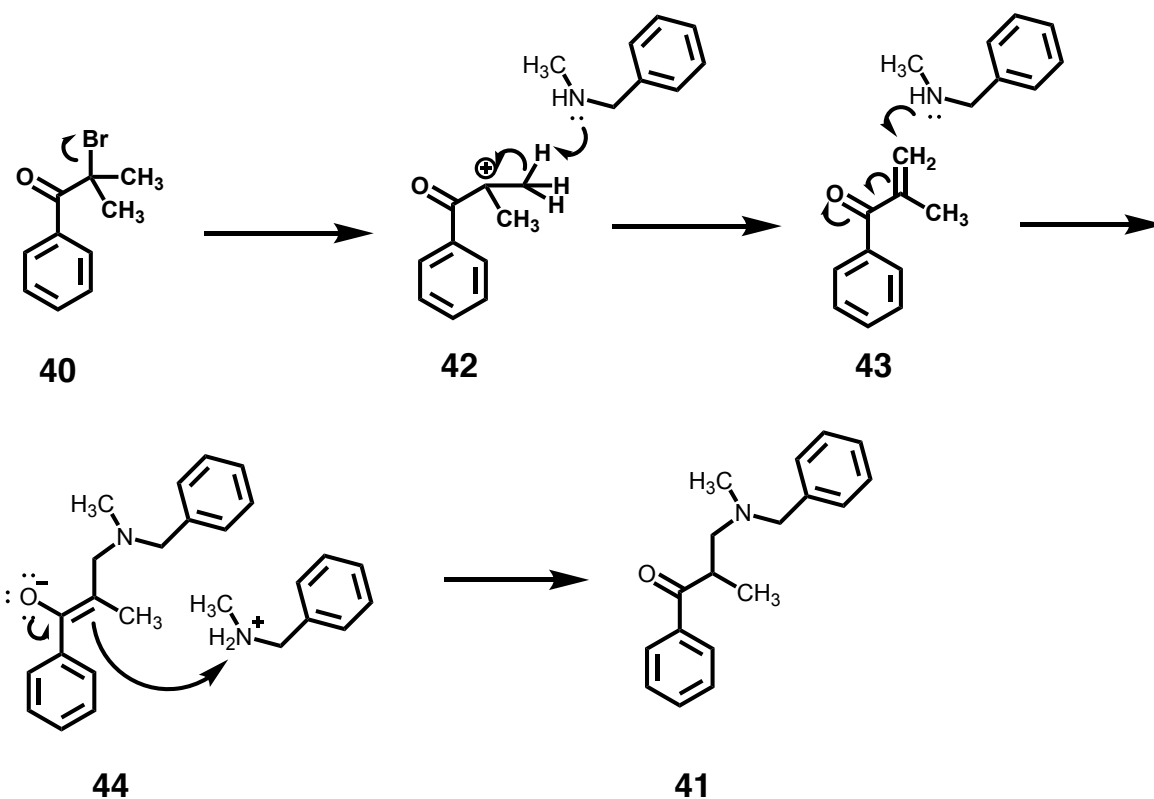


Figure 21. A potential mechanism via Michael addition for the transformation of **40** to **41**.

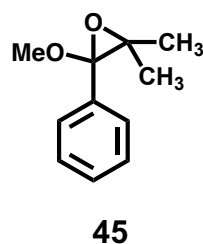
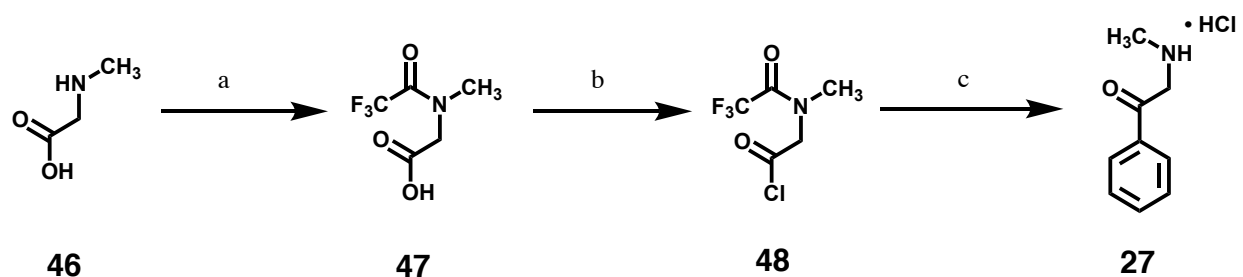


Figure 22. Epoxy intermediate **45**.

A literature search was conducted for alternative methods, leading to a 2008 patent from Perboni and Giubellina¹⁹³ on an “improved process of amide formation.” Within the patent was a specific route to α -aminoisobutyrophenones from α -bromoisobutyrophenones (i.e., **26** and **40**, respectively), which seemed perfectly suited to these investigations. In their method, the α -bromo intermediate was stirred with potassium carbonate and methanol for 3 hours, by which time it had formed a stable intermediate thought to be the epoxy compound by NMR analysis (i.e., **45**, Figure 22). Only after this intermediate formed was the amine added, resulting in the final compound.¹⁹³ The Perboni and Giubellina¹⁹³ procedure was used with success to afford the free base of target compound **26**, which was converted to its HCl salt.

Compound **27** was prepared by the same method recorded by Sakloth (Scheme 2, unpublished data). In this approach, a protected amine acid chloride **48** was prepared for Friedel-Crafts acylation of benzene by first protecting sarcosine (**46**) with TFAA, then converting it from the acid **47** to the acid chloride **48**. The Friedel-Crafts reaction was performed neat in great excess of benzene, and the amine was deprotected by stirring in HCl and *i*-PrOH to afford the HCl salt directly.

Scheme 2.^a Synthesis of Compound **27**.



^aReagents and conditions: (a) $\text{CF}_3\text{COOCOCF}_3$, CH_2Cl_2 , rt, 2 h; (b) ClCO_2 , benzene, pyridine, reflux, 1 h; (c) 1. Benzene, AlCl_3 , reflux, 4 h; 2. Conc. HCl, *i*-PrOH, 40 °C, 48 h.

2. Pharmacology

In the first known evaluation of MCAT isomers at the MATs, compounds were examined pharmacologically using a novel epifluorescence microscopy technique that utilized calcium as a biosensor for substrate activity.¹⁵⁰ Each agent was examined at multiple concentrations, allowing for the construction of concentration-response curves (Figure 23A). The achiral analogs were examined using the same technique, in the same series of experiments. Their dose-response curves are shown in Figure 23B.

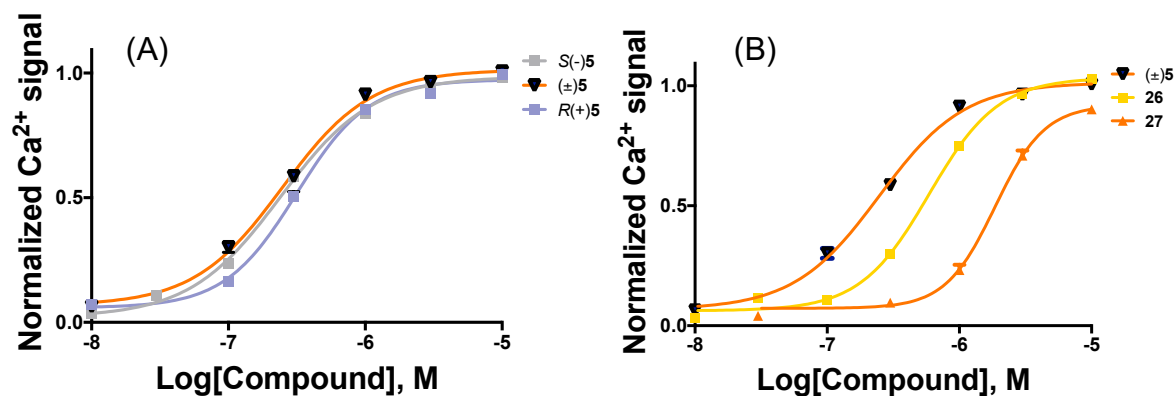


Figure 23. Dose-response curves for: (A) MCAT racemate and optical isomers; (B) MCAT racemate and MCAT achiral analogs **26** and **27**.

All agents were active as substrates at hDAT (Table 9). The *S*(-) isomer of MCAT (*S*(-)**5**) was significantly more potent than its *R*(+) enantiomer *R*(+)**5** at hDAT, but only by a small amount (i.e., approximately 1.3-fold). The racemate was not significantly less potent than the *S*(-) isomer.

Table 9. Potency of MCAT isomers and achiral analogs as substrates of hDAT in a calcium flux assay.

Species	hDAT EC ₅₀ , nM (± SEM)
<i>S</i> (-)MCAT (<i>S</i> (-) 5a)	240 ± 11 nM
<i>R</i> (+)MCAT (<i>R</i> (+) 5a)	315 ± 14 nM
(±)MCAT ((±) 5a)	248 ± 15 nM
α - <i>gem</i> -Dimethyl-MCAT (26)	590 ± 19 nM
α - <i>des</i> -Methyl-MCAT (27)	1860 ± 90 nM

In the case of the achiral MCAT analogs compounds **26** and **27**, removal of the chiral center resulted in a loss of potency, but both modifications were tolerated. The *gem*-dimethyl compound **26** was only approximately 2-fold less potent than the more potent isomer or the racemate, while the des-methyl analog **27** was approximately 8-fold less potent.

Similar experiments were conducted for the same set of compounds at hSERT by V. Nguyen, a student in the Eltit laboratory (Table 10). The *S*(-) isomer of MCAT *S*(-)**5**, but not *R*(+)**5**, was active as a substrate, with an EC₅₀ value of 15300 ± 1439 nM. The difference in potency for *S*(-)**5** between hSERT and hDAT was approximately 64-fold. The racemate (±)MCAT ((±)**5**) had an even greater preference for hDAT over hSERT (100-fold), whereas *R*(+)**5** was completely inactive at hSERT, making it selective as a substrate for hDAT over hSERT, without sacrificing much potency at hDAT as compared to its enantiomer (Table 9). For hSERT, removal of the chiral center was only tolerated by way of the *gem*-dimethyl modification (**26**), whereas the *α*-des-methyl analog (**27**) was inactive. With an hDAT/hSERT potency ratio of 22, **26** is the least selective of this series between the two transporters.

Table 10. Potency of MCAT isomers and achiral analogs as substrates of hSERT, and their selectivity for hDAT, in a calcium flux assay.

Compound	hSERT EC ₅₀ , nM(± SEM)	hDAT Selectivity ^a
<i>S</i> (-)MCAT (<i>S</i> (-)5a)	15300 ± 1439 nM ^b	64
<i>R</i> (+)MCAT (<i>R</i> (+)5a)	Inactive ^c	<i>DAT Selective</i>
(±)MCAT ((±)5a)	24750 ± 5745 nM	100
α- <i>gem</i> -Dimethyl-MCAT (26)	12860 ± 1270 nM	22
α- <i>des</i> -Methyl-MCAT (27)	Inactive ^d	<i>DAT Selective</i>

^aSelectivity was calculated as hDAT EC₅₀ ÷ hSERT EC₅₀; ^bHill slope for linear regression constrained to 2.0; ^ctested at concentrations up to 50000 nM; ^dtested at concentrations up to 60000 nM

The small difference between the isomers at hDAT, and the comparably considerable difference between the isomers at hSERT resulting in a corresponding difference in hDAT/hSERT selectivity, are of interest in light of previous behavioral studies. Previous investigations in our laboratory found that *S*(-)5a is more potent than *R*(+)5a in its ability to stimulate locomotor activity in mice (i.e. ED₅₀ = 0.5 mg/kg, 3.0 mg/kg, respectively).⁶⁰ Additionally, *S*(-)5a was more potent than *R*(+)5a in its discriminative stimulus potency (approximately 4-fold). We hypothesized that these differences would correspond to differences in potency, and found a small difference in potency at hDAT between the individual MCAT isomers (1.3-fold for *S*(-)5a as compared to *R*(+)5a). While the behavioral effects of synthetic cathinones are traditionally associated with activity at hDAT, increasing evidence suggests that hDAT/hSERT selectivity is an important variable in abuse liability of such compounds,⁶⁸ and that this selectivity emerges in the inspection of individual cathinone isomers.¹⁵² A greater difference between MCAT isomers was observed at hSERT, as *R*(+)5 was inactive at

concentrations over 3-fold higher than the EC⁵⁰ for *S*(-)**5**. Thus, the differences between isomers of MCAT in behavioral studies are possibly due to differences in hSERT potency, or in hDAT/hSERT selectivity. Future studies will include the investigation of abuse-related effects in ICSS, in which the more hDAT selective compounds are expected to show a greater degree of ICSS facilitation.

In the case of the achiral analogs **26** and **27**, both being active, this validates the concept of chiral center removal for future SAR studies. Based on these results, either approach might be useful for further SAR studies at hDAT. For hSERT, only **26** could be used. Previous studies have found that *α-des*-methyl cathinones are generally less potent in behavioral assays, and one study in vitro found similar results.¹⁸⁷ One goal of this aim was to further test whether actions at MATs contribute to the reduced potency of similar *des*-methyl cathinones. As **27** is 10-fold less potent at hDAT, and inactive at hSERT at concentrations of approximately 4-fold higher than the EC₅₀ for *S*(-)**5**, direct action at the MATs seems to be important. These studies are particularly strong in their support of direct action at MATs, as they were conducted in HEK-293 cells expressing the MATs without any of the other known ATS targets (e.g. VMAT1) endogenously expressed by animals in behavioral studies or in synaptosome-based assays.

3. Modeling

The four agents were docked to homology models of MATs to inform our results. Models of hDAT and hSERT were previously available in our laboratory.⁶⁹ The hNET models were generated in these investigations (*vide infra*). Common binding modes were identified for all compounds and were similar between transporters (Figure 24). For both hDAT and hNET, two similar binding modes were identified. In the first (hDAT-1 and hNET-1), the carbonyl oxygen

was oriented trans to the predicted basic nitrogen/aspartate interaction. An analogous binding mode for the compounds was found in hSERT (hSERT-1), which was likely strengthened by the addition of a hydrogen-bonding interaction with Tyr95, which is a phenylalanine residue in hDAT and hNET. In the second common binding mode observed at both hDAT and hNET (i.e., hDAT-2 and hNET-2), the carbonyl oxygen atoms of the compounds were oriented cis to the aspartate residues. This binding mode was not observed in hSERT, but an alternative binding mode was identified (hSERT-2), in which the compound is reversed and shifted out of the binding pocket. Previous X-ray crystallography studies have identified a second binding site in hSERT stacked just above and overlapping the common binding site used for docking in these studies.¹¹² Binding mode hSERT-2 could be shifted towards that second binding site. In general, the α -gem-dimethyl MCAT analog **26** was slightly shifted out of alignment with the other compounds. This could be due to lack of steric bulk tolerance in the occluded inner portion of the binding site, and may explain the slight reduction in potency as compared to either *S*(-)**5** or *R*(+)**5a**.

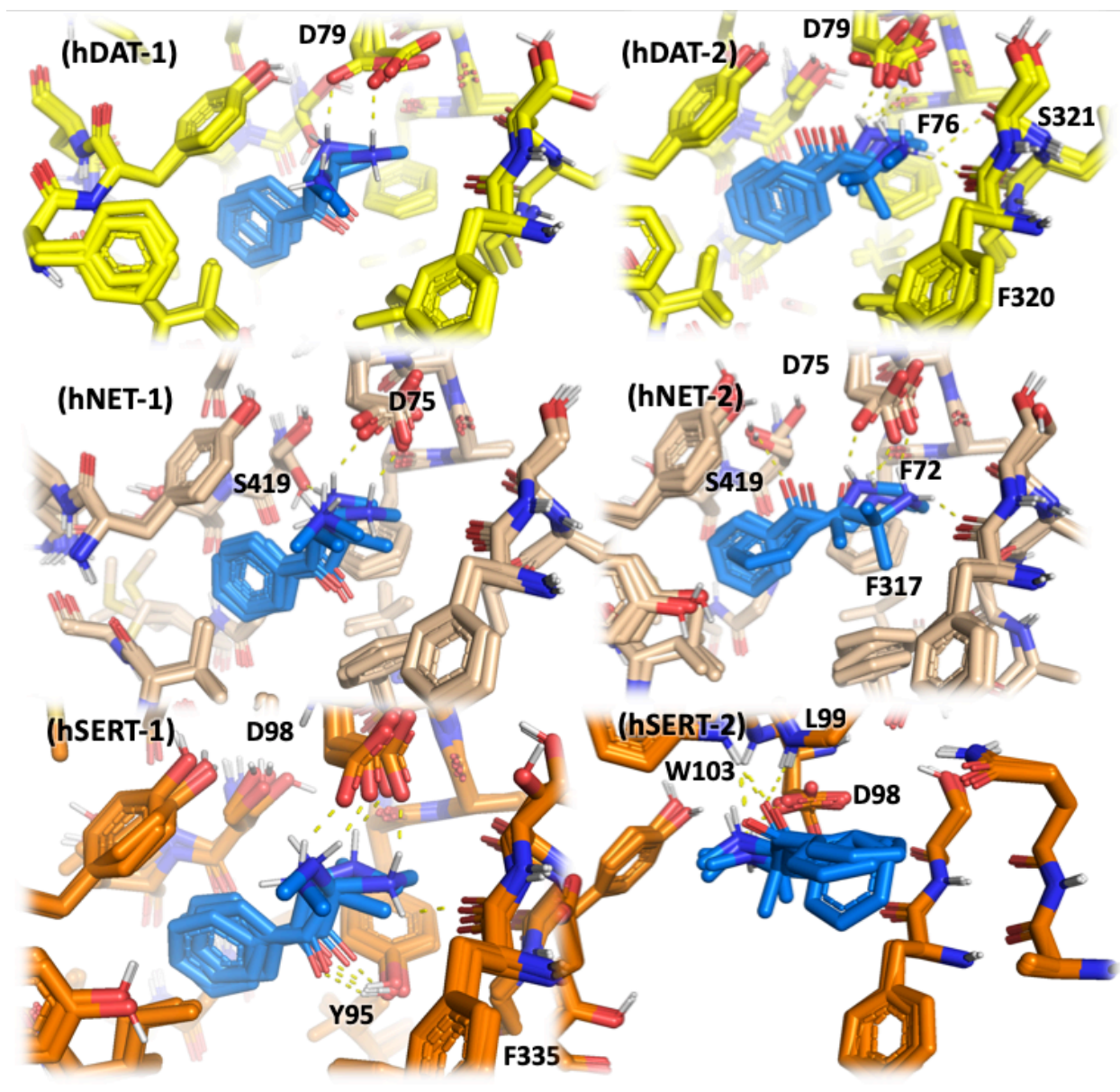


Figure 24. Common binding modes for Aim 1 compounds at hDAT (top), hNET (middle), and hSERT (bottom).

S(-)-MCAT docked similarly at hDAT (mode hDAT-1) to the binding of *S*(-)-amphetamine in the template crystal structure of dDAT (Figure 25A). A similar mode was identified for *S*(-)-5a at hNET as well (Figure 25B). The similar pose at hSERT varied more than the difference between the hDAT and hNET modes, in keeping with the high correlation between hNET and hDAT for MCAT-related compounds.^{67,181} These results support the hypothesis that

amphetamine and MCAT bind in a similar manner at the putative MAT binding site, at least when it comes to DAT. They provide incipient support for the general hypothesis that cathinones and other ATS bind in a similar manner during the transport process. Previous studies have shown that between MCAT and amphetamine, the difference in potency at MATs is negligible.⁶⁷ However, studies of other scaffolds (i.e., pyrrolidinophenones) have found 10-fold differences between keto and des-keto analogs.¹⁷⁴ Further studies should include parallel SAR between series of cathinone and amphetamines, in concert with docking studies, to further test the generalizability of this concept.

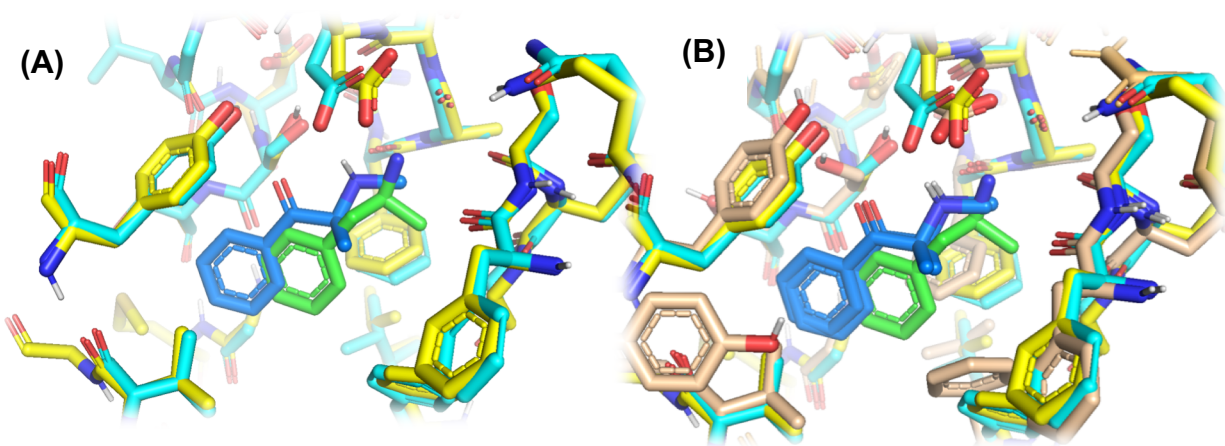


Figure 25. (A) *S(+)*Amphetamine (green) co-crystallized with dDAT (yellow, PDB ID:4XP9)⁶⁹ overlaid with *S(-)*5a (blue) docked at an hDAT homology model (yellow); (B) same as A, but overlaid with *S(-)*5a docked once to an hNET homology model (salmon).

B. Aim 2: To further establish SAR of α -pyrrolidinophenones.

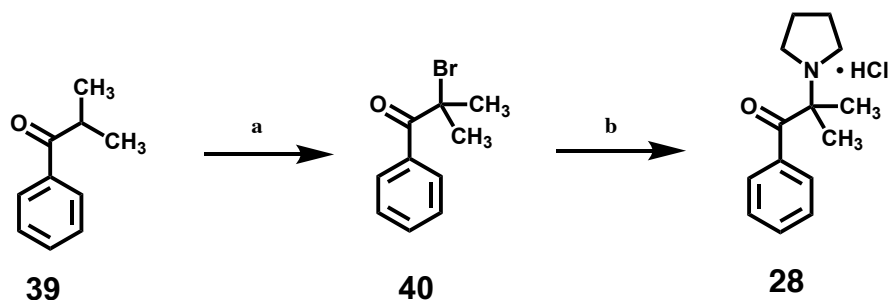
1. Aim 2.1: To assess the nature of stereoselectivity observed for α -pyrrolidinophenones by synthesizing and evaluating an achiral α -pyrrolidinophenone analog.

a. Synthesis Aim 2.1

The achiral analog was designed by adding a second methyl group to the α -carbon atom (i.e., **28**) of α -PPP (**70**; Table 6). The synthesis of the same compound was described in Perboni and Giubellina's¹⁹³ patent by the method described in the previous section: by employing

potassium carbonate and methanol to create an epoxy intermediate from α -bromoisobutyrophenone (**39**), to which the amine was added after stirring for several hours. As in the synthesis of gem-dimethyl-MCAT (**26**), the brominated intermediate **39** was synthesized from isobutyrophenone (**38**).

Scheme 3.^a Synthesis of Compound **28**.



^aReagents and Conditions: (a) Br₂, CHCl₃, rt, 24 h; (b) 1. K₂CO₃, MeOH, rt, 24 h; 2. MeNH₂, 70 °C, 14 h; 3. HCl/Et₂O.

b. Pharmacology Aim 2.1

Compound **28**, the gem-dimethyl analog of α -PPP (**70**) was evaluated in a modified calcium flux assay to assess blocker activity by B. Ruiz, a student in J. Eltit's laboratory. It was inactive at both MATs.

c. Modeling Aim 2.1

Compound **28** was docked at models of the MATs as described in Aim 1, but no sensible binding modes were identified. It did not dock in a similar manner to MCAT (i.e., the typical interaction between the amine nitrogen and aspartate residue was not present). This could explain the inactivity of the compound.

2. Aim 2.2: To establish QSAR for aryl-substituted pyrrolidinophenones, and determine similarity with MCAT activity via parallel SAR.

a. Synthesis Aim 2.2

α -PHP (**29**) had been previously synthesized by Kolanos et al. in the Glennon laboratory,²⁵ but was scaled up and resynthesized for the present investigations. The published procedure was followed exactly (Scheme 4), beginning with the commercially available

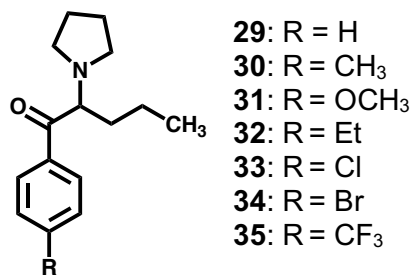
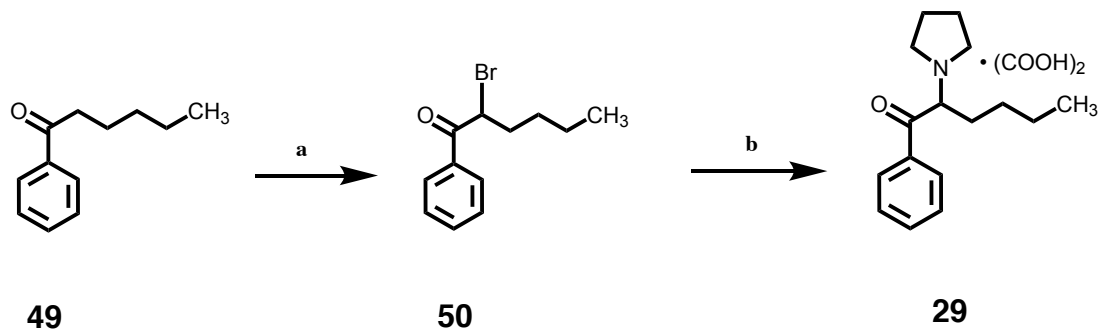


Figure 26. α -PHP analogs.

hexanophenone (**49**), which was treated with bromine to undergo carbonyl α -carbon halogenation, followed by substitution of the newly introduced bromine by pyrrolidine (Scheme 4).

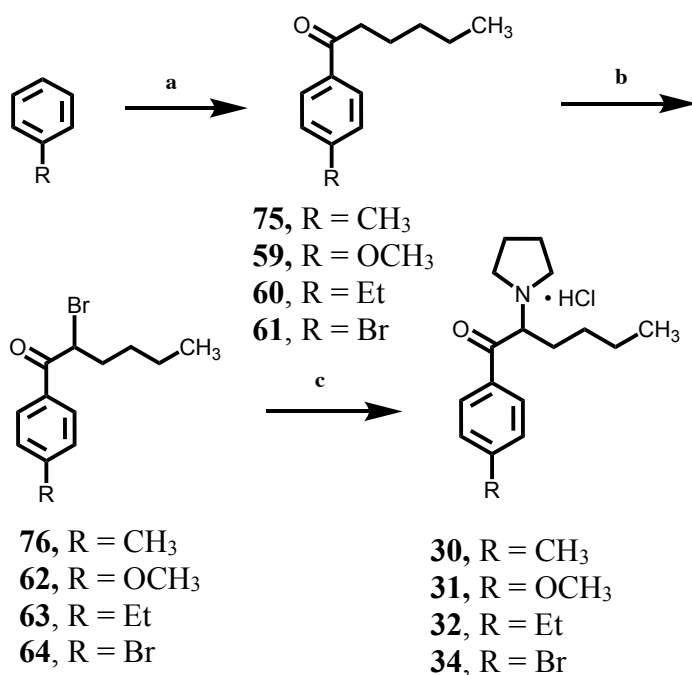
Scheme 4.^a Synthesis of Compound **29**.



^aReagents and Conditions: (a) Br₂, AlCl₃ (cat.), 0 °C, 30 min; 2. rt, 1 h (b) 1. Pyrrolidine, 0 °C, 10 min; 2. rt, 30 min; 3. Oxalic acid, Et₂O.

The synthesis of the α -PHP 4-substituted analog series (**30-35**, Figure 26) was achieved through two common synthetic routes. The first route was based on the approach to the unsubstituted α -PHP. However, in most cases, the 4-substituted hexanophenones were not commercially available, so these were synthesized from the appropriate substituted benzenes with hexanoyl chloride in a Friedel-Craft's acylation (Scheme 5). This was followed by halogenation of the carbonyl α -carbon with bromine, and subsequent substitution of the bromine with pyrrolidine. This process was effective for substrates with substituents that were electron-donating and *para*-directing either inductively (e.g. ethyl) or via resonance (e.g. bromo). For the electron-withdrawing and aromatic substitution-deactivating substituent trifluoromethyl, however, the transformation was unsuccessful even after several attempts.

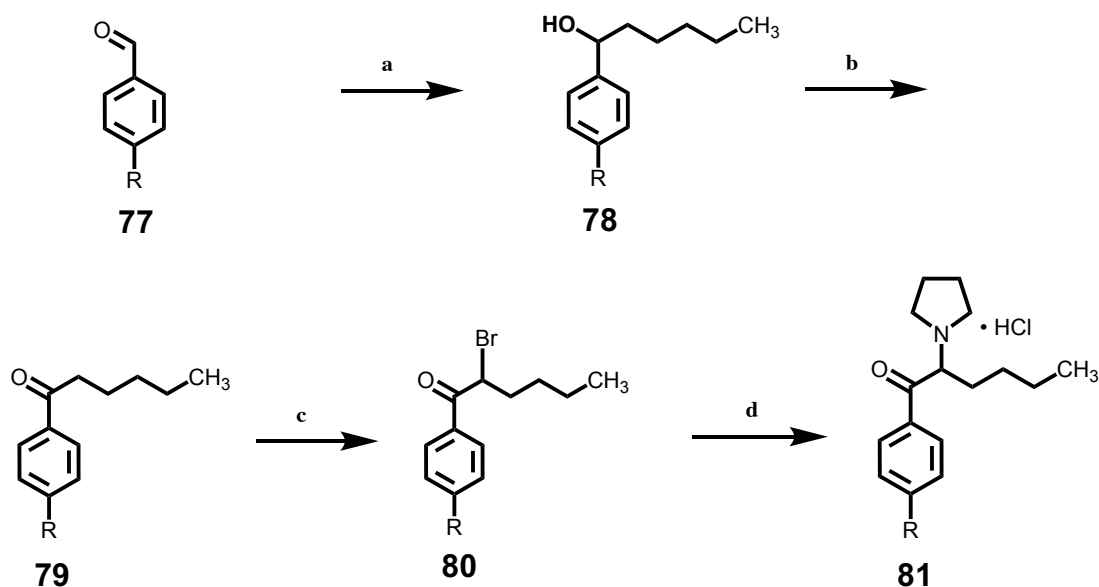
Scheme 5.^a Synthesis of Compounds **30**—**32** and **34**.



^aReagents and conditions: (a) 1. Hexanoyl chloride, AlCl₃ DCM, N₂, -10 °C, 30 min; 2. rt, 1-24 h; (b) 1. Br₂, AlCl₃ (cat.), 0 °C, 30 min; 2. rt, 1 h; (c) 1. Pyrrolidine, 0 °C, 10 min; 2. rt, 30 min.

A new approach was considered to synthesize the necessary 4-hexanophenones by oxidation from their corresponding alcohols, which would be generated by Grignard reaction with 4-substituted benzaldehydes (Scheme 6). The 4-trifluoromethyl alcohol intermediate (**67**) was successfully synthesized, validating the Grignard approach. The Grignard reagent was synthesized *in situ* using magnesium turnings freshly ground in a mortar and pestle, with several drops of 1,2-dibromoethane as an activator. The Grignard procedure was adapted from a similar procedure in a 2001 patent from Sebti and coworkers.¹⁹⁴

Scheme 6.^a Extended Grignard approach that was considered for making α -PHPs, as it had been used previously for related compounds.

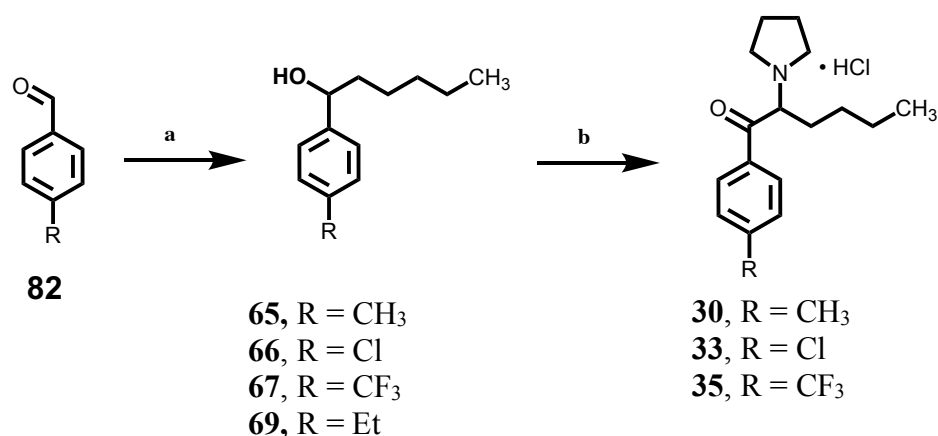


^aReagents and Conditions: (a) n-Bromopentane, magnesium, 1,2-dibromoethane, THF, N_2 , rt, 5-24 h; (b) Jones' Reagent; (c) 1. Br_2 , AlCl_3 (cat.), $0\text{ }^\circ\text{C}$, 30 min; 2. rt, 1 h; (d) 1. Pyrrolidine, $0\text{ }^\circ\text{C}$, 10 min; 2. rt, 30 min.

The alcohols would then be oxidized with Jones' Reagent, substituted with bromine, and then substituted with pyrrolidine, in a scheme that was similar to ones used previously in our laboratory. However, this scheme is long, and uses harsh reagents. An alternative was sought to simplify the procedure.

A one-pot procedure utilizing milder, more environmentally friendly and safer reagents (NBS in place of both Jones' Reagent and bromine), and which also simplified three steps into one (oxidation, bromination, and amine substitution) was discovered in the literature.¹⁹⁵ Guha and coworkers had pioneered this method in the synthesis of the closely related compound pyrovalerone and several related analogs in 2015.¹⁹⁵ In this procedure, the NBS is thought to oxidize the alcohol, then generate bromine in situ, which can be observed in a burst of brown gas that evolves from the reaction mixture. The method was employed successfully in the synthesis of several of the target compounds, including both electron-withdrawing and donating substituents (Scheme 7). Electron-withdrawing substituents, such as the 4-trifluoromethyl compound (**35**), required mild heating and longer times to initiate the evolution of bromine gas. The 4-methyl compound was prepared by both methods. The 4-ethyl compound was attempted, but the reaction resulted primarily in another product.

Scheme 7.^a Synthesis of Compound **30**, **33**, and **35**.



^aReagents and Conditions: (a) n-Bromopentane, magnesium, 1,2-dibromoethane, THF, N₂, rt, 5-24 h; (b) 1. NBS (1.3 equiv); 2. 1,4-dioxane, rt; 3. Pyrrolidine (24-48 h).

b. Pharmacology Aim 2.2

The series was evaluated for its ability to inhibit transport of hDAT substrate APP⁺ through hDAT expressed in HEK 293 cells, as measured by epifluorescence microscopy. Nonlinear regression using the Hill equation was performed on dose-response curves for each compound (Figure 27) to generate IC₅₀ potency values, which are shown in Table 11. The unsubstituted compound **29** was the most potent (IC₅₀ = 99.3 nM), and the trifluoromethyl analog **35** was the least potent (IC₅₀ = 5047 nM). The remainder of the series differed slightly but significantly from one another (less than 2-fold). Significance was determined using nonlinear regression in GraphPad Prism 6.0.

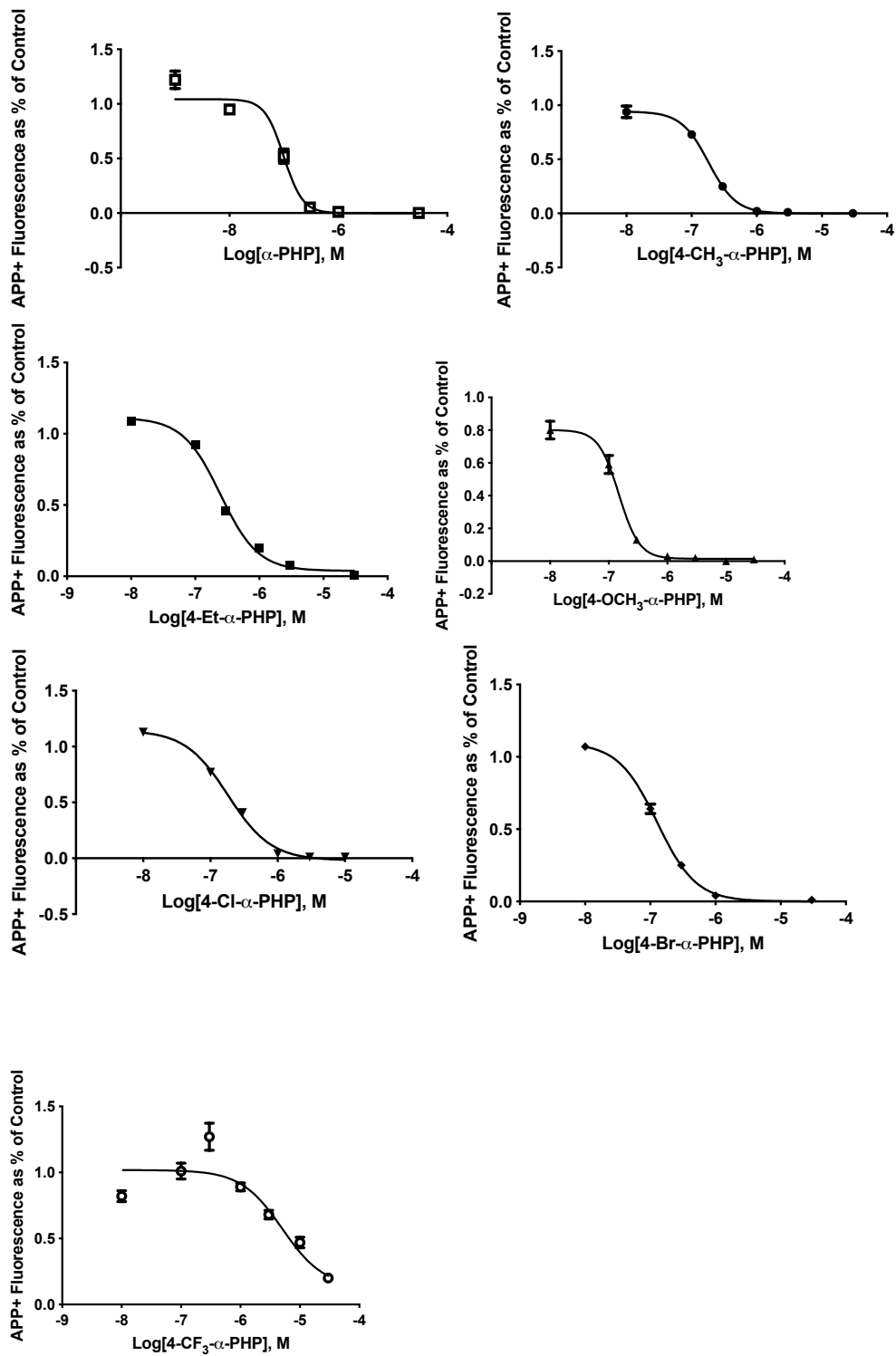


Figure 27. Concentration-response curves for inhibition of APP+ transport by 4-substituted α -PHP analogs.

Table 11. Inhibition of APP+ transport by α -PHP analogs in HEK cells, or release of [3 H]MPP+ by MCAT analogs from rat brain synaptosomes. MCAT data reproduced from Bonano et al. 2015.⁶⁸

Compound in α -PHP series	R	α -PHP series IC ₅₀ (\pm SEM), nM*	MCAT series EC ₅₀ , nM
α -PHP (29)	-H	99.3 \pm 7.9	12.5
4-CH ₃ - α -PHP (30)	-CH ₃	182.7 \pm 15.7	49.1
4-OCH ₃ - α -PHP (31)	-OCH ₃	149.1 \pm 13.4	506
4-CH ₂ CH ₃ - α -PHP (32)	-Et	246.6 \pm 15.8	n/a
4-Cl- α -PHP (33)	-Cl	182.8 \pm 25.3	42.2
4-Br- α -PHP (34)	-Br	127.0 \pm 7.5	59.4
4-CF ₃ - α -PHP (35)	-CF ₃	5047.0 \pm 2310	2700

*The APP+ assay can be summarized as follows. Plated cells, previously transfected with hDAT, were supplemented with doxycycline to induce expression of transporters. Test compounds or controls were exposed to the cells under constant perfusion. Fluorescence was observed at 460 nm excitation, then recoded for off-line analysis. At least 3 wells were examined per experiment, and 2 experiments were conducted for each compound to calculate the IC₅₀ values above. For reasons to be subsequently discussed, assays for **29**, **31**, and **35** were replicated. The new values were roughly consistent with the initial results (i.e., IC₅₀ \approx 29.4 nM, 93.6 nM, and 181100 nM, respectively; data points were not sufficient to calculate SEM in replicate experiment). The combined IC₅₀ values were highly consistent with the initial results (IC₅₀ \approx 96.5 \pm 3.7 nM, 111.4 \pm 6.5 nM, and 7503 \pm 3221 nM, respectively). However, the results shown in Figures 28-32 used the original data from this table.

c. Correlational Studies Aim 2.2

The α -PHP series was compared with a parallel series of MCAT analogs in which the 4-position had the same substituents.^{68,69} The potencies of the MCAT series are shown for comparison in Table 11. Pearson correlational analysis and linear regression revealed a statistically significant correlation coefficient between the two series ($r = 0.82$, $P = 0.046$, $n = 6$, Figure 28).

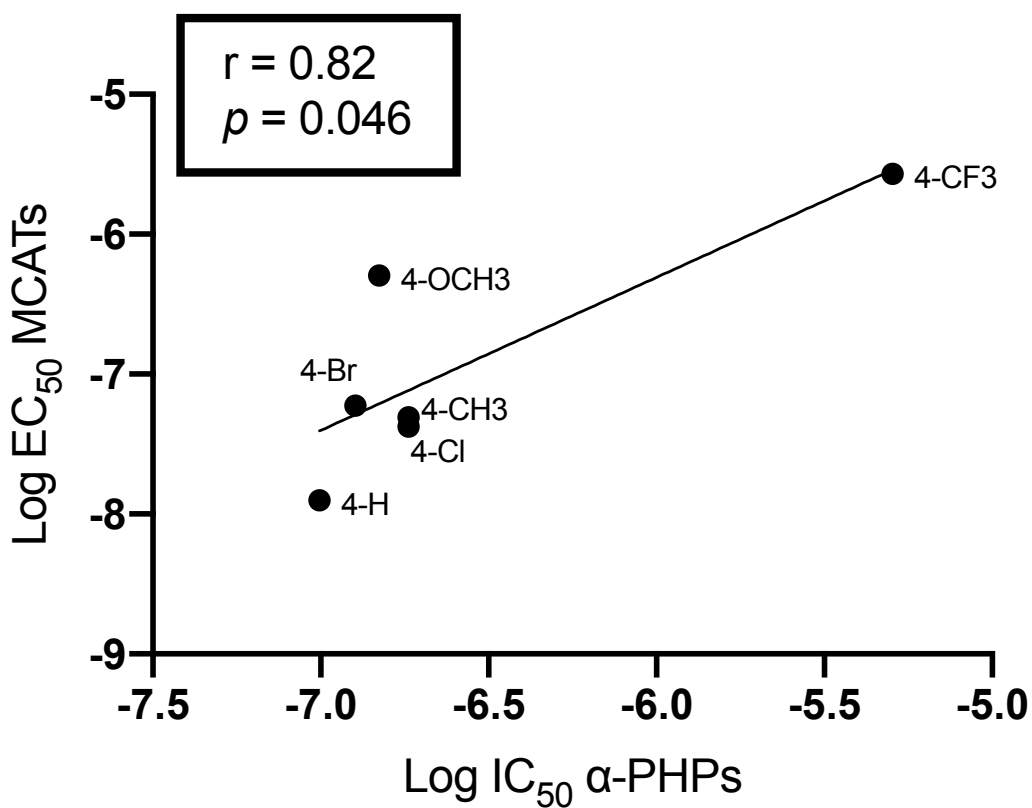


Figure 28. Correlation between potencies of α -PHP compounds and corresponding methcathinone analogs.

The most and least potent analogs of this α -PHP series were also the most and least potent analogs for a series of corresponding MCAT analogs previously synthesized in and published by the Glennon group.⁶⁹ However, these points, and particularly the weakest compound, the 4-trifluoromethyl, define the correlation. The remainder of the data points cluster together, with only slight variations in the potencies of the remaining compounds in the α -PHP series. With the 4-trifluoromethyl compound removed from the data set, the correlation is completely lost (Figure 29, $r = 0.36$, $P = 0.52$, $n = 5$). Therefore, while the original correlation is statistically significant, its validity is still questionable.

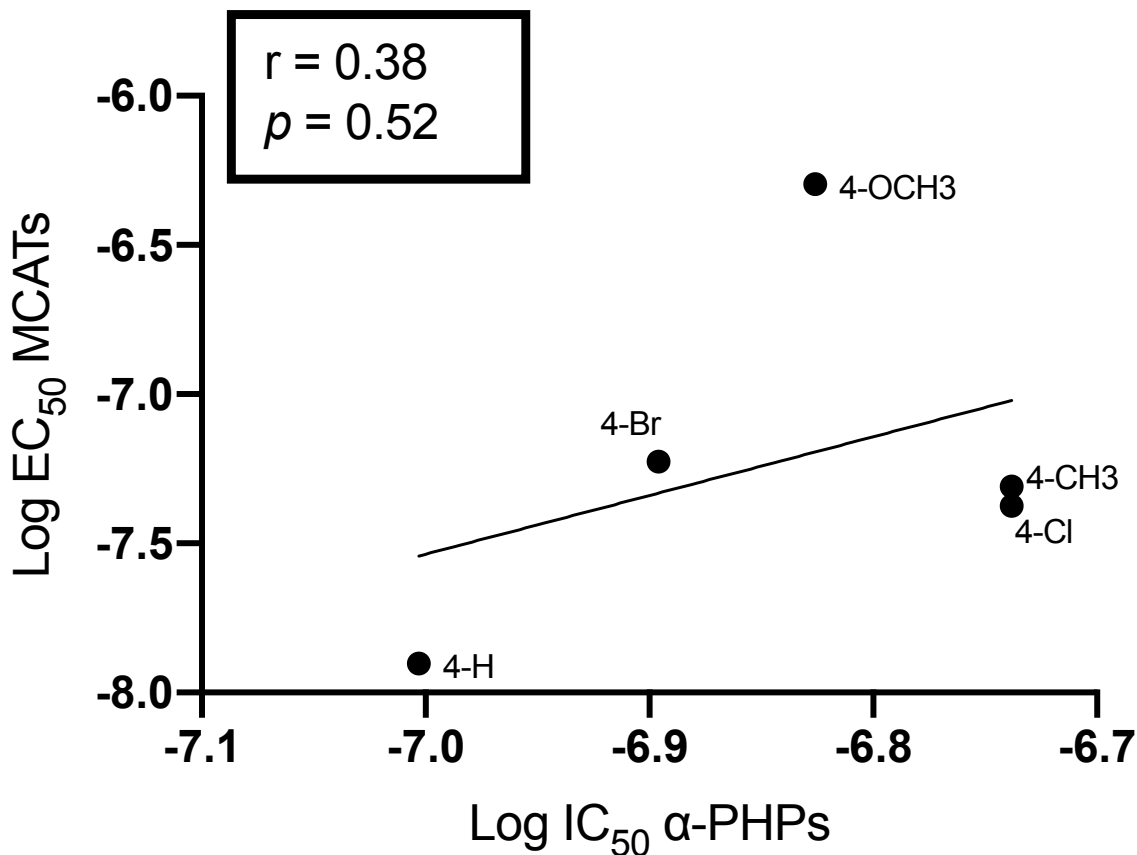


Figure 29. Correlation between α -PHPs and methcathinone analogs when 4-trifluoromethyl is removed.

The most conspicuous discrepancy between the two series is between the 4-methoxy compounds. In the MCAT series, the 4-methoxy compound is the second-least potent, and 10-fold less potent than the 4-methyl compound ($EC_{50} = 506$ nM and 49 nM, respectively). In the α -PHPs, the 4-methoxy appears relatively potent, and nearly equivalent in potency to the corresponding 4-methyl compound ($IC_{50} = 182.7$ nM and 149.1 nM, respectively). The GraphPad Prism automatic outlier test, which utilizes their ROUT method of outlier detection, identified the 4-methoxy data point as an outlier when Q (the maximum false discovery rate) was set to 33%. Below $Q = 33\%$, it was not identified as an outlier. No other points were identified as outliers at this Q value. The outlier test, and the placement of the 4-methoxy data point outside of the Gaussian distribution, are shown in Figure 30.

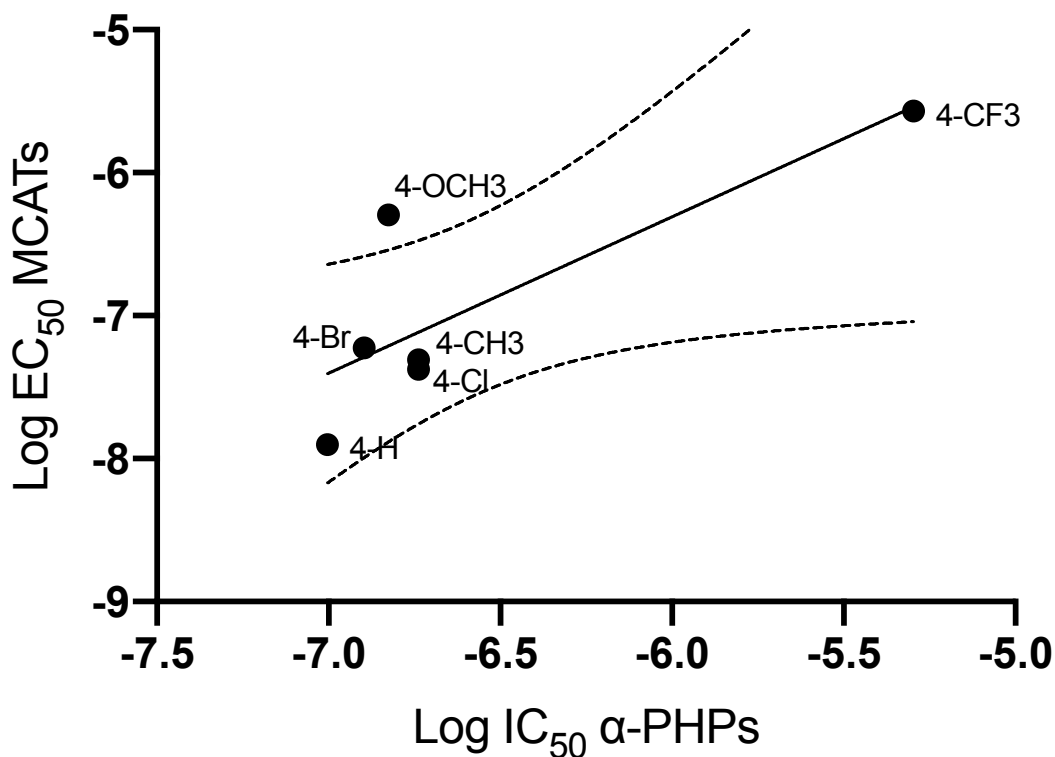


Figure 30. Linear regression of α -PHPs and MCATs with outlier test applied.

Pearson correlation was performed again between the MCAT and α -PHP series with the 4-methoxy compounds excluded, which resulted in a much more statistically significant correlation ($r = 0.97$, $P = 0.0046$, $n = 5$). The corresponding linear regression is shown in Figure 31. These results should be interpreted with a high degree of skepticism, considering the remaining importance of the trifluoromethyl compounds to the correlation, the high maximum false discovery rate applied in the outlier test, and the low number of XY pairs. Still, they suggest that it may be worth revisiting the methoxy compound for further testing.

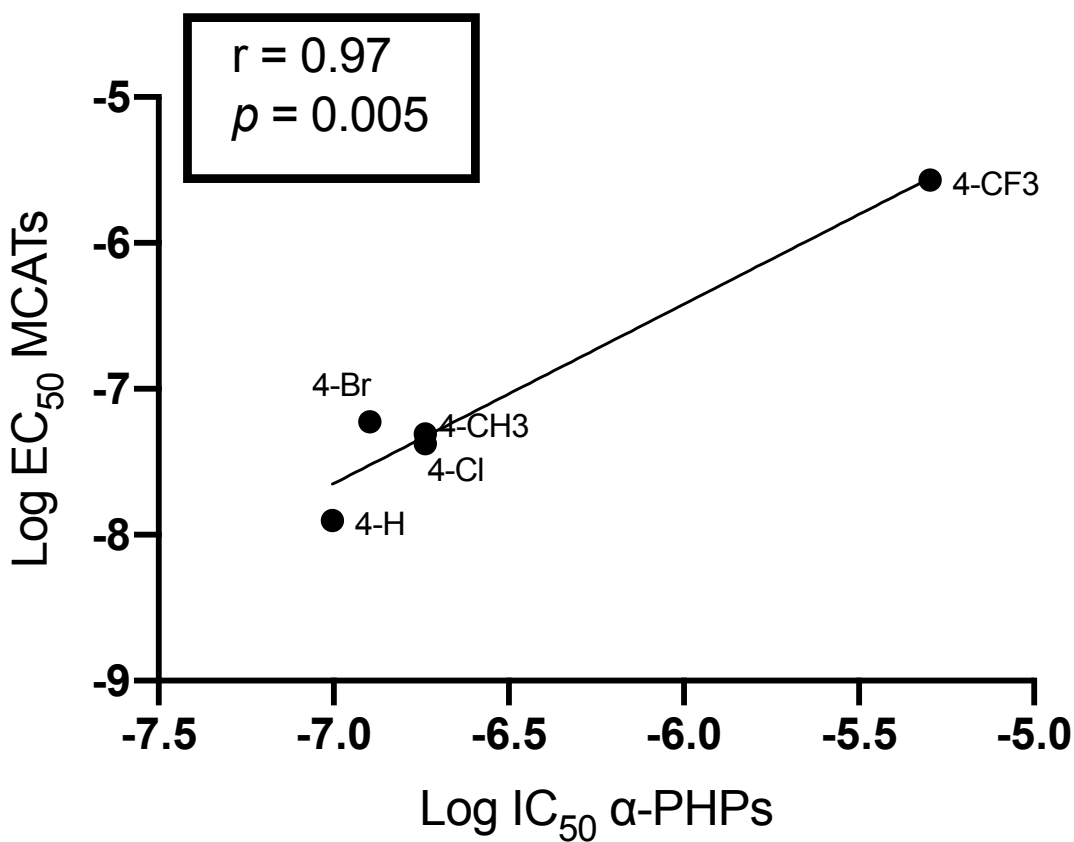


Figure 31. Linear regression analysis between α -PHP series and methcathinone series with 4-methoxy compounds excluded.

QSAR analysis was performed, considering variety of physicochemical parameters including electronic and steric factors. A statistically significant correlation ($r = -0.89$, $P = 0.013$, $n = 7$) was found with only one: Taft's steric E (E_s), a measure of steric bulk. Linear correlation was used to produce Figure 32. Again, these results must be interpreted with skepticism, as the 4-trifluoromethyl compound plays an important role in the significance of the correlation. Without the 4-trifluoromethyl compound, the correlation reduces to $r = -0.77$, and becomes insignificant ($P = 0.07$).

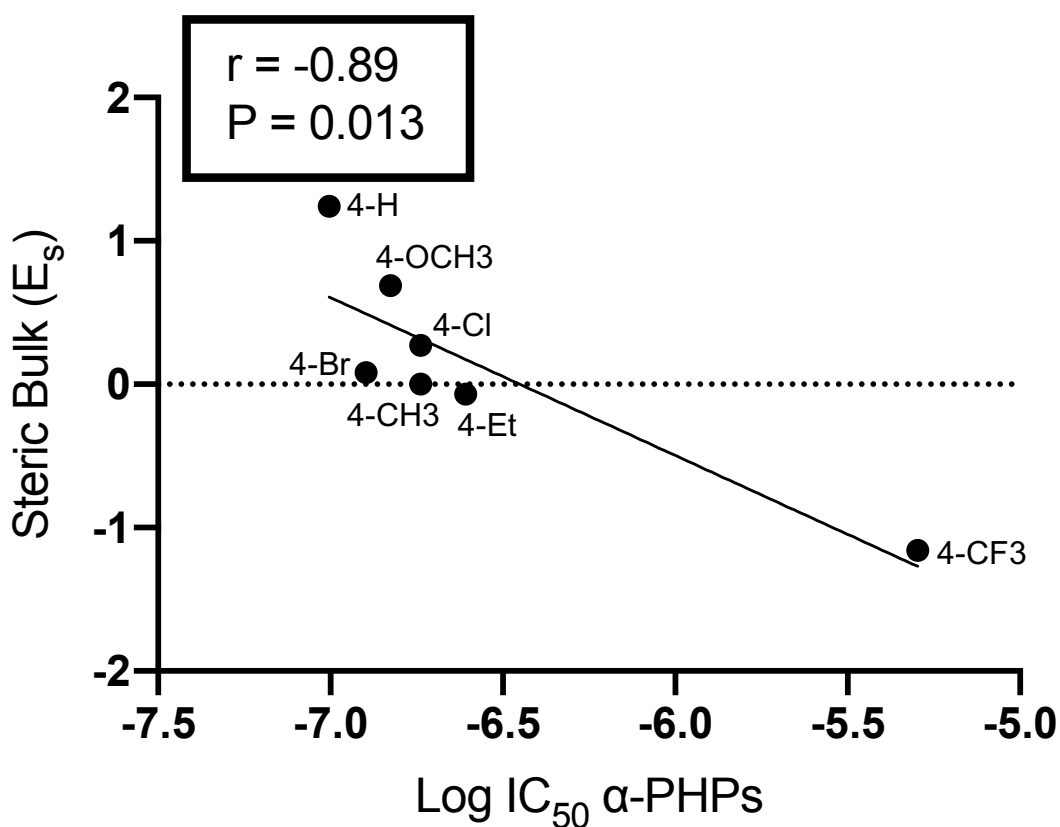


Figure 32. Linear regression of potency to inhibit DAT and Taft's steric E for α -PHP series.

In these studies, we were able to show that a wide range of aryl substituents are tolerated by hDAT at the 4-position of α -PHP. These substituents varied in size, electronic character, and lipophilicity, but there was less than a three-fold difference in the EC_{50} potency values for six out

of the seven analogs in the series. This suggests that aromatic substituents in the 4-position are not particularly important for activity at hDAT. The exception to this observation is the case of the 4-trifluoromethyl analog **35**, which defines a correlation with the potency values of a parallel MCAT series, and with steric parameter E_s . It might be that this compound helps to reveal these underlying, legitimate correlations, but the evidence for that claim is fairly weak. Another possibility is that 4-trifluoromethyl is universally bad for hDAT regardless of the agent under investigation, but for reasons that do not generalize to other substituents (i.e., they are not defined by a particular QSAR parameter in an operational manner).

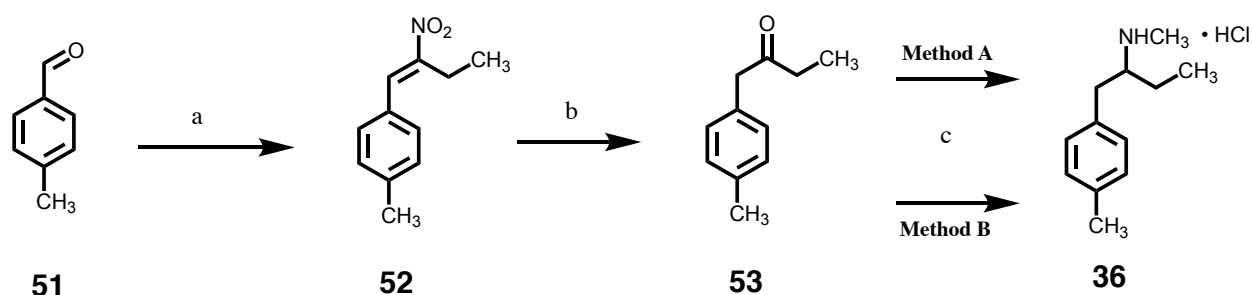
C. Aim 3: To synthesize analogs for progress in SAR of synthetic cathinone-related amphetamines at the α -carbon.

1. **Aim 3.1:** To synthesize analogs for the investigation of the impact of α -carbon alkyl chain extension on 4-methylamphetamines.

The α -ethyl 4-MMA analog **36** was synthesized from **53** in an analogous fashion to the common illicit synthesis route of methamphetamine from phenyl-2-propanone (i.e., P2P; Scheme 8). Two methods were employed for the reductive amination with methylamine. In method A, following Jacob and coworkers' procedure for a similar compound that had been successfully utilized by others in the Glennon laboratory,¹⁹⁶ a traditional reductive amination reagent (sodium cyanoborohydride) was used. In method B (Scheme 8), Parr hydrogenation in the presence of a platinum oxide catalyst was used for the reduction in an attempt to improve the yield. This was a new approach to the target compound **36**, but the general method of Heinzelman and Aspergrem¹⁹⁷ was used as a guideline. The ketone intermediate **53** was made by reduction of **52** with iron, following the Jacob et al.¹⁹⁶ approach. The nitroalkene **52** was produced by a

modified Henry reaction from *p*-tolualdehyde (**51**) following generally the procedure of Koremura and coworkers¹⁹⁸ for the same compound. Different quantities were used because they were working on a much larger scale, different times were used to allow the reaction to reach completion, and flash chromatography was used instead of distillation because previous attempted purification of **52** by Kugelrohr was unsuccessful.

Scheme 8.^a Synthesis of Compound **36**.

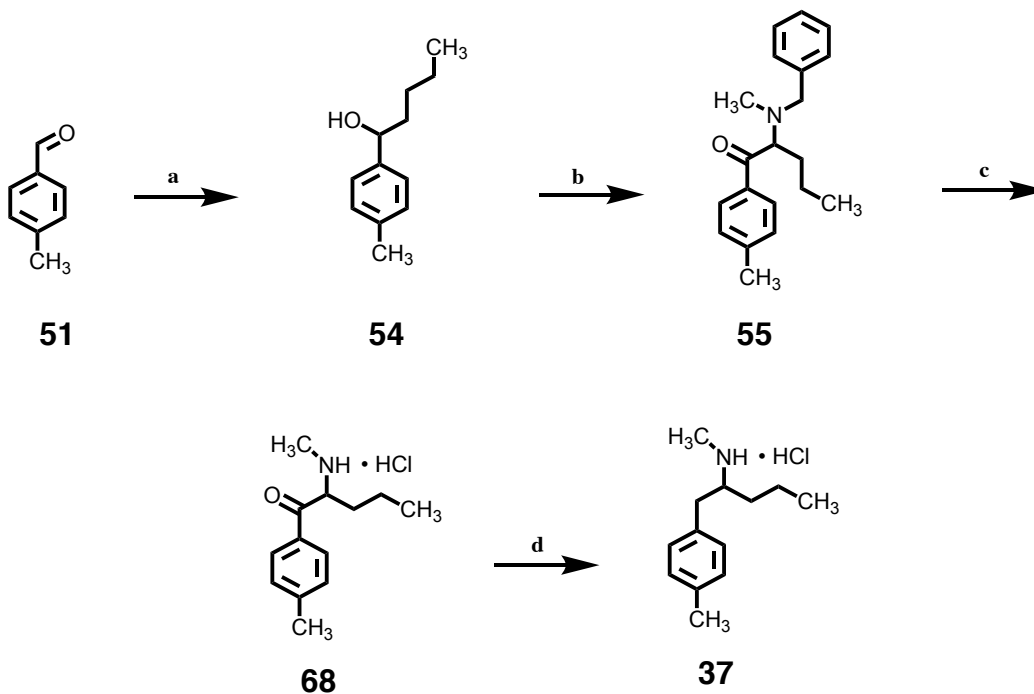


^aReagents and Conditions: (a) $\text{CH}_3(\text{CH}_2)_2\text{NO}_2$, $\text{CH}_3\text{COO}^-\text{NH}_4^+$, HOAc, reflux, 120°C , overnight (19.5 h); (b) Fe 90% aq. HOAc, 60°C , 20 min; (c) Method A: 40% aq. MeNH_2 , NaCNBH_3 , HOAc, MeOH, rt 40 min, HCl, Et_2O ; Method B: 33% MeNH_2 (EtOH), H_2 , Pt_2O , EtOH, rt 72 h, HCl, EtOAc.

The α -propyl compound **37** (Scheme 9) was approached through an entirely different route, as the iron reduction was difficult to stir. The same starting material (i.e., **51**) was converted to an alcohol (**54**) by Grignard reaction following a patent procedure.¹⁹⁴ Compound **54** was used in a modified form of Guha and coworkers' one-pot reaction (vide supra).¹⁹⁵ *N*-Benzylmethylamine, rather than methylamine, was used in order to control the equivalents in the reaction. The benzyl group was removed from **55** with chloroethyl chloroformate using Blough's procedure for similar compounds.¹⁹⁹ Finally, the keto group was reduced by Parr hydrogenation

with a palladium over carbon catalyst. The resulting product was impure, containing a large fraction of the ring-reduced cyclohexane counterpart to **37**.

Scheme 9.^a Synthesis of Compound **37**.



^aReagents and Conditions: (a) *n*-Butylmagnesium chloride, THF, N₂, rt, 24 h; (b) NBS, *N*-benzylmethylamine, 1,4-dioxane, rt, 40 h; (c) 1. 1-chloroethyl chloroformate, 2 h; 2. MeOH, reflux, 1 h; (d) H₂, Pd/C (10%), TFAA.

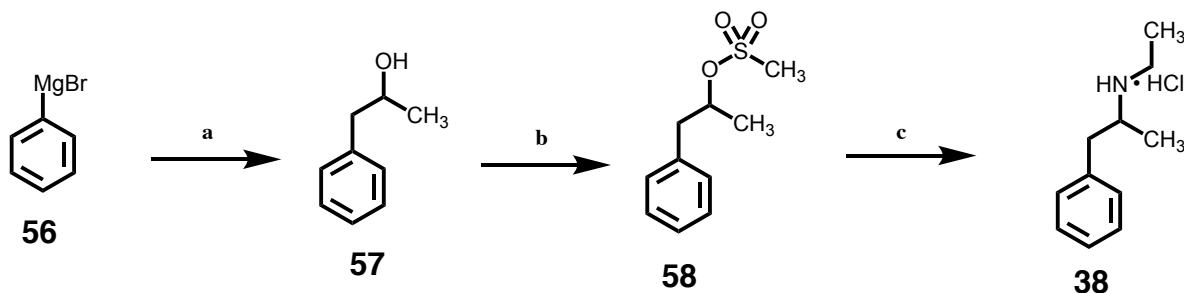
Biological data on compounds **36** and **37** have not at the time of writing been collected.

2. Aim 3.2: To stereoselectively synthesize *N*-ethylamphetamine isomers for future evaluation of ATS stereochemistry on DAT/NET/SERT selectivity

The isomers of **38** were synthesized according to a scheme developed in the Glennon laboratory that was used for similar compounds.¹⁹⁰ The *R* isomer *R*(**38**) was made in collaboration with U. Battisti, a former postdoctoral researcher in the Glennon group, who made the first two intermediates *S*(**57**) and *S*(**58**). Phenylmagnesium bromide was reacted with chiral

propylene oxides to give *S*(57) or *R*(57). The alcohol was converted to a mesylate to make it a better leaving group in compounds *S*(58) and *R*(58). The substitution of ethylamine for the mesylate proceeded by S_N2, resulting in inversion of the chiral center.

Scheme 10. Synthesis of Compounds *S*(+)38 and *R*(-)38.



Reagents and conditions: (a) *S*(-)Propylene oxide or *R*(+)propylene oxide, CuI, THF, -60 °C, 2 h, rt, 24 h; (b) MsCl, Et₃N, CH₂Cl₂, 0 °C to rt, 12 h; (c) (i) Ethylamine (70% aq.), DMF, 50 °C, 72 h, (ii) HCl, EtOH/Et₂O

At the time of writing, biological data for these compounds have not been collected.

D. Aim 4: To construct homology models of NET to inform MAT substrate studies.

1. Template

Previous modeling studies in our laboratory of hDAT and hSERT had used a 2013 dDAT crystal structure that was co-crystallized with reuptake inhibitor nortriptyline (PDB ID: 4M48).¹¹⁰ The 2015 substrate-bound structures solved by Wang et al.¹¹¹ had revealed shifted phenylalanine residues involved in substrate recognition, and as our hNET models were intended to inform substrate selectivity between MATs, a substrate-bound structure was thought to be preferable. Several structures of MATs bound to different substrates dopamine (PDB ID: 4XP1), *S*(+)methamphetamine (PDB ID: 4XP6), *S*(+)amphetamine (PDB ID: 4XP9), and 3,4-

dichlorophenethylamine (PDB ID: 4XPA) were available and considered as templates. As many of the synthetic cathinones under investigation in the Glennon group are secondary or tertiary amines, and fewer are primary amines, 4XP6 (with methamphetamine, **10**) was selected as a candidate template.

A comparison between the selected template (i.e. 4XP6), and the previous template used to build hDAT and hSERT models (i.e. 4M48),⁶⁹ was conducted in order to ascertain comparability of the resulting models for comparative modeling and docking studies between the MATs. Alignment and Root Mean Square Deviation (RMSD) analysis was performed in PyMOL, and showed that the difference between 4XP6 and 4M48 structure differed by only 0.398 Å (Figure 33). Considering that a population of 100 models was generated, introducing some degree of variation, that distance should not be significant to the outcome of the studies. Wang and coworkers¹¹¹ had identified a group of phenylalanine residues in the binding pocket that were shifted in substrate binding for the crystal structures. We observed this shift for Phe325 between the nortriptyline-bound structure and the methamphetamine-bound structure, strengthening the justification for the choice of template as the methamphetamine-bound structure (Figure 33).

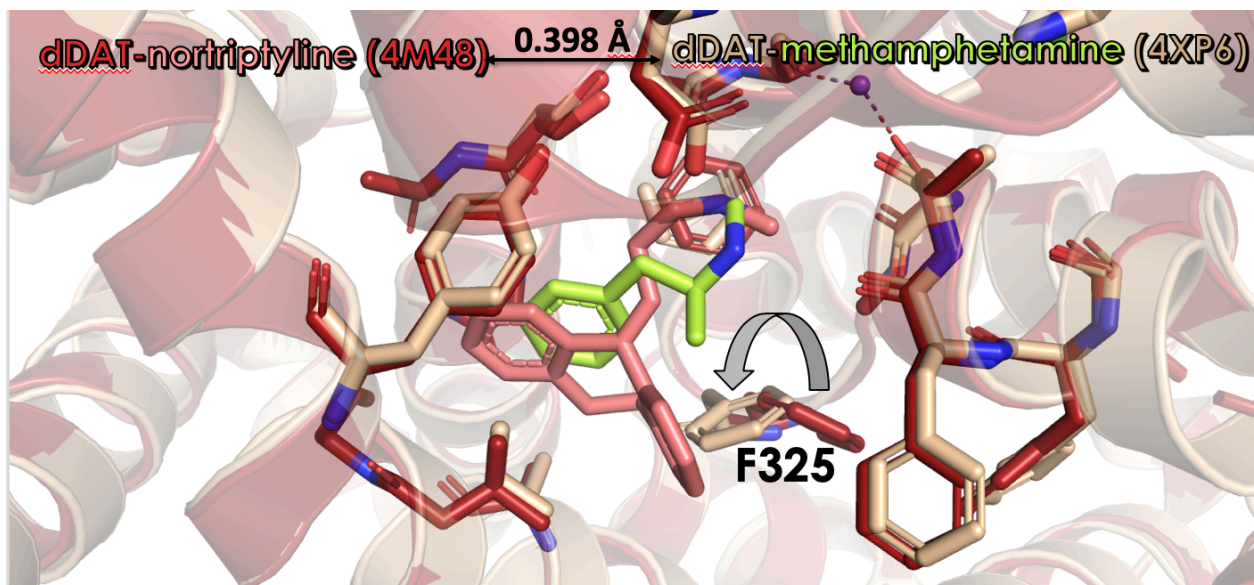


Figure 33. Alignment of dDAT/methamphetamine (beige/green, PDB ID: 4XP6) and dDAT/nortriptyline (red/pink, PDB ID: 4M48). Phe325 shift emphasized by grey arrow. Generated in PyMOL and Microsoft PowerPoint.

The more recent crystal structures of hSERT, solved by Coleman et al.,¹¹¹ were also considered as candidates for the hNET model template, as hSERT is of human origin, and dDAT is very much evolutionarily divorced from hNET (Figure 10, *vide supra*: C.4). Sequence identity was considered for four MATs transporters (dDAT, hDAT, hNET, and hSERT) by aligning their amino acid sequences. These were retrieved as FASTA from the National Center for Biotechnology Information (NCBI) using the Protein search function. The sequences were aligned using Clustal Omega (Figure 34).²⁰⁰ A percent identity matrix was generated directly from this alignment, which evaluated the identities between dDAT and hNET, and hSERT and hNET, as 56% and 50%, respectively (Figure 35). This supported the use of dDAT rather than hSERT for modeling of hNET, despite the species difference. Additionally, hSERT was co-crystallized with inhibitors paroxetine and citalopram, which suggested it might be less suitable for substrate docking, just as in the case of the dDAT/nortriptyline structure. Nevertheless, we compared the candidate templates (dDAT/methamphetamine, PDB ID:4XP6; hSERT/paroxetine,

PDB ID: 5I6X; hSERT/citalopram, Figure 36) to one another by alignment and RMSD analysis using PyMOL. The RMSD between dDAT/methamphetamine and hSERT/paroxetine or hSERT/citalopram were 1.024 Å and 0.998 Å, respectively.

hSERT	ME-----TTPLSNQKLSACEDGEDCQENGVLQKVVPTPGDKVESGQISNG----YSAVP 51	
dDAT	-----MS-----	-----PTG-HISKSKTP 13
hDAT	MSKSKCSVGLMSSVV--APAKEPNA-----VGPKEVELILVKEQNGVQLTSSTLT 48	
hNET	-----MLLARMNFQV--QPENNGAD---TGPEQPLRARKTAELLVVKERNVQCLLA--- 47	
	: .	* :
hSERT	SPGAGDDTRHSIPATTTTLVAELHQGERETWGKKVDFLLSVIGYAVDLGNVWRFPYICYQ 111	
dDAT	TPR-----DNDNNSISDERETWSGKVDFFLLSVIGFAVDLANVWRFPYLCYK 59	
hDAT	NPR-----Q--SPVEAQDRETWGKKIDFLLSVIGFAVDLANVWRFPYLCYK 92	
hNET	-PR-----DGDAQPRETWGKKIDFLLSVVGFVAVDLANVWRFPYLCYK 88	
	*	**** * :***** : * : * : * : * : * : * : * : * : * :
hSERT	NGGGAFLLPYTIMAIFGGIPLFYMELALGQYHRNGCISIWKRKICPIFKGIGYAIICIAFY 171	
dDAT	NGGGAFLLPYGIMLVVGGIPLFYMELALGQHNRKGAITCWGRVLPFLFKGIGYAVVLIIFY 119	
hDAT	NGGGAFLLPYLLFMVIAGMPLFYMELALGQFNREGAAGVWK-ICPILKGVGFTVILISLY 151	
hNET	NGGGAFLLPYTLFLIIAGMPLFYMELALGQYNRREGAATVWK-ICPFFKGVGYAVIILIALY 147	
	***** : * : . . . * : * : * : * : * : * : * : * : * : * : * : * :	
hSERT	IASYNTIMAWALYYLISSTFDQLPWTSCKNWNTGNCTNYFSEDNITWT----- 221	
dDAT	VDFYFNVI IAWSLRFFFASTNSLFWPWTSCNNWNTPNCRPFESQNASRVPVIGNYSDLYA 179	
hDAT	VGFFYNVI IAWALHLYLFSSTTELPWIHCNNSWNSPNCSDAHPGDSSG-DSSGL----- 204	
hNET	VGFFYNVI IAWSLYLYLFSSTLNLFPWTDGHTWNSPNTDPKLLNGSVLGNHTK----- 201	
	: * : * : * : * : * : * : * : * : * : * : * : * : * : * :	
hSERT	-----LHSTSPAEEFYTRHVLQIHRSKGLQDLGGISWQL 255	
dDAT	MGNQSLLYNETYMGSSLDTSVAVGHVEGFQSAASEYFNRYILELNRSEGIHDLGAIKWDM 239	
hDAT	-----NDTFG-TTPAAEYFERGVLHLHQSHGIDDLGPPRWQL 240	
hNET	-----YSKYK-FTPAAEFYERGVHLHLESGGIHDIQLPQWL 237	
	: * * : * : * : * : * : * : * : * : * : * :	
hSERT	ALCIMLIFTVIYFYSIWKGKVTSGKVVVWTATFPYIILSVLLVRGATLPGAWRGVLYLKP 315	
dDAT	ALCLLIVLYLICYFSLWKGISTSGKVVWFTALFPYAVLLILLIRGLTLPGSFLGIQYYLTP 299	
hDAT	TACLLVIVVLLYFSLWKGKVTSGKVVVITATMPYVVLTAALLRGVTLPGAIDGIRAYLSV 300	
hNET	LLCLMVVVIVLYFSLWKGKVTSGKVVVITATLPYFVFLVLLVHGVTLPASNGINAYLHI 297	
	* : : : : * : * : * : * : * : * : * : * : * : * : * : * : * : * : * :	
hSERT	NWQKLEETGVVIDAAAQIFFSLGPGFVLLAFASYNKFNNNCYQDALVTSVVNCMTSFVS 375	
dDAT	NFSAIYKAEVWVDAATQVFFSLGPGFVLLAYASYNKYHNNVYKDALLTSFINSATSFIA 359	
hDAT	DFYRLCEASVVIDAATQVCFSLGPGFVLLAFSSYNKFTNNCYRDAIVTTSINSLSFS 360	
hNET	DFYRLKEATVVIDAATQIFFSLGAGFVLLAFASYNKFDNNCYRDALLTSSINCITSFVS 357	
	: : : : * : * : * : * : * : * : * : * : * : * : * : * : * : * : * :	
hSERT	GFVIFTVLGYMAEMRNEVDVSEVAKDAGPSLLFITAYAEAIANMPASTFFAIIFFLMLITLG 435	
dDAT	GFVIFSFLGYMAHTLGVRIEDVAT-EGPGLVFFVYPAAIATMPASTFFWALIFFMMLLTLG 418	
hDAT	GFVVSFLGYMAQKHSVPIGDVAK-DGPGLIIFI IYPEAIATLPLSSAWAVVFFIMLLTLG 419	
hNET	GFAIFSILGYMAHEHKVNIEDVAT-EGAGLVF ILYPEAISTLSGSTFWAVVFFVMLLALG 416	
	* : * : * : * : * : * : * : * : * : * : * : * : * : * : * :	
hSERT	LDSTFAGLEGVITAVLDEFPHVWAKRRERFVLAVVITCFPGSLVTLTFGGAYVVKLLEEY 495	
dDAT	LDSSFGGSEAITALSDEFPKIK-RNRELFVAGLFLSLYFVVGVLACTQGGFYFFHLLDRY 477	
hDAT	IDSAMGGMESVITGLIDEFQLLH-RHRELFVIVLATFLLSLFCVNTGGIYVFTLLDHF 478	
hNET	LDSSMGGMEAVITGLADDFQVLK-RHRKLFVTFVTFSTFLALFICITKGGIYVLTLLDHF 475	
	: * : * : * : * : * : * : * : * : * : * : * : * : * : * :	
hSERT	ATGPAVLTVALIEAVVSWFYGITQFCRDVKEMLGFSPGWFWRICWVAISPLFLFIICS 555	
dDAT	AAGYSILVAVFFEAIASVWIYGTNRFSIEDIRDMIGFPPGRYQVCWRFVAPIFLFITVY 537	
hDAT	AAGTSILFVGLIEAIGVAVFYGVGFSDDIQQMTGQRPSLYWRLCWKLVSPCFLLFVVVV 538	
hNET	AAGTSILFAVLMIEAIGVSWFYGVDRFSNDIQMMGFRPGLYWRLCWKLVSPAFLLFVVVV 535	
	* : * : * : * : * : * : * : * : * : * : * : * : * : * : * :	
hSERT	FLMSPQLRLRFQYNYPYWSIILGYCIGTSSFCIPTIYAYRLIITPGTFKERIISKITPE 615	
dDAT	GLIGYEPLTYADYVYPSWANALGWCIAGSSVMIIPAVAFKLLSTPGSLRQRFITLTPW 597	
hDAT	SIVTFRPPHYGAYIFPDWANALGWVIATXSMAMVPIYAAYKFCSLPGSFREKLAYATAPE 598	
hNET	SIINFKPLTYDDYIFPPWANVWGWGIALSSMLVPIYVIYKFLSTQGSLEWRELAYGITPE 595	
	: : * : * : * : * : * : * : * : * : * : * : * : * : * : * :	
hSERT	TPTEIPCG----DIRLNAV----- 630	
dDAT	RDQQSMAMVNLNGVTTEVTVVRLTDTETAKEPVDV 631	
hDAT	KDRELVDV---GEVRQFTLRHWLKV----- 620	
hNET	NEHHLVAQ---RDIRQFQLQHWLAI----- 617	

Figure 34. Sequence alignments of dDAT, hDAT, hNET, and hSERT for comparison. Asterisks (*) indicate fully conserved amino acid residues, colons (:) indicate moderately conserved residues, and periods (.) indicate weakly conserved residues. Generated using Clustal Omega.

2. Model Generation and Evaluation

For the purposes of model building, the FASTA amino acid sequence for the dDAT template (PDB ID: 4XP6) was retrieved from the Protein Databank. The sequence of hNET was retrieved from the Universal Protein Resource database (UniProt accession code: P23975). These sequences were aligned using Clustal X and adjusted manually to account for sequence modifications to the crystal structure of 4XP6. Modeller v9.14 was used to build a population of 100 models based on this alignment.²⁰¹ The models were assessed on the basis of molpdf, DOPE score, and GA341 score (Table 12). GA341 scores, which assess the quality of models using the percentage sequence identity between model and template as a parameter, can range from zero to one, with a score of one being ideal.^{202,203} All the hNET models had a GA341 score of one, supporting their validity. Higher scores for the modeller objective function (molpdf) are considered ideal,²⁰¹ whereas lower DOPE (discrete optimized protein energy) scores are considered ideal. The DOPE score was used to select the best model, as DOPE is an optimized statistical method for assessing models.²⁰⁴ There is no benchmark for DOPE scores; all scores are relative and arbitrary. The lowest scoring model in the DOPE column was selected for further evaluation (homology model #66).

Table 12. Model evaluation using molpdf, DOPE, and GA341 scores, generated using Modeller v9.14. Conditional formatting was added using Microsoft Excel, using green to indicate relatively superior models on the basis of the scoring function for that column.

Model ID	molpdf	DOPE	GA341
1	2421.04932	-80946.734	1
2	2416.73022	-80840.398	1
3	2258.40137	-80466.148	1
4	2607.85181	-80457.203	1
5	2271.44482	-80720.109	1
6	2404.61133	-80343.016	1

7	2455.85986	-80334.164	1
8	2112.20264	-81030.297	1
9	2424.18335	-80679.773	1
10	2670.10693	-79913.219	1
11	2351.76392	-80887.664	1
12	2098.3147	-80702.273	1
13	2529.13599	-80404.414	1
14	2278.57056	-80643.984	1
15	2353.59277	-81009.648	1
16	2533.14722	-80913.695	1
17	2131.19824	-80772.617	1
18	2281.23096	-80600.289	1
19	2359.65161	-81225.242	1
20	2424.08374	-81164.797	1
21	2371.58667	-80596.969	1
22	2081.18506	-80982.039	1
23	2419.19873	-80890.75	1
24	2237.89258	-80521.883	1
25	2118.3186	-80697.211	1
26	2341.26807	-81039.297	1
27	2085.75781	-80442.164	1
28	2270.28296	-80887.891	1
29	2113.53442	-80824.617	1
30	2263.8186	-81263.703	1
31	2457.58789	-80873	1
32	2850.07983	-80300.164	1
33	2191.68188	-81000.773	1
34	2158.7561	-80540.07	1
35	2218.05664	-80795.469	1
36	2208.14014	-80151.023	1
37	2196.95093	-81002.586	1
38	2351.42041	-80557.898	1
39	2264.92407	-80626.875	1
40	2088.90649	-81059.133	1
41	2321.43286	-80958.469	1
42	2305.40112	-80800.563	1
43	2258.46582	-81222.836	1
44	2287.58594	-80977.406	1
45	2840.82178	-80186.875	1
46	2059.99951	-80844.906	1

47	2199.75562	-81180.797	1
48	2261.15869	-80733.078	1
49	2297.5564	-80903.969	1
50	2178.57251	-80375.148	1
51	2194.84961	-80670.898	1
52	2217.43994	-80835.859	1
53	2373.91528	-81056.742	1
54	2492.0022	-80714.625	1
55	2353.00537	-80898.742	1
56	2115.56787	-80553.297	1
57	2140.40454	-81125.68	1
58	2240.88623	-80981.133	1
59	2538.65967	-80843.594	1
60	2097.5022	-80590.531	1
61	2278.38379	-80965.398	1
62	2315.10254	-80464.977	1
63	2276.68726	-80240.555	1
64	2335.35132	-80978.047	1
65	2237.10986	-80735.789	1
66	2357.88745	-81298.203	1
67	2719.89062	-80617.375	1
68	2160.12109	-80786.305	1
69	2263.10913	-80971.703	1
70	2470.77026	-80265.836	1
71	2497.51489	-80293.984	1
72	2267.38086	-80721.344	1
73	2288.39795	-80812.063	1
74	2744.96997	-80152.367	1
75	2319.60376	-80594.078	1
76	2532.76953	-80920.414	1
77	2246.51392	-80802.156	1
78	2486.87012	-80580.813	1
79	2124.20068	-80516.82	1
80	2309.64868	-80761.984	1
81	2427.55835	-80430.789	1
82	2249.85938	-80793.789	1
83	2205.91138	-80527.406	1
84	2403.64966	-80706.984	1
85	2308.40161	-80717.531	1
86	2163.9563	-80779.164	1

87	2306.92822	-80651.492	1
88	2136.55273	-80786.703	1
89	2386.12451	-80416.367	1
90	2209.34473	-80970.094	1
91	2294.87183	-80202.742	1
92	2180.16797	-81048.109	1
93	2429.8584	-80373.031	1
94	2398.53198	-80368.875	1
95	2369.08984	-80816.422	1
96	2149.12427	-80747.383	1
97	2156.55591	-80753.289	1
98	2252.84424	-80353.633	1
99	2148.31299	-80806.344	1
100	2565.34888	-80920.672	1

PyMOL was used to visualize evaluate homology model #66 (Figure 37A), and PROCHECK was used to evaluate model #66 on the basis of allowed phi and psi angles.²⁰⁵ A Ramachandran plot was generated showing that 95.6% of residues were in the most favored regions, 4.2% were in additional allowed regions, 0.2% were in generously allowed regions, and 0.0% were in disallowed regions (Figure 37B). A model is considered high-quality if it has 90% or greater residues in the favored regions. Model 66, therefore, appears to be a very strong model. The one residue in the generously allowed region (Asp493) was inspected visually using PyMOL (Figure 37C). It was far from the putative binding site, and should not interfere with induced-fit docking studies.

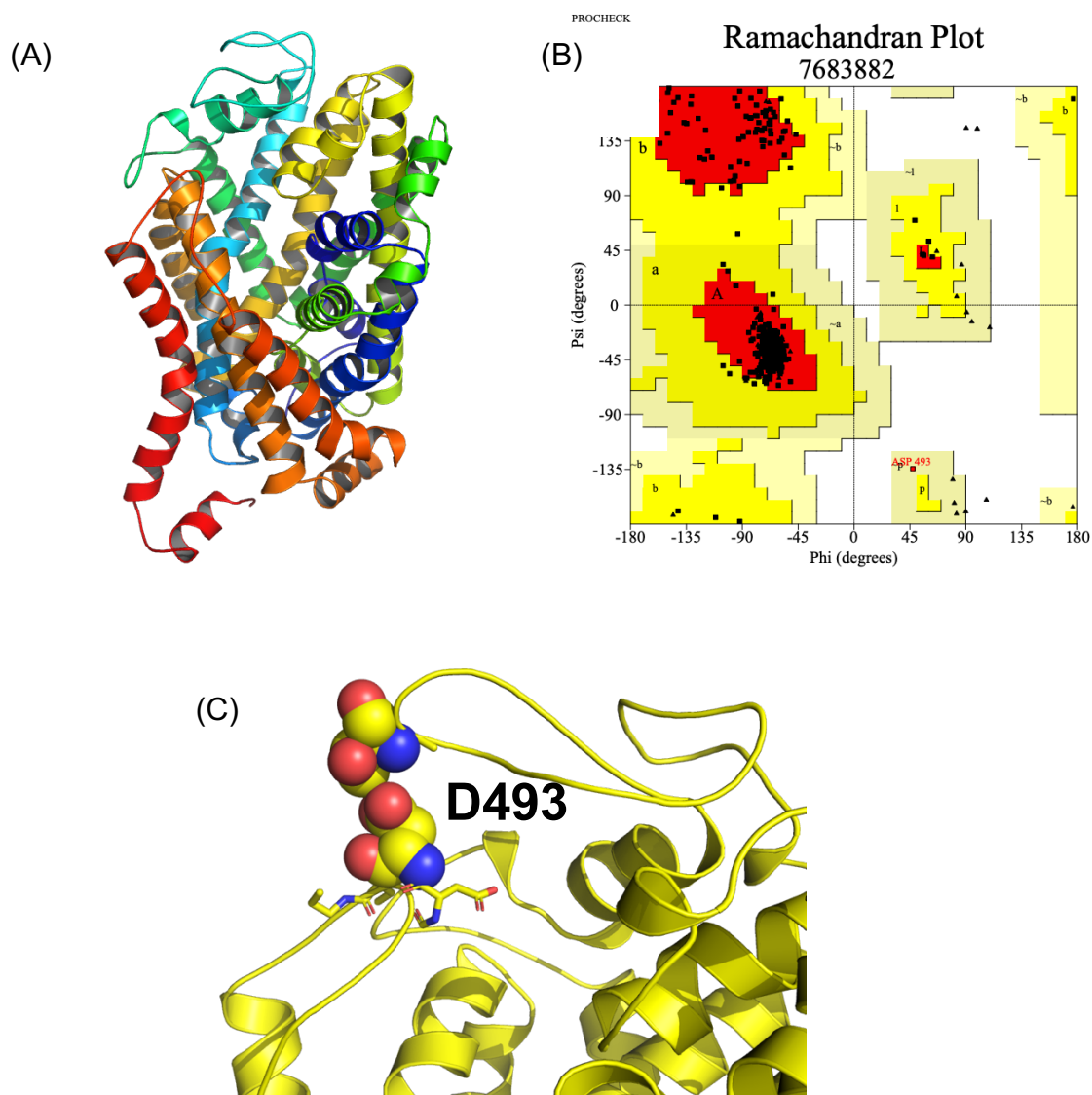


Figure 37. Model evaluation using PyMOL and PROCHECK. (A) Homology model #66 of hNET, generated in PyMOL; (B) Ramachandran plot of homology model #66, generated in PROCHECK; (C) Visualization of Asp493 and surrounding residues, generated in PyMOL.

In addition to evaluating the best model, the population of 100 models was maintained for future studies as a way to account for the plasticity of the substrate binding pocket and account for protein flexibility during docking studies. The consistent score of one using the objective GA341 scoring function supports the use of the entire population of models.

3. Docking endogenous substrates

Both to validate the models, and to gain insight into substrate binding at hNET, the endogenous substrates DA and NE were docked to the population of hNET models. With the common Asp residue (Asp75 for hNET) used to define a 12-Angstrom binding pocket, the substrates were docked to each of the 100 models 10 times using GOLD, thus accounting for both ligand and protein flexibility.

The docking solutions were sorted into clusters by similarity. The top-ranking cluster by GOLD score and population was labeled DA-1. Cluster DA-1 consisted of 62 out of 100 of the top docking solutions, outranking the next cluster in terms of population by 44 solutions, thereby indicating its superiority. This cluster also contained the highest scoring pose, with a GOLD score of 59.4. In this pose, a pi-pi interaction was predicted between the DA aryl ring and Tyr152. Notably, the protonated nitrogen of DA was shifted away from Asp75 (3.9 Å), favoring hydrogen-bonding interactions between the catechol hydroxyl groups and Ala145 and Ser420 (Figure 38A). This served as validation for the model, as the crystal structure of dDAT bound to DA (PDB ID: 4XP1) revealed a similar shift in binding of dopamine relative to the binding of amphetamine or methamphetamine, which favored closeness with the aspartate. This shift was observed in these hNET models, despite having used the methamphetamine-bound (PDB ID: 4XP6) rather than DA-bound (PDB ID: 4XP1) structure as the template (Figure 38B). DA-hNET binding pose and model were aligned with the co-crystal structure dDAT-DA (4XP1) using PyMOL (Figure 39B), resulting in an RMSD value of 0.496 Å.

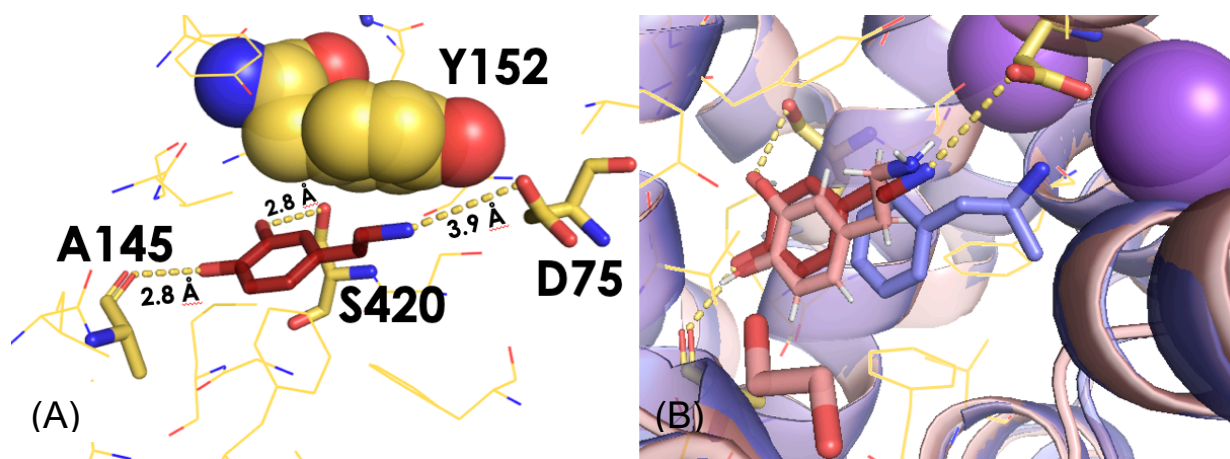


Figure 38. Induced-fit docking pose for DA at hNET. (A) DA-1 with predicted distances from potential residues of interaction emphasized. (B) DA-1 (red), DA as co-crystallized with dDAT (salmon, PDB ID: 4XP1), and methamphetamine as co-crystallized with dDAT (lavender, 4XP6).

For NE, there were two equally populated clusters of binding modes, each with a similar GOLD score. Cluster NE-1 consisted of 26 top poses, with a highest GOLD score of 57.59, and cluster NE-2 also consisted of 26 top poses, with a highest GOLD score of 57.52. In NE-1, the aryl ring of NE was sandwiched between two aromatic residue side-chains, forming pi-pi edge-to-face interactions with Tyr152 on one side, and Phe323 on the other. The β -hydroxyl group was predicted to form a hydrogen bond with the side-chain carbonyl oxygen atom of Phe317, while the NE protonated nitrogen forms ion-dipole interactions and hydrogen bonds with Phe72 and Ala73 (Figure 39A).

In cluster NE-2, the aryl ring was shifted away from the Asp75. However, the amine nitrogen was simultaneously shifted closer to the Asp residue, allowing for ionic interactions and hydrogen bonding. The aromatic interaction with Tyr152 is retained as well (Figure 39B). Cluster NE-2 was similar to DA-1. The two were overlaid in PyMOL, revealing that they were roughly equivalent (RMSD = 0.445; Figure 39D). Interestingly, the fourth-ranking cluster of DA poses by population (DA-4) was visually similar to NE cluster NE-1 (Figure 39C). Cluster DA-4 consisted of four top-scoring binding poses, and had a top GOLD score of 53.89. Cluster DA-4 was rotated at the aryl ring as compared to NE-1, sacrificing edge-to-face aromatic interactions for the less favorable face-to-face interactions, but both occupied roughly the same area in the binding pocket. In DA-4, the distance between the basic nitrogen atom and the aspartate residue was shortened to 2.5 Å, allowing for highly favored ionic interactions and hydrogen bonding.

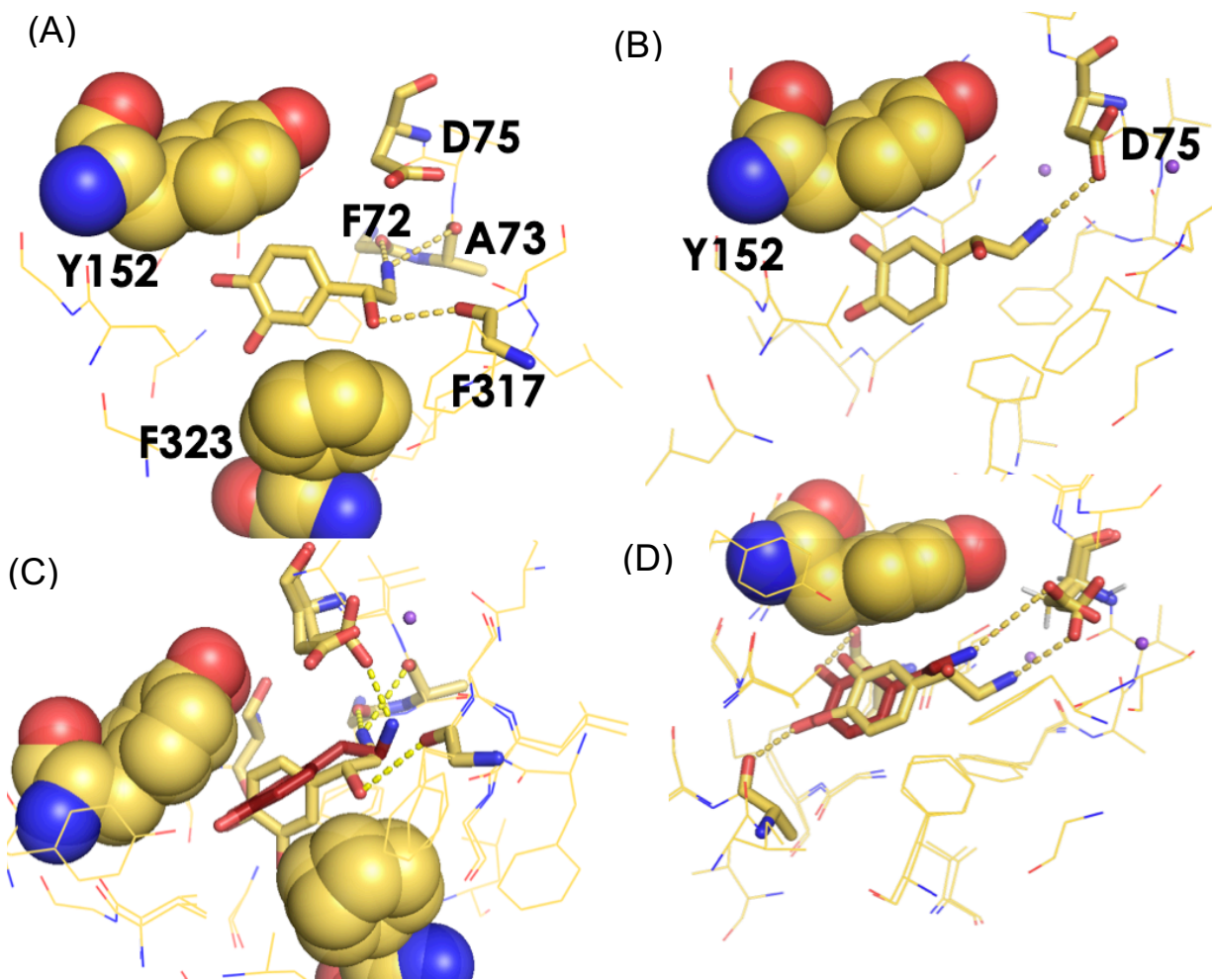


Figure 39. Induced-fit docking poses for NE at hNET. (A) NE-1; (B) NE-2; (C) NE-1 and DA-4 overlaid; (D) NE-2 and DA-1 overlaid. Image generated in PyMOL and Microsoft PowerPoint.

Overall, the docking of endogenous substrates DA and NE served to validate the hNET models further. They could be used to predict shifted binding that was observed in the crystal structure of hDAT, and to predict various modes of interaction, accounting for the dynamic nature of substrate transport. The predicted binding of DA and NE were roughly equivalent, though NE is considered the actual endogenous substrate of hNET. Though unintuitive, the lack of distinction between DA and NE binding is consistent with biological data. Binding studies using radiolabeled β -citalopram have found a negligible difference between DA and NE at hNET ($K_M = 0.24 \mu\text{M}$ and $0.58 \mu\text{M}$, respectively).²⁰⁶ Furthermore, uptake studies have shown that

hNET transports DA at a slightly faster rate (V_{\max} DA = 32 pmol/min/mg protein; V_{\max} NE = 17 pmol/min/mg protein).²⁰⁶ On the other hand, hDAT is more selective.²⁰⁶

4. Insights to MCAT selectivity

Previous modeling studies in our laboratory identified a particular non-conserved residue as responsible for the difference in selectivity of 4-substituted MCAT analogs between DAT and SERT.²⁵ That residue was a serine (Ser149) in hDAT and an alanine (Ala169) in hSERT. As the selectivity for hDAT over hSERT had been correlated with steric bulk (E_s),⁶⁸ volume,⁶⁹ and maximum width (B5) of the substituent,⁶⁹ it was proposed that the larger serine residue in hDAT, which was near the 4-substituent in the models, could not accommodate the larger substituent, thus conferring selectivity to hSERT in the case of a large substituent.

Later, the 4-substituted MCAT series was tested in rat brain synaptosomes at hNET. A high correlation between hDAT and hNET potency was observed.¹⁸¹ Therefore, DAT/SERT selectivity was roughly equivalent to NET/SERT selectivity for this series. In constructing the hNET models, it was expected that the same serine residue would be conserved between hDAT and hNET. However, the alignment of amino acid residues showed that hNET had an alanine residue at that position (Ala145), conserved with hSERT, suggesting that the residue cannot be responsible for the observed selectivity.

Docking studies were conducted to determine whether another residue in the region of the 4-substituent, which was not conserved between hDAT and hSERT, could explain the selectivity between the MATs. All residues that were conserved between hDAT and hNET, but non-conserved between hDAT and hSERT (highlighted in green in Table 13), were visualized after docking the series of 4-substituted MCAT analogs compounds at all three MAT models and

identifying common binding modes. All non-conserved residues were sterically more bulky in hSERT than in hDAT and hNET, ruling them out, with one exception: an alanine residue (Ala81 and Ala77 in hDAT and hNET, respectively) is a glycine residue in hSERT (Gly100). On the basis of these docking studies, these non-conserved residues appeared to be too far from the ligand to account for the discrepancy. In Figure 40, they are the top-most residue in the image of each MAT, showing its distance from the MCAT 4-substituent. On the basis of these docking studies, it seems unlikely that a non-conserved residue in the binding pocket can explain the selectivity of 4-substituted MCATs between hDAT and hSERT.

Table 13. Alignment of binding site residues between hDAT, hNET, and hSERT. Conserved alanine residue between hNET and hSERT highlighted in red. All those residues that are not conserved between hNET and hSERT are highlighted in green.

hDAT	F76	A77	V78	D79	L80	A81	N82	I148	S149	L150	V152		
hNET	F72	A73	V74	D76	L76	A77	N78	I144	A145	L146	V148		
hSERT	Y95	A96	V97	D98	L99	G100	N101	I168	A169	F170	I172		
hDAT	G153	F155	Y156	N157	C319	F320	S321	L322	G323	F326	V328	S422	A423
hNET	G149	Y151	Y152	N153	F316	F317	S318	L319	G320	F323	V325	S419	S420
hSERT	A173	Y175	Y176	N177	F334	F335	S336	L337	G338	F341	V343	S438	T439

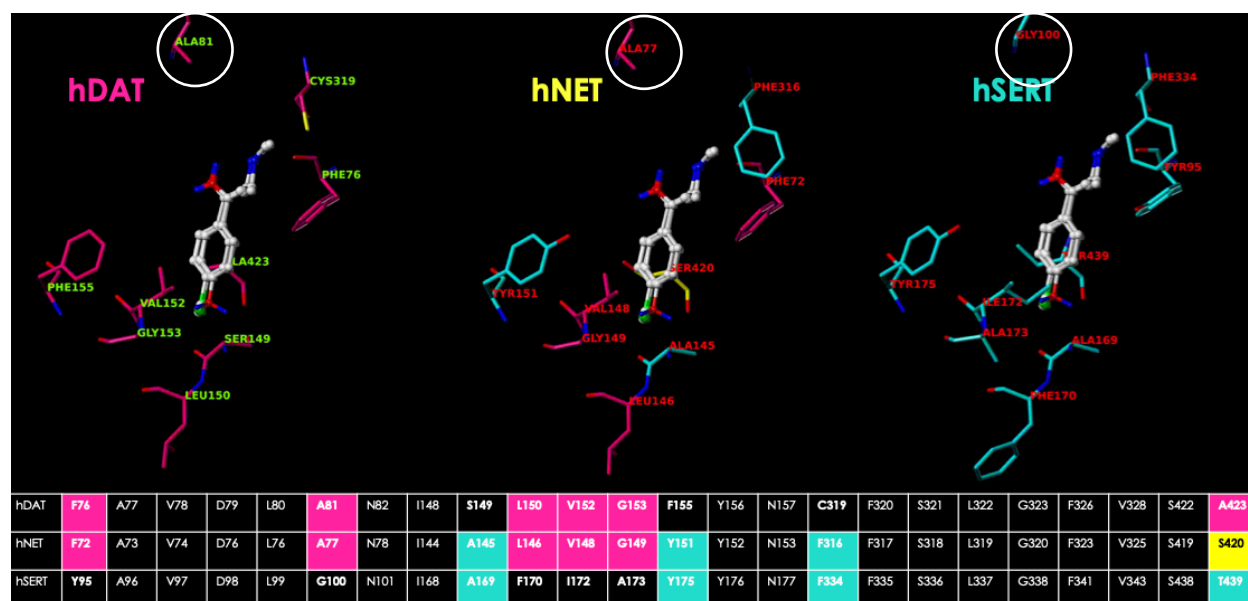


Figure 40. Side-by-side comparison of the docked 4-substituted MCATs at hDAT, hNET, and hSERT, with the alignment of their binding-site residues displayed below. In the hNET model, magenta and blue have been used to indicate residues conserved with hDAT and hSERT, respectively. The only residues that were conserved between hDAT and hNET (A81 and A77, respectively), but smaller in hSERT (G100) are circled in white.

Alternative means of evaluating the differences in the hDAT/hNET/hSERT binding pockets were considered. The volume of the binding pockets were calculated using Sybyl-X 2.1. The hSERT binding pocket was calculated to be substantially smaller (94 \AA^3) than the hDAT and hNET binding pockets, which were equal in size to one another (157 \AA^3). These values were in keeping with observations gleaned from the alignment of the binding site residues, which were mostly sterically larger in hSERT, but counterintuitive to the QSAR determined for the 4-MCAT series, in which a larger size molecule was favored at hSERT. Steric hindrance seemed unlikely to be the determining factor, and so it was hypothesized that the larger size of substituent might instead allow greater opportunity for hydrophobic interactions.

There was one exception to the conclusion that the alanine/serine non-conserved residue does not control selectivity. In the case of 4-methoxy-MCAT, unlike all the other compounds, the potencies at hNET and hSERT were similar, and dissimilar from hDAT ($EC_{50} = 111$ nM, 120 nM, and 506 nM, respectively). This is also the only long substituent of the series, and length was notably not found as a correlate of DAT/SERT selectivity. It is possible that the alanine/serine non-conserved residue controls selectivity in the case of long substituents, as shown in Figure 41.

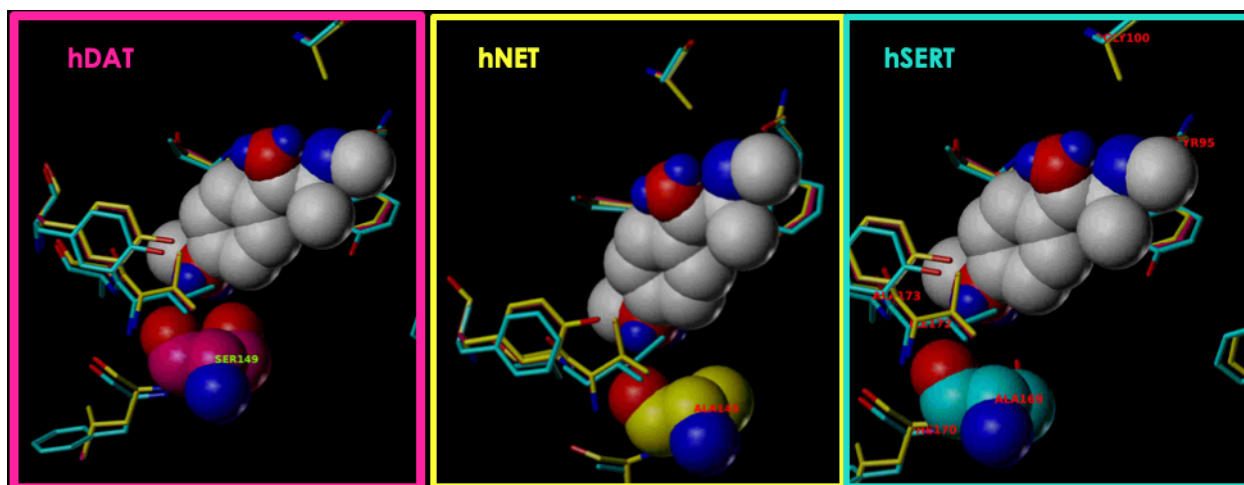


Figure 41. Docked poses of 4-methoxyMCAT at hDAT, hNET, and hSERT. Highlighted is a residue conserved between hNET and hSERT, but not hDAT. Image generated in Sybyl-X 2.1.

To further investigate and quantify hydrophobic interactions for substrates at MATs, Hydrophatic INTeraction (HINT) studies were conducted.²⁰⁷ Previous HINT studies had been conducted using the docked 4-MCATs at hSERT and hDAT. Here, HINT studies were conducted for the docked 4-MCATs at hNET, and compared to those from earlier investigations. The previous investigations had focused exclusively on the HINT scores for interactions with the 4-position substituent, so these were calculated for hNET as well (Table 14).

Table 14. HINT Scores for 4-MCATs at MATs.

Agent	HINT Score		
	hDAT	hNET	hSERT
MCAT	0	0	0
4-Fluoro-MCAT	22	15	51
4-MeO-MCAT	-88	-136	125
4-Methyl-MCAT	-23	-7	136
4-Cl-MCAT	2	-22	135
4-Br-MCAT	-13	-31	78
4-CF ₃ -MCAT	-5	16	97

Pearson correlational analysis was conducted between potency and HINT score for each MAT to test whether relationships existed between the potencies at individual transporters and polar or nonpolar interactions. Supporting the hypothesis that larger substituents provide opportunity for more favorable interactions at hSERT, significant correlations were found for polar contributions and hydrophobic contributions to hSERT potency, but not for either of the other transporters (Table 15).

Table 15. Pearson correlation between HINT scores and potency at individual transporters.

	Pearson Correlation: HINT and LogEC ₅₀		
	hDAT	hNET	hSERT
Total	R = 0.044 P = 0.93	R = 0.033 P = 0.94	R = -0.864 P = 0.01
Polar contribution	R = 0.103 P = 0.84	R = -0.036 P = 0.94	R = 0.841 P = 0.02
Hydrophobic contribution	R = 0.057 P = 0.90	R = 0.078 P = 0.87	R = -0.910 P < 0.01

V. Conclusions

These studies represent progress towards constructing comprehensive SAR for synthetic cathinones and related agents, with particular attention to the α -carbon atom. They represent the first studies of the MCAT isomers at MATs, and the first systematic SAR study of aryl substitution of α -pyrrolidinophenones. Additionally, synthetic strategies were developed and synthetic targets prepared to be used in further SAR studies, as well as drug development in the case of therapeutic ATS. Finally, a population of hNET models were produced, facilitating insights to substrate selectivity at MATs and completing the MAT docking picture.

In the first known studies to evaluate MCAT isomers at MATs, we find only a small (1.3-fold) difference in the potency between *S*(-)**5**, *R*(+)**5**, and (\pm)**5** is less than 1.3-fold at hDAT. However, considerable differences were found for the isomers at hSERT, suggesting hSERT is less tolerant of *R*-isomers for synthetic cathinone substrates, as greater hDAT selectivity has also been observed for *R*-mephedrone in other studies.¹⁵² In future studies, it might be of interest to test whether *R*-isomers of synthetic cathinone substrates are reliably more selective for hDAT over hSERT by evaluating a series of 4-substituted MCATs. The MCAT isomers, racemate, and achiral analogs **26** and **27** are at the time of writing being evaluated in ICSS to determine their abuse-related effects. As hDAT/hSERT selectivity predicts abuse potential, the *R* isomer may show greater abuse-related effects in the ICSS study. Though the compounds are all more selective for hDAT by greater than 20-fold, the *R*(+)**5** is completely hDAT selective, even when testing it at hSERT at concentrations over 3-fold higher than the EC₅₀ of *S*(-)**5**. This, without paying much of a penalty in potency at hDAT. The gem-dimethyl analog is the least selective for

hDAT, suggesting diminished abuse potential. It is also slightly less potent at hDAT. The *gem*-dimethyl modification should be more thoroughly investigated for therapeutic applications, as a moderate potency at hDAT and a diminished abuse potential could be clinically useful.

Though the chiral center seems preferred, the study goal to remove it was realized in both achiral MCAT analogs. Both were active as substrates, suggesting that either achiral modification might be a viable pathway for future studies and drug development. Indeed, these scaffolds are found among phenylalkylamines available for clinical use (i.e., phentermine, phenylephrine, Figure 42), though they have not been observed in clinically used cathinones. The chiral center is preferable, but the *gem*-dimethyl compound was less potent by only 2-fold, suggesting the penalty is minor for this modification.

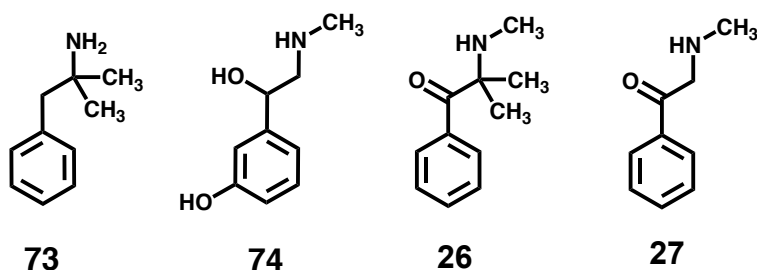


Figure 42. Clinically available achiral phenylalkylamines phentermine (**73**) and phenylephrine (**74**), alongside structurally similar achiral MCAT analogs from these studies **26** and **27**.

Future SAR studies at the β -carbon atom might be able to utilize either achiral modification to the α -carbon atom to facilitate the investigation. The *gem*-dimethyl scaffold might be a superior choice, as it is only two-fold less potent than the racemate, and isomers, as opposed to the des-methyl modification, which is 10-fold less potent. Further studies are needed to fully validate this design concept. Parallel SAR studies utilizing the *gem*-dimethyl modification might be of interest.

The use of $K_2CO_3/MeOH$ in the introduction of the amine via bromine substitution was found to be necessary for the *gem*-dimethyl product. This step theoretically allows the substitution to proceed via an epoxide intermediate that prevents the formation of the Michael addition product observed in the course of these studies. A mechanism was proposed herein for the Michael product. Forgoing this step might result in Michael addition products for other target compounds, resulting in synthetic difficulties and inefficiency of SAR investigations. Literature support exists for the utility of these reagents to produce amines through an epoxide intermediate. Stevens and Chang²⁰⁸ first wrote about the utility of “epoxy ethers” in the formation of “alpha-amino ketones” (i.e., cathinones) in 1962. De Kimpe et al.²⁰⁹ proposed a mechanism for the epoxide intermediate in the synthesis of similar compounds in 1983. Further synthetic studies might compare the routes with and without $K_2CO_3/MeOH$ for other target *gem*-dimethyl cathinones, to further establish the necessity of these reagents and the relationship to the *gem*-dimethyl chemical environment.

These studies demonstrate that there are multiple viable routes to alpha-pyrrolidinophenone analogs. The one-pot method described by Guha et al.¹⁹⁵ was a particularly useful method, as it utilized less toxic, more environmentally friendly reagents, simplified several steps into one and, unlike the Friedel-Craft’s-based approach, allows for access to analogs with a wide variety of *para*-substituents, including strongly electron-withdrawing groups (e.g. 4- CF_3).

These SAR studies were enriched by the addition of molecular modeling, in which a population of hNET models were produced. The inclusion of these models allowed for insight into the nature of substrate discrimination at the MATs. On the basis of endogenous substrate docking, it was concluded that substrate selectivity between hNET and hDAT is unlikely to

occur in the predicted hNET binding pocket. This pocket is non-discriminatory between DA and NE, in keeping with biological data. On the other hand, hDAT is more selective, transporting its endogenous substrate DA at a significantly higher rate, and binding DA with greater selectivity.²⁰⁶ Further studies might benefit from docking the endogenous substrates NE and DA at hDAT and comparing the binding modes to those obtained here at hNET.

A population of hNET models was included for the first time in the examination of synthetic cathinone interactions with MATs. This allowed for an update to a previously published model of the structural basis for hDAT/hSERT selectivity among synthetic cathinone substrates. An alanine residue, which was proposed to be responsible for hDAT/hSERT selectivity in a series of aryl-substituted MCAT analogs,⁶⁹ was in fact conserved between hSERT and hNET, despite the high correlation between hDAT and hNET substrate activity.¹⁸¹ On the basis of these studies, it was concluded that the previous explanation could no longer be accepted as the primary deciding factor in hDAT/hSERT selectivity. As no other non-conserved residues between hDAT and hSERT in the region of the varied substituent could be identified, it can be concluded that other aspects of substrate transport are more important to substrate selectivity. Such features are important to understand, as the hDAT/hSERT ratio is clearly important to abuse potential.^{68,152} Future studies might include blind docking to the MAT models used in these studies, or docking to potential allosteric sites.

There was one caveat to the dismissal of the alanine/serine residue model for explaining substrate selectivity. In the 4-substituted MCAT series, one compound (4-methoxy-MCAT) was similar in potency between hNET and hSERT, and not hDAT. For all the other compounds tested, the hNET and hDAT values were very similar (Table 8). Methoxy was the only long substituent tested, and this could be more important when it comes to steric hindrance with the

hDAT serine residue. Further studies might investigate other 2-atom-length substituents or longer at this position, testing the hypothesis that one could develop a substrate selective for hNET and hSERT over hDAT. Such compounds would be predicted to be of reduced abuse potential, and potentially high in therapeutic potential.

In future studies, the 4-ethyl-MCAT might be a valuable target compound, as it would be isosteric to the 4-methoxy-MCAT, but without the hydrogen-bonding potential of the oxygen atom. If a similar correlation between hSERT and hNET was found for this compound, it would support the hypothesis that length at this position can bias the compounds in favor of hSERT. This would be valuable information for discriminating between compounds of high abuse and therapeutic potential in future drug development efforts. The 4-ethyl-MCAT compound would also be valuable to test in order to further test the parallel SAR concept that is tenuously proposed based on these investigations of α -pyrrolidinophenones.

Overall, there are many long-term translational applications to this project, particularly in informing development of agents for the treatment of StUD and other mental health disorders. In terms of regulatory issues, the applications are more direct. Over the past century, the prohibition of psychoactive and addictive substances has driven the development of more potent compounds on the basis of the iron law (i.e., it is more efficient to illicitly transport pure ethanol or “moonshine” than diluted formulations like beer, so that is what was manufactured during alcohol prohibition). Over the past decade, with the emergence of internet drug markets and the development of clandestine chemistry infrastructure in India, China, and Mexico, the problem of high-potency NPS has accelerated, and the “khat and mouse game” between clandestine chemists and regulators got out of control. The synthetic cathinones are a case in point, as the scheduling of the original “bath salts” constituents directly led to the development and marketing

of novel pyrrolidinophenone analogs, such as α -PHP, that were dramatically increased in potency and hDAT-selectivity.

The natural next step for regulatory authorities is to schedule α -PHP, along with other emerging synthetic cathinones. Our studies suggest that this effort would be futile and counter-productive. The chemical space of synthetic cathinones is wide open with compounds that are potent hDAT releasers or blockers, including the achiral MCAT analogs and the aryl-substituted PHPs of these investigations. It is entirely possible that an even more dangerous synthetic cathinone is around the corner from the next scheduling motion.

VI. Experimentals

A. Synthesis

Compound identity was determined by proton nuclear magnetic resonance spectrometry (^1H NMR), infrared (IR) spectroscopy, melting point (mp), and mass spectrometry (MS). Purity was determined by carbon, hydrogen, and nitrogen elemental analysis (CHN), which was conducted by Atlantic Microlab Inc. (Norcross, GA). The compounds were considered pure if the experimental values were within 0.4% of those calculated on the basis of theory. Melting points were obtained using a Thomas-Hoover melting point apparatus and are uncorrected. ^1H NMR spectra were obtained using a Bruker ARX 400 MHz spectrometer with tetramethylsilane as an internal standard. IR was conducted on a Thermo Nicolet instrument. Where flash chromatography was used, this was performed on a CombiFlash Companion/TS (Telodyne Isco Inc., Lincoln, NE) with RediSep Rf normal-phase silica flash columns as stationary phases, and silica gel (230-400 mesh) as adsorbent. Reaction monitoring was accomplished by thin-layer chromatography with silica gel plates (250 μ , 2.5 \times 10 cm; Analtech Inc., Newark, DE). MS was obtained using electrospray ionization in positive ion mode. Optical rotation, where necessary, was obtained using a Jasco P-2000 polarimeter with a sodium lamp. Water-soluble salts of final target compounds were prepared (hydrochloride or oxalate) for the purposes of biological studies.

α -Methylaminoisobutyrophenone Hydrochloride (26)

Compound **26** is known,²¹⁰ but was synthesized according to a patent procedure for a similar compound.¹⁹³ In a sealed tube at room temperature, **40** (3.00 g, 13.2 mmol) was added to a stirred solution of potassium carbonate (5.53 g, 39.6 mmol) in MeOH (75 mL). The reaction

mixture was allowed to stir for 5 h, at which time methylamine gas was bubbled in. The temperature was increased to 57 °C, and the mixture stirred overnight. Upon cooling to room temperature, Et₂O (50 mL) was added to dilute the mixture, which was then filtered. Solvent was evaporated under reduced pressure, and the resulting crude mixture was dissolved in EtOAc, then acidified and extracted with HCl (1 M, 5 mL, 6x). The aqueous portion was basified with NaOH (1 M, 50 mL), and extracted with EtOAc (30 mL). The combined organic portion was dried (Na₂SO₄), and solvent was removed under reduced pressure, to yield 1.40 g of the free base as a yellow oil.

The free base was dissolved in EtOAc (30 mL), a saturated solution of gaseous HCl in Et₂O (10 mL) was added, and the reaction mixture was allowed to stir at room temperature for 2 h. The solvent was removed by filtration to yield a white powder that was recrystallized from EtOH/Et₂O to yield 0.60 g (21%) of **26** as a white solid: mp 218-220 °C (lit.²¹⁰ mp 212-214 °C); ¹H NMR (DMSO-*d*₆) δ 1.75 (s, 6H, 2 x CH₃), 2.53 (s, 3H, CH₃), 7.57 (dd, *J* = 7.6, 7.9 Hz, 2H, ArH), 7.70 (t, *J* = 7.4, 1H, ArH), 7.95 (dd, *J* = 8.5, 1.2, 1H, ArH), 9.49 (br s, 2H, NH²⁺).

2-Methylamino-1-phenylethan-1-one Hydrochloride (27)

Compound **27** was prepared in a three-step reaction sequence in which the intermediates were used directly without further purification, as described by Sakloth, but their transformations are described here individually (**47**, **48**). Compound **27** is known in the literature,⁷² but synthesis by this method was reported to result in low yields by Sakloth, so the compound was made by a literature procedure for similar compounds.²¹¹ AlCl₃ (9.20 g, 69 mmol) was added in a portionwise manner to a stirred solution of **48** (61 mmol) in anhydrous benzene (40 mL) under

an N₂ atmosphere. The stirred reaction mixture was heated at reflux for 4 h, allowed to cool to room temperature, quenched by addition of conc. HCl (12 mL) and ice (10 g). The organic layer was separated, washed with saturated NaHCO₃ (3 x 15 mL) and brine (2 x 10 mL), dried (Na₂SO₄), and evaporated under reduced pressure. The resulting brown oil was then dissolved in conc. HCl (50 mL) and *i*-PrOH (75 mL) and stirred at 40 °C for 48 h. The solvent was evaporated to yield 0.50 g of residue, which was recrystallized twice from *i*-PrOH to yield 0.56 g of **27** (5%) as off-white crystals: mp 205-208 °C (lit.⁷² mp 219 °C). Though the observed mp is lower than the reported lit. mp, it was exactly consistent with the mp obtained by Sakloth (unpublished data). ¹H NMR (DMSO-*d*⁶) δ 2.63 (s, 3H, CH₃), 4.77 (s, 2H, CH₂), 7.60 (t, *J* = 7.7 Hz, 2H, ArH), 7.74 (t, *J* = 7.8 Hz, 1H, ArH), 8.00 (d, *J* = 7.4 Hz, 2H, ArH), 9.48 (br s, 2H, NH⁺).

***α*-gem-Dimethyl-*α*-pyrrolidinopropiophenone Hydrochloride (28)**

The compound is known in the patent literature without physical data, and was synthesized according to its literature procedure.¹⁹³ In a 2-neck flask under nitrogen, **40** (0.57 g, 2.5 mmol) was added to a stirred solution of potassium carbonate (1.00 g, 7.2 mmol) in MeOH (5.0 mL). After three hours of stirring at room temperature, pyrrolidine (0.53 g, 7.5 mmol) was added, and the mixture was stirred at reflux overnight (14 h). Upon cooling the reaction mixture to room temperature, EtOAc (75 mL) was added to dilute the mixture, which was then filtered. Solvent was removed from the filtrate under reduced pressure, and the resulting crude mixture was dissolved in EtOAc (75 mL) and washed with H₂O (20 mL). The mixture was acidified and extracted with HCl (1 N, 2 mL, 3x), the resulting aqueous portion of which was basified with NaOH (3 M, 2 mL) and extracted with EtOAc (10 mL). The organic portion was dried (Na₂SO₄)

and solvent was removed under reduced pressure, resulting in a yellow liquid (0.10 g), which solidified upon cooling.

The free base was dissolved in Et₂O (30 mL), a saturated solution of gaseous HCl in Et₂O (5 mL) was added, and the reaction mixture was allowed to stir at room temperature for 2 h. The solvent was removed by filtration to yield a white powder that recrystallized from EtOH/Et₂O to afford 0.08 g (13%) of **28** as a white solid: mp 134-137 °C (EtOH/Et₂O); ¹H NMR (DMSO-*d*₆) δ 1.80 (s, 6H, 2 x CH₃), 1.92-2.00 (m, 4H, 2 x CH₂), 3.17-3.40 (m, 4H, 2 x CH₂), 7.36 (m, 2H, ArH), 6.67-7.77 (m, 1H, ArH), 7.92 (d, *J* = 7.4, 2H, ArH), 11.0 (br s, 1H, NH⁺); Anal. Calcd. For (C₁₄H₁₉NO•HCl•0.2H₂O) C, 65.33; H, 7.99; N, 5.44. Found: C, 65.29; H, 7.71; N, 5.36.

α-Pyrrolidinohexanophenone Oxalate (29)

The compound is known,²⁵ and was synthesized according to the literature procedure. Compound **50** (11.3 g, 44 mmol) was stirred in pyrrolidine (6.0 mL) overnight (24 h). Et₂O (50 mL) was added to dilute the mixture, followed by acidification and extraction with HCl (3 N, 20 mL, 3x). The combined aqueous portion of was basified with NaHCO₃ (200 mL) and extracted with Et₂O (3 x 15 mL). The combined organic portion was washed with brine, dried (Na₂SO₄), and solvent was removed under reduced pressure, resulting in a brown liquid (4.48 g), which was dissolved in Et₂O and added dropwise to a saturated solution of oxalic acid (1.8 g) in Et₂O (129 mL). The mixture was allowed to stir at room temperature overnight. The solvent was removed by filtration to yield a white powder that recrystallized from *i*-PrOH to afford 4.37 g (29%) of **29** as a white solid: mp 128-130 °C (*i*-PrOH; lit.²⁵ mp 129-131 °C); ¹H NMR (DMSO-*d*₆) δ 0.76 (t, *J* = 7.1, 3H, CH₃), 0.98-1.08 (m, 4H, 2 x CH₂), 1.89-1.96 (m, 6H, 3 x CH₂), 2.07-2.09 (m, 4H, 2 x

CH₂), 3.15 (br s, 1H, OH), 4.8-5.0 (m, 1H, CH), 7.56-7.63 (m, 2H, ArH), 7.75 (t, $J = 7.4$, 1H, ArH), 8.06-8.08 (m, 2H, ArH).

4-Methyl- α -pyrrolidinohexanophenone Hydrochloride (30)

The compound is known in a patent with no physical data,²¹² but was synthesized according to a different procedure for similar compounds.¹⁹⁵ Under open atmosphere and constant stirring, *N*-bromosuccinimide (1.21 g, 6.8 mmol) was added directly to **65** (1.01 g, 5.26 mmol) at room temperature. The mixture turned yellow, then orange, and released a burst of brown gas over the course of 2 min, at which time 1,4-dioxane (4 mL) was added. After 10 min of stirring, pyrrolidine (1.3 mL, 1.12 g, 16 mmol) was added dropwise to the mixture, which became cloudy and colorless, then returned to clear yellow. The mixture was allowed to stir, loosely covered, at room temperature for 36 h. The mixture was washed with NaHCO₃ (20 mL), then acidified with HCl (1N, 50 mL, to pH 1). The aqueous portion was separated, basified with NaOH (3M, 50 mL, to pH 13), and extracted with EtOAc (3 x 20 mL). The combined organic portion was dried (Na₂SO₄) and evaporated under reduced pressure, resulting in a yellow-colored oil.

The yellow oil was dissolved in anhydrous Et₂O (5 mL) at room temperature. Under constant stirring, a saturated solution of gaseous HCl in Et₂O (10 mL) was added) and the reaction mixture was allowed to stir at room temperature overnight. The solvent was evaporated to yield a brown solid that was recrystallized from acetonitrile to yield 0.23 g (15%) of **30** as a beige solid: mp 179-182 °C (acetonitrile); ¹H NMR (DMSO-*d*₆) δ 0.77 (t, $J = 7.1$ Hz, 3H, CH₃), 0.99-1.29 (m, 4H, 2 x CH₂), 1.94-2.09 (m, 6H, 3 x CH₂), 2.45 (s, 3H, CH₃), 3.05-3.07 (m, 1H, CH₂), 3.20-3.29 (m, 1H, CH₂), 3.49-3.51 (m, 1H, CH₂), 3.63-3.64 (m, 1H, CH₂), 5.47-5.50 (m, 1H, CH), 7.47 (d,

$J = 8.1$ Hz, 2H, ArH), 8.02 (d, $J = 8.3$ Hz, 2H, ArH), 10.47 (br s, 1H, NH⁺); Anal. Calcd for (C₁₇H₂₅NO•1.0 HCl•0.6 H₂O) C, 66.58; H, 8.94; N, 4.57. Found: C, 66.56; H, 8.83; N, 4.47; HRMS-ESI⁺ (m/z) calcd for C₁₇H₂₆NO⁺ (M+H⁺) 260.2014, found 260.2017, calcd for C₁₇H₂₅NONa⁺ (M+Na⁺) 282.1834, found 282.1831.

4-Methoxy- α -pyrrolidinohexanophenone Hydrochloride (31)

The compound is previously unknown. It was prepared according to a general procedure for substitution of a halogen by an amine. Compound **62** (460 mg, 1.8 mmol) was stirred in pyrrolidine (2.0 mL, 24.0 mmol) for 1 h at room temperature. The stirred reaction mixture was quenched by careful addition of ice-cold H₂O (10 mL), acidified with HCl (6 N, 3 x 5 mL, to pH 1), and extracted with EtOAc (3 x 10 mL). The combined acidic portion was basified with NaOH (3 M, 3 x 5 mL, to pH 13), and re-extracted with Et₂O (3 x 15 mL). The combined organic portion was washed with brine (15 mL), dried (Na₂SO₄), and evaporated under reduced pressure. The crude free base was dissolved in anhydrous Et₂O (2 mL), to which saturated ethereal HCl solution was added dropwise at -78 °C (dry ice/acetone) under constant stirring. The mixture was allowed to stir at room temperature for 24 h, after which the solvent was evaporated to yield a white solid that was recrystallized from acetonitrile to yield 97 mg (19%) of **31** as white needles: mp 195-198 °C; ¹H NMR (DMSO-*d*₆) δ 0.76 (t, $J = 7.1$ Hz, 3H, CH₃), 1.01-1.26 (m, 4H, 2 x CH₂), 1.93-2.09 (m, 6H, 3 x CH₂), 3.00-3.01 (m, 1H, CH₂), 3.17-3.25 (m, 1H, CH₂), 3.36-3.48 (m, 1H, CH₂), 3.60-3.61 (m, 1H, CH₂), 3.90 (s, 3H, CH₃), 5.43-5.51 (m, 1H, CH), 7.16 (d, $J = 8.8$ Hz, 2H, ArH), 8.08 (d, $J = 8.9$ Hz, 2H, ArH), 10.28 (br s, 1H, NH⁺); Anal. Calcd for (C₁₇H₂₅NO₂·HCl) C, 65.48; H, 8.40; N, 4.49. Found: C, 65.76; H, 8.54; N, 4.46.

4-Ethyl- α -pyrrolidinohexanophenone Hydrochloride (32)

The compound is previously unknown. It was prepared according to a general procedure for substitution of a halogen by an amine. Compound **63** (520 mg, 1.8 mmol) was stirred in pyrrolidine (2.0 mL, 24.0 mmol) for 1 h at room temperature. The stirred reaction mixture was quenched by careful addition of ice-cold H₂O (10 mL), acidified with HCl (1 N, 3 x 15 mL, to pH 1), and extracted with Et₂O (3 x 5 mL). The combined acidic portion was basified with NaOH (3 M, to pH 13), and re-extracted with Et₂O (3 x 15 mL). The combined organic portion was washed with brine (15 mL), dried (Na₂SO₄), and evaporated under reduced pressure. The crude free base was dissolved in anhydrous Et₂O (2 mL), to which saturated ethereal HCl solution was added dropwise at -78 °C (dry ice/acetone) under constant stirring. The mixture was allowed to stir at room temperature for 24 h, solids were collected by filtration and recrystallized from acetonitrile to yield 152 mg (27%) of **32** as yellow crystals: mp 182-184 °C; ¹H NMR (DMSO-*d*₆) δ 0.75 (t, *J* = 7.0 Hz, 3H, CH₃), 0.92-1.27 (m, 7H, 2 x CH₂, CH₃), 1.87-2.09 (m, 6H, 3 x CH₂), 2.73 (q, *J* = 7.6 Hz, 2H, CH₂), 2.97-3.10 (m, 1H, CH₂), 3.21-3.28 (m, 1H, CH₂), 3.45-3.49 (m, 1H, CH₂), 3.60-3.61 (m, 1H, CH₂), 5.42-5.47 (m, 1H, CH), 7.49 (d, *J* = 8.2 Hz, 2H, ArH), 8.01 (d, *J* = 8.3 Hz, 2H, ArH), 10.24 (br s, 1H, NH⁺); Anal. Calcd for (C₁₈H₂₇NO·HCl) C, 69.77; H, 9.11; N, 4.52. Found: C, 69.81; H, 9.21; N, 4.57.

4-Chloro- α -pyrrolidinohexanophenone Hydrochloride (33)

The compound is unknown, and was synthesized according to a procedure for similar compounds.¹⁹⁵ Under open atmosphere and constant stirring, *N*-bromosuccinimide (5.49 g, 31 mmol) was added directly to **66** (5.08 g, 24 mmol) at room temperature. The temperature was increased to 30 °C, and the mixture was stirred for 1 h. Upon the release of brown gas, 1,4-

dioxane (10 mL) was added. The mixture turned clear yellow after 10 min of stirring at room temperature, and pyrrolidine (5.90 mL, 5.09 g, 72 mmol) was added dropwise. The mixture was allowed to stir, loosely covered, at room temperature overnight. The mixture was washed with NaHCO₃ (20 mL) and extracted with EtOAc (3 x 20 mL). To the organic portion was added HCl (3N, 15 mL, to pH 1), and the aqueous portion was separated, basified with NaHCO₃ (3M, 50 mL, to pH 13), and extracted with EtOAc (3 x 20 mL). The combined organic portion was dried (Na₂SO₄) and evaporated under reduced pressure, resulting in 3.5 g of a crude brown oil.

The residual oil was dissolved in anhydrous Et₂O (5 mL) at room temperature. Under constant stirring, a saturated solution of gaseous HCl in Et₂O (10 mL) was added and the reaction mixture was allowed to stir at room temperature overnight. The precipitate was filtered to yield a brown solid that was recrystallized from *i*-PrOH/Et₂O resulting in 0.15 g (2%) of **33** as an off-white powder: mp 198-200 °C; ¹H NMR (DMSO-*d*₆) δ 0.74 (t, *J* = 7.2 Hz, 3H, CH₃), 0.89-1.27 (m, 4H, 2 x CH₂), 1.93-2.05 (m, 6H, 3 x CH₂), 3.07-3.29 (m, 2H, CH₂), 3.41-3.61 (m, 2H, CH₂), 5.54-5.55 (m, 1H, CH), 7.72 (d, *J* = 8.6 Hz, 2H, ArH), 8.10 (d, *J* = 8.6 Hz, 2H, ArH), 10.59 (br s, 1H, NH⁺); Anal. Calcd for (C₁₆H₂₂ClNO•HCl) C, 60.76; H, 7.33; N, 4.43. Found: C, 60.66; H, 7.21; N, 4.53.

4-Bromo- α -pyrrolidinohexanophenone Hydrochloride (34)

The compound is previously unknown. It was prepared according to a general procedure for substitution of a halogen by an amine. Compound **64** (860 mg, 2.6 mmol) was stirred in pyrrolidine (3.0 mL, 36.0 mmol) for 30 min at room temperature. The stirred reaction mixture was quenched by careful addition of ice-cold H₂O (10 mL), acidified with HCl (2 N, to pH 1),

and extracted with Et₂O (3 x 10 mL). The combined acidic portion was basified with NaOH (15%, 20 mL, to pH 13), and re-extracted with Et₂O (3 x 20 mL). The combined organic portion was washed with brine (15 mL), dried (Na₂SO₄), and evaporated under reduced pressure. The residual oil was purified by flash chromatography (silica gel; hexanes/EtOAc; 95/5 to 80/20) to afford the free base as a yellow oil. The free base was dissolved in anhydrous Et₂O (2 mL) under N₂ atmosphere, and HCl gas was bubbled in. The precipitate was recrystallized from acetonitrile to yield 152 mg (27%) of **34** as an off-white powder: mp 199-201 °C; ¹H NMR (DMSO-*d*₆) δ 0.75 (t, *J* = 6.7 Hz, 3H, CH₃), 1.19 (m, 1H, CH₂), 1.78-1.94 (m, 3H, 2 x CH₂), 1.78-2.05 (m, 6H, 3 x CH₂), 2.99-3.07 (m, 1H, CH₂), 3.21 (m, 1H, CH₂), 3.49 (m, 1H, CH₂), 3.61 (m, 1H, CH₂), 5.39-5.58 (m, 1H, CH), 7.88 (d, *J* = 7.6 Hz, 2H, ArH), 8.01 (d, *J* = 8.5 Hz, 2H, ArH), 10.38 (br s, 1H, NH⁺); Anal. Calcd for (C₁₆H₂₂BrNO·HCl·0.4 H₂O) C, 52.23; H, 6.52; N, 3.81. Found: C, 52.01; H, 6.30; N, 3.96.

4-Trifluoromethyl- α -pyrrolidinohexanophenone Hydrochloride (35)

The compound is unknown, and was synthesized according to a procedure for similar compounds.¹⁹⁵ Under open atmosphere and constant stirring, *N*-bromosuccinimide (2.08 g, 11.7 mmol) was added directly to **67** (2.21g, 9.0 mmol) at room temperature. The temperature was increased to 30 °C, and the mixture was stirred for 40 min. Upon the release of brown gas, 1,4-dioxane (10 mL) was added. After stirring the reaction mixture for 10 min, pyrrolidine (2.21 mL, 1.92 g, 26.9 mmol) was added to the mixture, dropwise. The mixture was allowed to stir, loosely covered, at room temperature overnight. The mixture was quenched carefully with NaHCO₃ (20 mL) at 0 °C and extracted with Et₂O (3 x 20 mL). To the organic portion was added HCl (3N, 15 mL, to pH 1), and the aqueous portion was separated, basified with NaHCO₃ (3M, 50 mL, to pH

13), and extracted with Et₂O (3 x 20 mL). The combined organic portion was dried (Na₂SO₄) and evaporated under reduced pressure. The resulting crude oil was dissolved in anhydrous Et₂O (5 mL) at room temperature. Under constant stirring, gaseous HCl was bubbled in and the reaction mixture was allowed to stir at room temperature overnight. The precipitate was filtered to yield a brown solid that was recrystallized from EtOH/Et₂O resulting in 0.17 g (5%) of **35** as a white powder: mp 219-222 °C; ¹H NMR (DMSO-*d*₆) δ 0.74 (t, *J* = 7.2 Hz, 3H, CH₃), 0.99-1.25 (m, 4H, 2 x CH₂), 1.96-2.07 (m, 6H, 3 x CH₂), 3.13-3.26 (m, 2H, CH₂), 3.52-3.62 (m, 2H, CH₂), 5.61 (m, 1H, CH), 8.03 (d, *J* = 8.1 Hz, 2H, ArH), 8.28 (d, *J* = 8.2 Hz, 2H, ArH), 10.59 (br s, 1H, NH⁺); Anal. Calcd for (C₁₇H₂₂F₃NO•HCl) C, 58.37; H, 6.63; N, 4.00. Found: C, 58.18; H, 6.45; N, 3.99.

α-Ethyl-4-methylmethamphetamine Hydrochloride (36)

The compound is known,²¹³ but was synthesized by two different methods for comparison. The first (Method A) was a procedure for a similar compound, as this procedure had been used successfully by others in the lab.¹⁹⁶ The second (Method B) followed a literature procedure for similar compounds.¹⁹⁷

Method A

Methylamine (21.5 mL, 40% in H₂O, 248 mmol) was diluted with MeOH (34 mL) and adjusted to pH 6 with HOAc (15 mL) at 0 °C. Compound **53** (0.44 g, 2.7 mmol) was added to the stirred solution along with additional MeOH (20 mL), and followed by NaB(CN)H₃ (0.53 g, 8.5 mmol). The ice bath was removed and gas evolution was observed. The contents were allowed to stir at room temperature for 40 min, then were quenched by the careful addition of NaOH (3M, 5 mL),

extracted with EtOAc (10 mL), and dried (Na₂SO₄). Solvent was removed under reduced pressure, and the resulting gummy solid was dissolved in EtOH (5 mL). A saturated hydrochloric acid solution in anhydrous Et₂O (5 mL) was added and the mixture was allowed to warm to room temperature and stirred overnight. The precipitate was collected by filtration to yield a white-colored solid which upon recrystallization from EtOH/Et₂O afforded 0.030 g (5%) of **36** as a white solid: mp 159-160 °C (lit.²¹³ mp 159°C); IR (solid, cm⁻¹) 1447, 2463, 2709, 2745, 3187; ¹H NMR (DMSO-*d*₆) δ 0.89 (t, *J* = 7.5 Hz, 3H, CH₃), 1.46-1.63 (m, 2H, CH₂), 2.29 (s, 3H, CH₃), 2.54 (s, 3H, CH₃), 2.74 (dd, *J* = 9.3, 13.7 Hz, 1H, CH₂), 3.07 (dd, *J* = 4.7, 13.7 Hz, 1H, CH₂), 7.13-7.22 (m, 4H, ArH), 8.99 (br s, 2H, NH₂⁺).

Method B

Methylamine (16 mL, 33% in EtOH, 130 mmol), **53** (0.23 g, 1.4 mmol) and platinum (II) oxide (5.0 mg, 0.020 mmol) in EtOH (25 mL) were shaken with hydrogen gas (>50 psi) at room temperature. The reaction never went to completion, but was stopped after 72 hours and filtered to remove the catalyst. The mixture was evaporated to dryness under reduced pressure, resulting in a yellow mixture of oil and solid, which was diluted with Et₂O (10 mL) and filtered. The mixture was acidified with HCl (1N, to pH 1) and extracted with deionized water (35 mL). The aqueous portion was basified with NaOH (3M, to pH 13), and extracted with Et₂O (10 mL). The combined organic portion was dried (Na₂SO₄), and solvent was removed under reduced pressure to yield 160 mg of yellow oil. A saturated HCl solution in anhydrous EtOAc (3 mL) was added, and the mixture was stirred at room temperature for 30 hours. The precipitate was collected by filtration to yield a white solid which, upon recrystallization from EtOH, afforded 23 mg (8%) of **36** as a white solid: mp 158-159 °C (lit.²¹³ mp 159°C); IR (solid, cm⁻¹) 2463; ¹H NMR (DMSO-

d_6) δ 0.89 (t, $J = 7.5$ Hz, 3H, CH₃), 1.46-1.63 (m, 2H, CH₂), 2.29 (s, 3H, CH₃), 2.54 (s, 3H, CH₃), 2.74 (dd, $J = 9.3, 13.7$ Hz, 1H, CH₂), 3.07 (dd, $J = 4.7, J = 13.7$, 1H, CH₂), 7.13-7.22 (m, 4H, ArH), 8.99 (br s, 2H, NH₂⁺).

***N*-Methyl-1-(*p*-tolyl)pentan-2-amine Hydrochloride (37)**

To a solution of **68** (150 mg, 0.63 mmol) in TFA (5.0 mL) at room temperature was added palladium on carbon (10%, 0.085). The mixture was shaken at 55 psi until the pressure was reduced to 50 psi (1 h), at which time pressure was restored to 55 psi, and the mixture allowed to shake for 60 h. The reaction was stopped by the addition of NaHCO₃ and filtered to remove the catalyst. The mixture was extracted with Et₂O (3 x 10 mL). The combined organic portion was dried (Na₂SO₄), and solvent was removed under reduced pressure to yield 160 mg of yellow oil. A saturated HCl solution in anhydrous Et₂O (3 mL) was added, and the mixture was stirred at room temperature for 30 hours. The precipitate was collected by filtration to yield a white-colored solid which, upon recrystallization from EtOH, afforded **37** as a white solid: mp 162-167 °C; ¹H NMR (DMSO- d_6) δ 0.80 (t, $J = 7.2$ Hz, 3H, CH₃), 1.17-1.40 (m, 4H, 2 x CH₂), 2.29 (s, 3H, CH₃), 2.72 (dd, $J = 9.1, 13.7$ Hz, 1H, CH₂), 3.01-3.08 (m, 2H, CH + CH₂), 7.14-7.20 (m, 4H, ArH), 8.64 (br s, 2H, NH₂⁺); Anal. Calcd. for (C₁₃H₂₁N·HCl·0.7 H₂O) C, 64.95; H, 9.81; N, 5.83. Found: C, 65.13; H, 9.74; N, 6.15.

***R*(-)*N*-Ethylamphetamine Hydrochloride (*R*(-)-38)**

The compound is known,²¹⁴ but it was synthesized according to a new procedure. The Kondekar procedure was used as a guideline.²¹⁵ Aqueous ethylamine (70%, 19 mL, 230 mmol) was added

to a solution of *S*(+)**58** (2.5 g, 12 mmol) in DMF (70 mL) at room temperature. After the mixture was stirred at 50 °C for 36 h, another portion of aqueous ethylamine solution (70%, 5.0 mL, 63 mmol) was added. The resulting mixture was stirred for 12 h at 50 °C, and another portion of ethylamine (70%, 7.0 mL, 88 mmol) was added. After stirring for another 12 h at 50 °C, the mixture was diluted with Et₂O (100 mL) and water (30 mL). The aqueous phase was extracted with Et₂O (3 x 50 mL) and washed with brine (3 x 20 mL). The combined extracts were dried (Na₂SO₄), and the solvent was evaporated under reduced pressure to yield 1.4 g of oil. The oil was dissolved in anhydrous Et₂O (5 mL), and a saturated HCl solution in anhydrous Et₂O (5 mL) was added. The mixture was allowed to stir overnight. The precipitate was collected by filtration to yield a white solid, which upon recrystallization from EtOH/Et₂O afforded 0.38 g (16%) of *R*(-)**38** as a white solid: mp 152-154 °C (lit.²¹⁴ mp 155 °C); ¹H NMR (DMSO-*d*₆) δ : 1.09 (d, *J* = 6.5 Hz, 3H, CH₃), 1.25 (t, *J* = 7.2 Hz, 3H, CH₃), 2.63 (dd, *J* = 2.4 Hz, 10.5 Hz, 1H, CH₂), 2.92-3.06 (m, 2H, CH₂), 3.27 (dd, *J* = 3.6, 9.4 Hz, 1H, CH₂), 3.35-3.39 (m, 1H, CH), 7.25 (d, *J* = 3.0 Hz, 1H, ArH), 7.27 (s, 2H, ArH), 7.34 (dd, *J* = 7.1, 7.6 Hz, 2H, ArH), 9.12 (br s, 2H, NH₂⁺); α _D²⁰ = -17.7 ° (*c* = 0.99 H₂O); Anal. Calcd for (C₁₁H₁₇N•HCl) C, 66.15; H, 9.08; N, 7.01. Found: C, 65.96; H, 9.13; N, 6.92.

***S*(+)*N*-Ethylamphetamine Hydrochloride (*S*(+)**38**)**

The compound is known,²¹⁴ but it was synthesized according to a new procedure. The Kondekar procedure for similar compounds was used as a guideline.²¹⁵ Aqueous ethylamine (70%, 20 mL, 240 mmol) was added to a solution of *R*(-)**58** (3.5 g, 16 mmol) in DMF (70 mL) at room temperature. After the mixture was stirred at 50 °C for 32 h, another portion of aqueous ethylamine solution (9.0 mL, 110 mmol) was added. The resulting mixture was stirred overnight

(12 h) at 50 °C, and another portion of ethylamine (9.0 mL, 110 mmol) was added. After stirring for another 24 h at 50 °C, the mixture was diluted with Et₂O (100 mL) and water (30 mL). The aqueous phase was extracted with Et₂O (3 x 40 mL) and washed with brine (3 x 20 mL). The combined extracts were dried (Na₂SO₄), and solvent was evaporated under reduced pressure to yield 1.60 g of yellow liquid. A saturated HCl solution in anhydrous Et₂O (20 mL) was added to a solution of this liquid dissolved in anhydrous Et₂O (10 mL); this mixture was allowed to warm to room temperature and stirred overnight. The precipitate was collected by filtration to yield a white solid, which upon recrystallization from EtOH/Et₂O afforded 0.41 g (13%) of *S*(+)**38** as a white solid: mp 152-154 °C (lit.²¹⁴ mp 154.2 °C); ¹H NMR (DMSO-*d*₆) δ: 1.09 (d, *J* = 6.5 Hz, 3H, CH₃), 1.25 (t, *J* = 7.2 Hz, 3H, CH₃), 2.63 (dd, *J* = 2.4 Hz, 10.5 Hz, 1H, CH₂), 2.92-3.06 (m, 2H, CH₂), 3.27 (dd, *J* = 3.6, 9.4 Hz, 1H, CH₂), 3.35-3.39 (m, 1H, CH), 7.25 (d, *J* = 3.1 Hz, 1H, ArH), 7.27 (s, 2H, ArH), 7.34 (dd, *J* = 7.1, 7.6 Hz, 2H, ArH), 9.12 (br s, 2H, NH₂⁺); α^D₂₀ = +15.9 ° (*c* = 1.0 H₂O).

α-Bromoisobutyrophenone (40)

Compound **40** was synthesized according to a modified literature procedure for the same compound.¹⁹¹ Bromine (3.2 g, 20 mmol) diluted 10-fold with CHCl₃ (8.9 mL) was added in a dropwise manner to a stirred solution of isobutyrophenone (3.0 g, 20 mmol) in CHCl₃ (15 mL). The reaction mixture was allowed to stir at room temperature overnight (24 h), at which time it was extracted with CHCl₃ (40 mL), washed with NaHCO₃ (50% aq., 50 mL) and brine (15 mL), and dried (Na₂SO₄). Solvent was removed under reduced pressure to yield 4.9 g (>99%) of **40** as a yellow liquid (>99%) that was used without further purification. ¹H NMR (CDCl₃) δ 2.04 (s,

6H, 2 x CH₃), 7.45 (t, *J* = 7.4 Hz, 2H, ArH), 7.53 (t, *J* = 7.4 Hz, 1H, ArH), 8.12 (d, *J* = 7.4 Hz, 2H, ArH).

3-(Benzyl(methyl)amino)-2-methyl-1-phenylpropan-1-one Oxalate (41)

The compound is known in the literature as a free base,²¹⁶ but was prepared according to the general method of Blough et al.¹⁹² for substitution of a halogen by *N*-benzylmethylamine. In a 2-neck flask, *N*-benzylmethylamine (3.0 g, 12 mmol) was added to a stirred solution of **40** (1.5 g, 6 mmol) in THF (10 mL). The mixture was stirred at reflux overnight (24 h). Upon cooling to room temperature, THF was removed under reduced pressure, and the mixture was dissolved in EtOAc (50 mL). The mixture was washed with saturated NaHCO₃ (50 mL) and DIH₂O (100 mL). The organic portion was washed with brine, dried (Na₂SO₄), and solvent was removed under reduced pressure. The crude base was purified by flash chromatography (silica gel; hexanes/EtOAc; 75/25), resulting in 1.5 g (91%) of the free base as an oil. After difficulty making the HCl salt, the oxalate salt was prepared by stirring a portion of the free base (0.2 g) in a saturated solution of oxalic acid (74 mg) in Et₂O (20 mL) for 72 h at room temperature. The solids were filtered and dried in an abderhalden, resulting in 0.2 g (64%) of **41** as a white powder: mp 165-180 °C (Et₂O); ¹H NMR (DMSO-*d*₆) δ 1.13 (d, *J* = 6.9 Hz, 3H, CH₃), 2.12 (s, 3H, CH₃), 2.42 (dd, *J* = 7.2 Hz, 5.3 Hz, 1H, CH₂), 2.81 (dd, *J* = 7.2 Hz, 5.3 Hz, 1H, CH₂), 3.44 (d, *J* = 2.9 Hz, 2H, CH₂), 3.62-3.71 (m, 1H, CH), 7.12-7.17 (m, 5H, ArH), 7.37-7.41 (m, 2H, ArH), 7.47-7.51 (m, 1H, ArH), 7.87-7.90 (m, 2H, ArH); Anal. Calcd. For C₁₈H₂₁NO•(COOH)₂: C, 67.21; H, 6.49; N, 3.92. Found: C, 67.11; H, 6.44; N, 3.93.

N-Trifluoroacetyl Sarcosine (47)

Compound **47** was prepared by a literature procedure for the same compound.²¹⁷ Trifluoroacetic anhydride (8.60 mL, 61.78 mmol) was added in a dropwise manner at 0 °C to a stirred suspension of sarcosine (5.00 g, 56.16 mmol) in anhydrous CH₂Cl₂ (14 mL) under an N₂ atmosphere. The reaction mixture was allowed to stir at room temperature for 2 h. The solvent was evaporated under reduced pressure to give 11.3 g (>99%) of **47** as a yellow solid that was used without further purification.

N-Trifluoroacetyl Sarcosinyl Chloride (48)

Compound **48** was known in the literature without any physical data,²¹⁷ but was prepared according to a literature procedure for the same compound.²¹¹ Oxalyl chloride (5.7 mL, 8.57 g, 68 mmol) was added in a dropwise manner over 5 min to a stirred solution of **47** (11.3 g, 185 mmol) and pyridine (3 drops) in anhydrous benzene (22 mL) under an N₂ atmosphere. The stirred reaction mixture was heated at reflux for 1 h, allowed to cool to room temperature and solvents were removed under reduced pressure to give a brown-colored liquid that was brought under N₂ atmosphere and used directly without further purification, to avoid degradation.

α-Bromohexanophenone (50)

The compound is known, and was prepared according to the method described previously,²⁵ but using Et₂O as a solvent. Bromine (9.06 g, 57 mmol) was added at 0 °C (ice-bath) to a stirred solution of hexanophenone (10 g, 57 mmol) in anhydrous Et₂O (20 mL). The reaction mixture was stirred at room temperature for 2 h. The reaction was quenched by the careful addition of H₂O (100 mL) and extracted with Et₂O (3 x 25 mL). The combined organic portion was washed

with brine (40 mL), dried (Na₂SO₄), and evaporated under reduced pressure to afford 11.3 g (78%) of **50** as a clear yellow oil: ¹H NMR (CDCl₃) δ 0.93 (t, *J* = 7.1 Hz, 3H, CH₃), 1.33-1.56 (m, 4H, 2 x CH₂), 2.08-2.26 (m, 2H, CH₂), 5.12 (t, *J* = 7.1 Hz, 1H, CH), 7.49 (t, *J* = 7.6 Hz, 2H, ArH), 7.57-7.61 (m, 1H, ArH), 8.01 (dd, *J* = 8.2, 1.0 Hz, 2H, ArH).

1-(*p*-Tolyl)-2-nitrobut-1-ene (52)

The compound is known, and was synthesized generally following a modified version of the published procedure.¹⁹⁸ Different quantities were used because they were working on a much larger scale, different times were used to allow the reaction to reach completion, and flash chromatography was used instead of distillation because previous attempted purification by Kugelrohr was unsuccessful. In a 3-neck flask, *p*-tolualdehyde (1.00 g, 8.3 mmol) and 1-nitropropane (0.74 g, 8.3 mmol) were added to a stirred solution of NH₄OAc (0.33 g, 4.3 mmol) in HOAc (4.2 mL). The stirred reaction mixture was heated at reflux overnight (19.5 h), cooled to room temperature, and solvent was evaporated under reduced pressure. The resulting orange-colored oil was purified by flash chromatography (silica gel; 100% hexanes) to afford 0.72 g (45%) of **52** as a yellow oil: ¹H NMR (CDCl₃) δ 1.41 (t, *J* = 7.4 Hz, 3H, CH₃), 2.53 (s, 3H, CH₃), 3.01 (q, *J* = 7.4 Hz, 2H, CH₂), 7.39 (d, *J* = 3.9, 2H, ArH), 7.46 (d, *J* = 8.18, 2H, ArH).

1-(*p*-Tolyl)butan-2-one (53)

The compound is known,²¹⁸ but was synthesized by a procedure for a similar compound because the one for similar compounds was used with success by others in the lab.¹⁹⁶ Iron powder (2.70 g, 44.9 mmol) was added to a stirred solution of aqueous HOAc (90%) at room temperature. Temperature was increased to 60 °C followed by dropwise addition of **52** (0.75 g) to the mixture.

After stirring for 20 min, during which time gas evolution and a reddening of color was observed, the mixture was quenched carefully with H₂O (20 mL), extracted with EtOAc (20 mL), dried (Na₂SO₄) and evaporated to dryness under reduced pressure. The mixture was purified by flash chromatography (silica gel; 100% hexanes) and solvent removed under reduced pressure, resulting in 0.43 g (68%) of **53** as a yellow oil: ¹H NMR (CDCl₃) δ 1.18 (t, *J* = 7.1 Hz, 3H, CH₃), 2.26 (s, 3H, CH₃), 2.35-2.41 (m, 2H, CH₂), 2.34 (s, 2H, CH₂), 7.01-7.07 (m, 4H, ArH).

1-(*p*-Tolyl)hexan-1-ol (54)

The compound is known, but was synthesized according to a literature procedure for a similar compound.¹⁹⁴ To a stirred solution of *p*-tolualdehyde (1.2 g, 10 mmol) in THF (10 mL), under N₂ at 5 °C, was added butylmagnesium chloride in THF (2 M, 10 mL). The reaction mixture was allowed to stir at room temperature overnight (17 h), at which time it was cooled below 5 °C and quenched carefully with H₂O (5 mL) and HCl (2 N, 10 mL). A white precipitate was observed. Extraction with THF (3 x 10 mL) resulted in a pale-yellow liquid which was dried (Na₂SO₄), and evaporated under reduced pressure to yield a clear purple liquid. This was further purified by Kugelrohr and flash chromatography (silica gel; hexanes/EtOAc, 70:30) to afford **54** as a clear, colorless oil (0.75 g, 42%). ¹H NMR (CDCl₃) δ 0.886 (t, *J* = 7.0 Hz, 3H, CH₃), 1.20-1.29 (m, 2H, CH₂), 1.31-1.44 (m, 2H, CH₂), 1.65-1.85 (m, 2H, CH₂), 2.35 (s, 3H, CH₃), 4.61-4.65 (m, 2H, CH₂), 7.16 (d, *J* = 7.9 Hz, 2H, ArH), 7.24 (d, *J* = 8.0 Hz, 2H, ArH).

2-(Benzyl(methyl)amino)-1-(*p*-tolyl)pentan-1-one (55)

The compound is unknown, but was synthesized according to a procedure for similar compounds.¹⁹⁵ Under open atmosphere and constant stirring, *N*-bromosuccinimide (0.97 g, 5.4

mmol) was added directly to **54** (0.75 g, 4.2 mmol) at room temperature. The mixture turned yellow, then orange, and released a burst of brown gas over the course of 2 min, at which time 1,4-dioxane (4.0 mL) was added, resulting in a clear yellow solution. After 10 min of stirring, *N*-benzylmethylamine (1.3 mL, 12 mmol) was added dropwise, and the mixture became cloudy and colorless, then returned shortly to yellow. It was allowed to stir, loosely covered, at room temperature for 36 h. The reaction was quenched carefully with NaHCO₃ (20 mL), extracted with EtOAc (3 x 20 mL), dried (Na₂SO₄), and evaporated to dryness under reduced pressure, resulting in a yellow liquid that was further purified by flash chromatography (silica gel; hexanes/EtOAc, 95:5). This afforded 0.68 g (55%) of **55** as a yellow oil: ¹H NMR (CDCl₃) δ 0.94 (t, *J* = 7.4 Hz, 3H, CH₃), 1.26-1.37 (m, 2H, CH₂), 1.66-1.75 (m, 1H, CH₂), 1.88-1.97 (m, 1H, CH₂), 2.26 (s, 3H, CH₃), 2.41 (s, 3H, CH₃), 3.69 (dd, *J* = 10.6, 13.6 Hz, 2H, CH₂), 4.16 (dd, *J* = 3.5, 5.2 Hz, 1H, CH), 7.22-7.30 (m, 7H, ArH), 7.83 (d, *J* = 8.2 Hz, 2H, ArH).

***R*(-)-1-Phenylpropan-2-ol (*R*(-)**57**)**

The compound is not known, but it was synthesized according to a procedure for similar compounds.²¹⁹ In a 2-neck flask, under N₂ atmosphere, at -60 °C, CuI (1.14 g, 6.0 mmol) was added to solution of phenylmagnesium bromide (1 M, 30.0 mmol) in anhydrous THF (15 mL). The reaction mixture was allowed to stir for about 30 min, when a solution of *R*(-)-propylene oxide (1.8 g, 30.0 mmol) in 15 mL of anhydrous THF was added slowly with a syringe. Stirring was continued for 2 h at -60 °C and for 24 h at room temperature. The reaction mixture was quenched (NH₄Cl), and the aqueous phase was extracted with EtOAc (3 x 50 mL). The combined organic portions were washed with brine, dried (MgSO₄), and evaporated under reduced pressure to give an oil. The crude compound was purified using flash chromatography

(silica gel; hexanes/EtOAc; 88/12) to afford 3.60 g of *R*(-)**57** (89%) as a clear, colorless oil. ¹H NMR (CDCl₃) δ: 1.17 (d, *J* = 6.1 Hz, 3H, CH₃), 1.44 (d, *J* = 3.4 Hz, OH), 2.61 (dd, *J* = 7.9, 13.6 Hz, 1H, CH), 2.72 (dd, *J* = 4.8, 13.6 Hz, 1H, CH), 3.89-4.00 (m, 1H, CH), 7.10- 7.18 (m, 3H, ArH), 7.24 (dd, *J* = 6.9, 7.5 Hz, 2H, ArH); α^D₂₀ = - 32.7 (*c* = 2.2 CHCl₃).

***S*(+)-1-Phenylpropan-2-ol (*S*(+)**57**)**

This compound was prepared by U. Battisti. The compound is not known, but it was synthesized according to a procedure for similar compounds.²¹⁹ This procedure was used because it allows for stereospecific phenylpropan-2-ol synthesis. In a 2-neck flask under N₂ atmosphere at -35 °C, CuI (1.14 g, 6.0 mmol) was added to solution of phenylmagnesium bromide (1 M, 30.0 mmol) in anhydrous THF (30 mL). The reaction mixture was allowed to stir for about 30 min, when a solution of *S*(+)-propylene oxide (1.75 g, 30.0 mmol) in 15 mL of anhydrous THF was added slowly with a syringe. Stirring was continued for 2 h at -35 °C and for 2 h at room temperature. The reaction mixture was quenched with aqueous ammonium chloride solution, and the aqueous phase was extracted with EtOAc (3 x 40 mL). The combined organic portions were washed with brine, dried (MgSO₄), and evaporated under reduced pressure to give a black oil. The crude compound was purified using flash chromatography (silica gel; hexanes/EtOAc; 80/20) to afford 4.08 g of *S*(+)**57** (99%) as a colorless oil. ¹H NMR (CDCl₃) δ: 1.17 (d, *J* = 6.1 Hz, 3H, CH₃), 1.44 (d, *J* = 3.4 Hz, OH), 2.61 (dd, *J* = 7.9, 13.6 Hz, 1H, CH), 2.72 (dd, *J* = 4.8, 13.6 Hz, 1H, CH), 3.89-4.00 (m, 1H, CH), 7.10- 7.18 (m, 3H, ArH), 7.24 (dd, *J* = 6.9, 7.5 Hz, 2H, ArH); α^D₂₀ = + 37.1 (*c* = 1.0 CHCl₃).

***R*(-)-1-Phenylpropan-2-yl Methanesulfonate (*R*(-)-58)**

The compound is not known but it was synthesized according to a procedure for similar compounds.²¹⁵ Methanesulfonyl chloride (4.40 g, 39 mmol) was added dropwise over 15 min to an ice-cold stirred solution of *R*(-)**57** (3.50 g, 26 mmol) and Et₃N (7.9 g, 78 mmol) in anhydrous CH₂Cl₂ (30 mL). The resulting mixture was allowed to warm to room temperature and stirred for 12 h. After the addition of CH₂Cl₂ (100 mL), the solution was washed with water (3 x 40 mL) and brine, dried (Na₂SO₄), and evaporated under reduced pressure. The crude product was further purified by flash chromatography (silica gel; hexanes/EtOAc; 80/20) to afford 4.50 g (81%) of *R*(-)**58** as yellow crystals. ¹H NMR (CDCl₃) δ: 1.40 (d, *J* = 6.2 Hz, 3H, CH₃), 2.43 (s, 3H, SO₂CH₃), 2.83 (dd, *J* = 5.3, 13.9 Hz, 1H, CH), 2.91 (dd, *J* = 8.1, 13.9 Hz, 1H, CH), 4.73-4.89 (m, 1H, CH), 7.11-7.21(m, 3H, ArH), 7.22-7.29 (m, 2H, ArH); α^D₂₀ = -35.2 (*c* = 1.2 CHCl₃).

***S*(+)-1-Phenylpropan-2-yl Methanesulfonate (*S*(+)-58)**

The compound was synthesized by U. Battisti. The compound is not known but it was synthesized according to procedure for similar compounds.²¹⁵ Methanesulfonyl chloride (6.5 g, 45.0 mmol) was added dropwise over 15 min to an ice-cold stirred solution of *S*(+)**57** (4.08 g, 30 mmol) and Et₃N (9.1 g, 90 mmol) in anhydrous CH₂Cl₂ (50 mL). The resulting mixture was allowed to warm to room temperature and stirred for 12 h. After the addition of CH₂Cl₂ (25 mL), the solution was washed with water (3 x 30 mL) and brine, dried (Na₂SO₄), and evaporated under reduced pressure. The crude product was purified by flash chromatography (silica gel; hexanes/EtOAc; 80/20) to afford 5.6 g (87%) of *S*(+)**58** as yellow crystals: mp 60-62 °C; ¹H NMR (CDCl₃) δ: 1.40 (d, *J* = 6.2 Hz, 3H, CH₃), 2.43 (s, 3H, SO₂CH₃), 2.83 (dd, *J* = 5.3, 13.9 Hz,

1H, CH), 2.91 (dd, $J = 8.1, 13.9$ Hz, 1H, CH), 4.73-4.89 (m, 1H, CH), 7.11-7.21(m, 3H, ArH), 7.22-7.29 (m, 2H, ArH); $\alpha_{D_{20}} = +35.0$ ($c = 1.1$ g CHCl_3).

4-Methoxyhexanophenone (59)

Compound **59** is known, and was synthesized according to a literature procedure for the same compound.²²⁰ In a 2-neck flask, hexanoyl chloride (1.4 g, 10.2 mmol) was added to a solution of AlCl_3 (1.36 g, 10.2 mmol) in anhydrous DCM (10 mL) under a N_2 atmosphere and cooled to -10 °C (salt/ice-bath). The contents were allowed to stir at -10 to -5 °C for 10 min. A solution of anisole (1.00 g, 9.3 mmol) in anhydrous DCM (10 mL) was added in a dropwise manner over 30 min at -10 to -3 °C. The ice bath was removed and the contents were allowed to stir at room temperature for 1 h, quenched by the careful addition of ice-cold HCl (1N, 50 mL), and extracted with DCM (3x 20 mL). The combined organic portion was washed with brine (20 mL), dried (Na_2SO_4), and evaporated under reduced pressure to yield 1.71 g (90%) of **59** as a yellow-colored waxy solid: mp 34 - 36 °C (lit.²²⁰ mp 38 °C); ^1H NMR (CDCl_3) δ 0.91 (t, $J = 5.5$ Hz, 3H, CH_3), 1.32-1.41 (m, 4H, 2 x CH_2), 1.67-1.76 (m, 2H, CH_2), 2.90 (t, $J = 7.3$, 2H, CH_2), 3.86 (s, 3H, CH_3), 7.93 (d, $J = 7.0$, 2H, ArH), 7.94 (d, $J = 8.9$, 2H, ArH).

4-Ethylhexanophenone (60)

Compound **60** is known, and was synthesized according to a literature procedure for the same compound.²²⁰ In a 2-neck flask, hexanoyl chloride (1.4 g, 10.2 mmol) was added to a solution of AlCl_3 (1.36 g, 10.2 mmol) in anhydrous DCM (10 mL) under a N_2 atmosphere and cooled to -10 °C (salt/ice-bath). The contents were allowed to stir at -10 to -5 °C for 10 min. A solution of ethylbenzene (1.1 g, 9.3 mmol) in anhydrous DCM (10 mL) was added in a dropwise manner

over 30 min at -10 to -3 °C. The ice bath was removed and the contents were allowed to stir at room temperature for 1 h, quenched by the careful addition of ice-cold HCl (1N, 50 mL), and extracted with DCM (3x 20 mL). The combined organic portion was washed with brine (20 mL), dried (Na₂SO₄), evaporated under reduced pressure, and used without further purification, yielding 1.88 g (>99%) of **60** as a yellow-colored oil: ¹H NMR (CDCl₃) δ 0.93 (t, *J* = 3.0 Hz, 3H, CH₃), 1.28 (t, *J* = 7.6 Hz, 3H, CH₃), 1.33-1.45 (m, 4H, 2 x CH₂), 1.72-1.79 (m, 2H, CH₂), 2.73 (q, *J* = 7.6, 2H, CH₂), 2.96 (t, *J* = 7.4, 2H, CH₂), 7.30 (d, *J* = 8.1, 2H, ArH), 7.91 (d, *J* = 8.2, 2H, ArH).

4-Bromohexanophenone (61)

Compound **61** is known,²²¹ but was synthesized according to a literature procedure for a similar compound²²⁰ because it had been used successfully for the 4-methoxy analog **59**. In a 2-neck flask, hexanoyl chloride (1.9 g, 14.0 mmol) was added to a solution of AlCl₃ (1.9 g, 14.0 mmol) in anhydrous DCM (10 mL) under a N₂ atmosphere and cooled to -10 °C (salt/ice-bath). The contents were allowed to stir at -10 to -5 °C for 10 min. A solution of bromobenzene (2.0 g, 12.7 mmol) in anhydrous DCM (10 mL) was added in a dropwise manner over 30 min at -10 to -3 °C. The ice bath was removed and the contents were allowed to stir at room temperature for 1 h, quenched by the careful addition of ice-cold HCl (1N, 50 mL), and extracted with DCM (3x 20 mL). The combined organic portion was washed with brine (20 mL), dried (Na₂SO₄), and evaporated under reduced pressure. The residual semi-solid was crystallized from hexanes, yielding 0.9 g (27%) of **61** as a yellow-colored solid: mp 61-65 °C (lit.²²¹ mp 59-60 °C); ¹H NMR (CDCl₃) δ 0.91 (t, *J* = 4.1 Hz, 3H, CH₃), 1.25-1.41 (m, 4H, 2 x CH₂), 1.68-1.76 (m, 2H, CH₂), 2.91 (t, *J* = 7.4, 2H, CH₂), 7.59 (d, *J* = 7.9, 2H, ArH), 7.81 (d, *J* = 7.9, 2H, ArH).

4-Methoxy- α -bromohexanophenone (**62**)

The compound is known,²²² but was prepared according to a literature procedure for a similar compound.²²³ AlCl₃ (5 mg) was added at room temperature to a stirred solution of **59** (1.7 g, 8.3 mmol) in anhydrous Et₂O (10 mL). After cooling the reaction mixture to 0 °C (ice-bath), a solution of bromine (1.3 g, 8.3 mmol) in anhydrous Et₂O (10 mL) was added in a dropwise manner over 20 min, and the reaction mixture was stirred at room temperature for 1 h. The reaction was quenched by the careful addition of H₂O (30 mL), washed with brine (10 mL), dried (Na₂SO₄), and evaporated under reduced pressure resulting in 1.45 g of a yellow-colored oil, which upon crystallization from hexane afforded 1.2 g (50%) of **62** as a yellow-colored solid: mp 51-53 °C (lit.²²² mp 51-52 °C); IR (solid, cm⁻¹) 1667 (s, C=O); ¹H NMR (CDCl₃) δ 0.92 (t, J = 6.9 Hz, 3H, CH₃), 1.52-1.59 (m, 4H, 2 x CH₂), 2.05-2.25 (m, 2H, CH₂), 3.89 (s, 3H, CH₃), 5.10 (t, J = 7.2 Hz, 1H, CH), 6.96 (d, J = 8.9 Hz, 2H, ArH), 8.00 (d, J = 8.9, 2H, ArH).

4-Ethyl- α -bromohexanophenone (**63**)

The compound is unknown, and was prepared according to a procedure for bromination of a similar compound.²²³ AlCl₃ (5 mg) was added at room temperature to a stirred solution of **60** (1.05 g, 5.14 mmol) in anhydrous Et₂O (10 mL). After cooling the reaction mixture to 0 °C (ice-bath), a solution of bromine (0.81 g, 5.14 mmol) in anhydrous Et₂O (10 mL) was added in a dropwise manner over 20 min, and the reaction mixture was stirred at room temperature for 1 h. The reaction was quenched by the careful addition of H₂O (30 mL), washed with brine (10 mL), dried (Na₂SO₄), and evaporated under reduced pressure. The residual oil was purified by flash chromatography (silica gel; hexanes/EtOAc; 80/20) to afford 0.52 g (36%) of **63** as a clear

yellow oil: ^1H NMR (CDCl_3) δ 0.85 (t, $J = 7.1$ Hz, 3H, CH_3), 1.18-1.21 (m, 3H, CH_3), 1.25-1.47 (m, 4H, 2 x CH_2), 1.97-2.19 (m, 2H, CH_2), 2.65 (q, $J = 7.6$ Hz, 2H, CH_2), 5.05 (t, $J = 6.9$, 1H, CH), 7.25 (d, $J = 8.3$, 2H, ArH), 7.87 (d, $J = 8.3$, 2H, ArH).

4-Bromo- α -bromohexanophenone (64)

The compound is unknown, and was prepared according to a procedure for bromination of a similar compound.²²³ AlCl_3 (5 mg) was added at room temperature to a stirred solution of **61** (890 mg, 3.5 mmol) in anhydrous Et_2O (10 mL). After cooling the reaction mixture to 0 °C (ice-bath), a solution of bromine (550 mg, 3.5 mmol) in anhydrous Et_2O (10 mL) was added in a dropwise manner over 30 min, and the reaction mixture was stirred at room temperature for 6 h. Additional bromine was added (270 mg, 1.7 mmol) at 0 °C (ice-bath), and the reaction was allowed to stir for 30 min. The reaction was quenched by the careful addition of NaHCO_3 (60 mL), extracted with Et_2O , washed with brine (10 mL), dried (Na_2SO_4), and evaporated under reduced pressure. The resulting 860 mg (74%) white solid, **64**, was used without further purification: mp 37-38 °C; ^1H NMR (CDCl_3) δ 0.92 (t, $J = 7.1$ Hz, 3H, CH_3), 1.32-1.57 (m, 6H, 3 x CH_2), 2.06-2.26 (m, 2H, CH_2), 5.04 (dd, $J = 7.7$, 6.6 Hz, 1H, CH), 7.63 (d, 8.7 Hz, 2H, ArH), 7.87 (d, 8.7 Hz, 2H, ArH).

1-(*p*-Tolyl)hexan-1-ol (65)

The compound is known, but was synthesized according to a literature procedure for a similar compound.¹⁹⁴ In a three-neck flask under N_2 at room temperature, 1-bromopentane (2.5 mL, 20 mmol) and 1,2-dibromoethane (several drops) diluted by THF (12 mL) were added dropwise to a stirred solution of magnesium (0.48 g, 20 mmol) in THF (8.0 mL). After stirring at room

temperature for two hours, the mixture was cooled to 0 °C and *p*-tolualdehyde (2.4 mL, 20 mmol) was added dropwise over the course of 20 min. The mixture was allowed to come to room temperature while stirring overnight (24 h). The reaction was quenched carefully with NH₄Cl (50 mL) and extracted with EtOAc (3 x 20 mL). The combined organic portions were washed with brine (30 mL), dried (Na₂SO₄), and evaporated under reduced pressure, resulting in an orange liquid. This was further purified by flash chromatography (silica gel; hexanes/EtOAc; 80/20) to afford **65** as a clear, yellow oil: (1.01 g, 26%) ¹H NMR (CDCl₃) δ 0.89 (t, *J* = 6.2 Hz, 3H, CH₃), 1.11-1.31 (m, 6H, 3 x CH₂), 1.42-1.53 (m, 1H, OH), 1.55-1.77 (m, 2H, CH₂), 2.37 (s, 3H, CH₃), 4.61-4.65 (m, 1H, CH), 7.16 (d, *J* = 7.9 Hz, 2H, ArH), 7.24 (d, *J* = 8.0 Hz, 2H, ArH).

1-(4-Chlorophenyl)hexan-1-ol (66)

The compound is known, but was synthesized according to a literature procedure for a similar compound.²²⁴ Magnesium turnings (2.4 g, 100 mmol), ground with a mortar and pestle, were added to a three-neck flask, brought under N₂ at room temperature, and THF was added (12 mL). The suspension was stirred for 5 min, after which 1,2-dibromoethane (several drops) was added. The mixture was stirred for 10 min, when it turned opaque gray, and 1-bromopentane (11.0 mL, 89 mmol) was added, followed by additional THF (6 mL). The mixture was stirred at room temperature for 2 h, and heated at reflux for 1 h. Upon cooling to 0 °C (ice-bath), 4-chlorobenzaldehyde (10.0, 71 mmol) was added dropwise over the course of 20 min. The mixture was allowed to come to room temperature while stirring for 1 h. The reaction was quenched carefully with H₂O, followed by the addition of NH₄Cl (50 mL). The organic portion was washed with brine (30 mL), dried (Na₂SO₄), and evaporated under reduced pressure to afford **66** as a clear, yellow oil: (5.45 g, 36%). ¹H NMR (CDCl₃) δ 0.89 (t, *J* = 5.8 Hz, 3H, CH₃),

1.22-1.45 (m, 6H, 3 x CH₂), 1.64-1.83 (m, 2H, CH₂), 1.88 (d, $J = 3.0$, 1H, OH), 4.65-4.70 (m, 1H, CH), 7.28-7.35 (m, 4H, ArH).

1-(4-(Trifluoromethyl)phenyl)hexan-1-ol (67)

The compound is known, and was synthesized according to a slightly modified literature procedure. The modification was to the time, as the reaction was stopped when all starting material was gone as determined by TLC.²²⁵ Magnesium turnings (0.72 g, 30 mmol), ground in a mortar and pestle, were added to anhydrous THF (6 mL) at room temperature, under constant stirring and N₂ atmosphere. A solution of 1-bromopentane (3.6 mL, 29 mmol) and 1,2-dibromoethane (several drops) in anhydrous THF (5 mL) was added dropwise to the stirred solution. After stirring at room temperature for two hours, the mixture was cooled to 0 °C (ice-bath) and 4-(trifluoromethyl)benzaldehyde (1.3 mL, 29 mmol) was added dropwise over the course of 20 min. The mixture was allowed to come to room temperature and stirred for 5 h. The reaction was quenched carefully with saturated aqueous NH₄Cl (50 mL). The mixture was adjusted to pH 4 with HCl (2N) and extracted with EtOAc (3 x 15 mL). The combined organic portions were washed with brine (30 mL), dried (MgSO₄), evaporated under reduced pressure, and purified by flash chromatography (silica gel; hexanes/EtOAc; 80/20) to afford **67** as a clear, yellow oil: (2.36 g, 33%) ¹H NMR (CDCl₃) δ 0.88 (t, $J = 6.7$ Hz, 3H, CH₃), 1.25-1.46 (m, 6H, 3 x CH₂), 1.64-1.82 (m, 2H, CH₂), 1.95 (d, $J = 2.9$, 1H, OH), 4.72-4.76 (m, 1H, CH), 7.46 (d, $J = 8.1$ Hz, 2H, ArH), 7.60 (d, $J = 8.1$ Hz, 2H, ArH).

2-(Methylamino)-1-(*p*-tolyl)-pentan-1-one Hydrochloride (68)

The compound is unknown, but was synthesized according to a procedure for similar compounds.¹⁹² To a stirred solution of **55** (0.68 g, 2.3 mmol) in dichloroethane (10 mL) was added 1-chloroethyl chloroformate (0.66 g, 4.6 mmol). The mixture was heated at reflux for 2 h, after which it was evaporated to dryness under reduced pressure. The residue was dissolved in MeOH (10 mL), stirred at reflux for 1 h, and evaporated to dryness again. This residue was dissolved in Et₂O (10 mL) and stirred overnight (18 h). The resulting precipitate was filtered, washed with Et₂O (10 mL), and recrystallized from EtOH/Et₂O to afford 0.30 g (54%) of **68** as a white solid: mp 216-219 °C; ¹H NMR (DMSO-*d*₆) δ 0.79 (t, *J* = 7.3 Hz, 3H, CH₃), 1.02-1.15 (m, 1H, CH₂), 1.24-1.37 (m, 1H, CH₂), 1.78-1.95 (m, 2H, CH₂), 2.42 (s, 3H, CH₃), 2.56 (s, 3H, CH₃), 5.20 (t, *J* = 5.3 Hz, 1H, CH), 7.43 (d, *J* = 8.3 Hz, 2H, ArH), 7.97 (d, *J* = 8.2 Hz, 2H, ArH), 9.37 (br s, 2H, NH₂⁺); Anal. Calcd. for (C₁₃H₁₉NO·HCl) C, 64.59; H, 8.34; N, 5.79. Found: C, 64.31; H, 8.32; N, 5.76.

B. Computational Modeling

1. Homology Modeling.

a. hDAT and hSERT

The hDAT and hSERT models used were generated by former Glennon laboratory student F. Sakloth, as described in the literature.⁶⁹

b. hNET

The sequences of dDAT and hNET were obtained as FASTA files from the NCBI using the protein search tool, and aligned using Clustal Omega. Artifacts of the crystallization process

and co-crystallized ligands were removed from dDAT (PDB ID:4XP6) leaving only the dDAT protein for the template structure. To generate a population of 100 three-dimensional models of hNET based on its alignment with the template dDAT, Modeller v9.14 (University of California San Francisco, San Francisco, CA) was used,²⁰¹ resulting in a population of 100 models of various conformations. These were evaluated using molpdf, DOPE, and GA341 scoring functions. Ramachandran plots were generated for the best-scoring models using PROCHECK v.3.5.4.²⁰⁵

2. Docking

Compounds were sketched in Sybyl-X 2.1. Docking was performed using GOLD.²²⁶ Each agent was docked 10 times to each of the population of 100 models of either hNET, hSERT, or hDAT. The common Asp residue between them was used to define a 12 Angstrom binding pocket (Asp73 in hNET). Using in-house scripts, docking solutions were clustered by similarity (within 2.0 angstroms RMSD) and the clusters were ranked by population and GOLD score. Clustered solutions were then sorted visually in Sybyl-X 2.1 to identify plausible binding modes. Clusters were additionally created between compounds to help identify common binding modes for a group of related structures. Selected binding modes were energy minimized in Sybyl-X 2.1 and further visualized in PyMOL.²²⁷

C. Cell Culture and expression of MATs

Ca²⁺ imaging for the purpose of measuring substrate or blocker activity at MATs was performed according to procedures developed in J. Eltit's laboratory.^{190,228–230} hDAT or hSERT was expressed in HEK-293 cells using the FlpIn-TREx system (Invitrogen). The culture media

was Dulbecco's modified eagle medium (DMEM), which was supplemented with fetal bovine serum (FBS). Cells were plated in 96-well flat-bottom plates.

D. Ca²⁺ Imaging for evaluation of test compounds

Plated cells were transfected with the cardiac isoform of voltage-gated Ca²⁺ channel Cav1.2, its auxiliary subunits, and transfection marker EGFP. Plasmids $\alpha 1$, $\beta 3$, $\alpha 2\delta 1$, and EGFP in a ratio of 0.9:0.5:0.75:0.25, in μg , along with Fugene 6 (Promega) in OptiMEM media. The media was later supplemented with doxycycline (1 $\mu\text{g}/\text{mL}$) in DMEM to induce expression of transporters. Ca²⁺ determinations were made with Fura2, a ratiometric Ca²⁺ sensor.

Experiments performed in imaging solution (IS; 130 mM NaCl, 4 mM KCl, 2 mM CaCl₂, 1 mM MgCl₂, 10 mM HEPES, 10 mM glucose, pH = 7.3). Test compounds or controls were exposed to the cells under constant perfusion at 35 °C (ThermoClamp-1, Automate Scientific). Fluorescence was observed using an Olympus IX70 microscope using a 20 \times 0.75 numerical aperture (NA) objective with a fluorescence imaging attachment (Till Photonics). Ratio images were obtained at 340 nm and 380 nm excitation, then recoded for off-line analysis. Each well was used for a single concentration of test agent. 2 to 5 wells were collected per concentration per compound per experiment, and 2 to 5 experiments were conducted for each compound at multiple concentrations. Each well contained multiple cells, which were individually evaluated for either substrate or blocker activity using the following protocols. Concentration-response curves were generated using GraphPad Prism 6.0.

1. Substrate activity using Ca²⁺ imaging

Substrate activity was measured using the following protocol. Cells were perfused with IS for 10 s, followed by perfusion of a positive control (DA for hDAT or hNET, 5-HT for hSERT; 10 μM) for 5 s. Following a 30 s washout with IS, the test compound was perfused for 5s, followed by an additional 5 s washout with IS.

2. Blocker activity using Ca²⁺ imaging

Blocker activity was measured using the following protocol. Cells were perfused with IS for 10 s, followed by perfusion of a positive control (DA for hDAT or hNET, 5-HT for hSERT; 10 μM) for 5 s. Following a 30 s washout with IS, the test compound was perfused for 30 s, followed by the test compound at a given concentration with the positive control for 5 s, and a final washout of 30 s with IS.

E. APP+ Imaging for assessing blocker activity

Plated cells were transfected with dsRed as a transfection marker, along with Fugene 6 (Promega) in OptiMEM media. The media was later supplemented with doxycycline in DMEM to induce expression of transporters. Experiments performed in IS (130 mM NaCl, 4 mM KCl, 2 mM CaCl₂, 1 mM MgCl₂, 10 mM Hepes, 10 mM glucose, pH = 7.3). Test compounds or controls were exposed to the cells under constant perfusion. Fluorescence was observed using an Olympus IX70 microscope using a 20× 0.75NA objective with a fluorescence imaging attachment (Till Photonics). Images were obtained at 460 nm excitation, then recoded for off-line analysis. Each well was used for a single concentration of test agent. 2 to 5 wells were collected per concentration per compound per experiment, and 2 experiments were conducted for each compound at multiple concentrations. Each well contained at least 40 cells, which were

evaluated by measuring the amplitude of fluorescence and taking an average value per well, then comparing test compounds to positive controls. Dose-response curves were generated using GraphPad Prism 6.0.

Blocker activity was assessed by the following protocol. Cells were perfused with IS for 10 s, followed by perfusion of the test compound or control (IS) for 40 s. Then, a mixture of APP+ (3 μ M) and the test compound or control (IS) were perfused for 30 s.

Inhibition potency (IC_{50}) was calculated by fitting data to the Hill equation (equation 1).

$$V = \frac{V_{max}[S]^n}{(K_{0.5})^n + [S]^n}$$

Equation 1. The Hill equation, used for calculating IC^{50} potency values.

VII. Bibliography

1. Centers for Disease Control and Prevention, National Center for Health Statistics. Multiple cause of death 1999-2017 on CDC WONDER online database, released December, 2018.
2. *National Drug Threat Assessment*; Product no. 2011-Q0317-001; U.S. Department of Justice National Drug Intelligence Center: Johnstown, PA, 2011.
3. *The Underestimated Cost of the Opioid Crisis*; The Council of Economic Advisers, Executive Office of the President of the United States, 2017.
4. Quinones, S. *Dreamland: The True Tale of America's Opiate Epidemic*; Bloombury Press: New York, 2016.
5. Cicero, T. J.; Ellis, M. S. Abuse-deterrent formulations and the prescription opioid abuse epidemic in the United States: lessons learned from Oxycontin. *JAMA Psychiatry* **2015**, *72*, 424–429.
6. *World Drug Report 2018* (United Nations publication, Sales No. E.18.XI.9).
7. Borek, H. A.; Holstege, C. P. Hyperthermia and multiorgan failure after abuse of “bath salts” containing 3,4-methylenedioxypropylone. *Ann. Emerg. Med.* **2012**, *60*, 103–105.
8. Karila, L.; Benyamina, A. The effects and risks associated with synthetic cathinones use in humans. In *Current Topics in Neurotoxicity*; Zawilska, J., Ed.; Springer, Cham, 2018; Vol. 12, pp 191–202.
9. Schedules of Controlled Substances: Temporary placement of three synthetic cathinones into Schedule I. *Fed. Regist.* **2011**, *76*, 65371–65375.
10. Saha, K.; Partilla, J. S.; Lehner, K. R.; Seddik, A.; Stockner, T.; Holy, M.; Sandtner, W.; Ecker, G. F.; Sitte, H. H.; Baumann, M. H. “Second-generation” mephedrone analogs, 4-

MEC and 4-MePPP, differentially affect monoamine transporter function.

Neuropsychopharmacology **2015**, *40*, 1321–1331.

11. Brandt, S. D.; Sumnall, H. R.; Measham, F.; Cole, J. Analyses of second-generation “legal highs” in the UK: initial findings. *Drug Test. Anal.* **2010**, *2*, 377–382.
12. Karila, L.; Lafaye, G.; Scocard, A.; Cottencin, O.; Benyamina, A. MDPV and α -PVP use in humans: the twisted sisters. *Neuropharmacology* **2017**, *134*, 65-72.
13. Gannon, B. M.; Galindo, K. I.; Mesmin, M. P.; Sulima, A.; Rice, K. C.; Collins, G. T. Relative reinforcing effects of second-generation synthetic cathinones: acquisition of self-administration and fixed ratio dose-response curves in rats. *Neuropharmacology* **2018**, *134*, 28–35.
14. Gatch, M. B.; Dolan, S. B.; Forster, M. J. Comparative behavioral pharmacology of three pyrrolidine-containing synthetic cathinone derivatives. *J. Pharmacol. Exp. Ther.* **2015**, *354*, 103–110.
15. Marusich, J. A.; Antonazzo, K. R.; Wiley, J. L.; Blough, B. E.; Partilla, J. S.; Baumann, M. H. Pharmacology of novel synthetic stimulants structurally related to the “bath salts” constituent 3,4-methylenedioxypropylvalerone (MDPV). *Neuropharmacology* **2014**, *87*, 206–213.
16. Pourmand, A.; Mazer-Amirshahi, M.; Chistov, S.; Li, A.; Park, M. Designer drugs: review and implications for emergency management. *Hum. Exp. Toxicol.* **2018**, *37*, 94–101.
17. Klavž, J.; Gorenjak, M.; Marinšek, M. Suicide attempt with a mix of synthetic cannabinoids and synthetic cathinones: case report of non-fatal intoxication with AB-CHIMNACA, AB-FUBINACA, alpha-PHP, alpha-PVP and 4-CMC. *Forensic Sci. Int.*

- 2016**, 265, 121–124.
18. Glennon, R. A. The 2014 Philip S. Portoghese medicinal chemistry lectureship: the “phenylalkylaminome” with a focus on selected drugs of abuse. *J. Med. Chem.* **2017**, 60, 2605–2628.
 19. O’Donnell, J. K.; Halpin, J.; Mattson, C. L.; Goldberger, B. A.; Gladden, R. M. Deaths involving fentanyl, fentanyl analogs, and u-47700 - 10 states, July-December 2016. *MMWR. Morb. Mortal. Wkly. Rep.* **2017**, 66, 1197–1202.
 20. Cowan, R. How the narcs created crack. *National Review*. 1986, pp 26–31.
 21. Glennon, R. A.; Yousif, M.; Naiman, N.; Kalix, P. Methcathinone: a new and potent amphetamine-like agent. *Pharmacol. Biochem. Behav.* **1987**, 26, 547–551.
 22. Shulgin, A.; Shulgin, A. *PIHKAL: A Chemical Love Story*; Transform Press: La Fayette, 1995.
 23. Alles, G. A. The comparative physiological actions of dl- β -phenylisopropylamines I. Pressor effect and toxicity. *J. Pharmacol. Exp. Ther.* **1933**, 47, 339–354.
 24. Glennon, R. A.; Young, R.; Hauck, A. E.; McKenney, J. D. Structure-activity studies on amphetamine analogs using drug discrimination methodology. *Pharmacol. Biochem. Behav.* **1984**, 21, 895-901.
 25. Kolanos, R.; Sakloth, F.; Jain, A. D.; Partilla, J. S.; Baumann, M. H.; Glennon, R. A. Structural modification of the designer stimulant α -pyrrolidinovalerophenone (α -PVP) influences potency at dopamine transporters. *ACS Chem. Neurosci.* **2015**, 6, 1726–1731.
 26. Montague, K. A. Catechol compounds in rat tissues and in brains of different animals. *Nature* **1957**, 180, 244–245.

27. Björklund, A.; Dunnett, S. B. Fifty years of dopamine research. *Trends Neurosci.* **2007**, *30*, 185–187.
28. Dakin, H. D. The synthesis of a substance allied to adrenalin. *Proc. R. Soc. London, Ser. B.* **1905**, *76*, 491–497.
29. Takamine, J. The isolation of the active principle of the suprarenal gland. *J. Physiol.* **1902**, *27*, xxix–xxx.
30. Bennett, M. R. One hundred years of adrenaline: the discovery of autoreceptors. *Clin. Auton. Res.* **1999**, *9*, 145–159.
31. Rapport, M. M.; Green, A. A.; Page, I. H. Serum vasoconstrictor (serotonin) IV. isolation and characterization. *J. Biol. Chem.* **1948**, *176*, 1243–1251.
32. McGrath, N. A.; Brichacek, M.; Njardarson, J. T. A graphical journey of innovative organic architectures that have improved our lives. *J. Chem. Educ.* **2010**, *87*, 1348–1349.
33. Hilliard, W. T.; Barloon, L.; Farley, P.; Penn, J. V.; Koranek, A. Bupropion diversion and misuse in the correctional facility. *J. Correct. Health Care* **2013**, *19*, 211–217.
34. Strike, M.; Hatcher, S. Bupropion injection resulting in tissue necrosis and psychosis: previously undocumented complications of intravenous bupropion use disorder. *J. Addict. Med.* **2015**, *9*, 246–250.
35. *Abuse of the amphetamines and pharmacologically related substances*; New drugs and developments in therapeutics: council on drugs' statements; *J. Am. Med. Assoc.* February 1963; Vol. 183, pp. 362-363.
36. Jones, C. M. *The Latest Prescription Trends for Controlled Prescription Drugs*; Office of Public Health Strategy and Analysis, Office of the Commissioner, Food and Drug Administration; September 2015, [Online] <https://www.drugabuse.gov/news->

- events/meetings-events/2015/09/latest-prescription-trends-controlled-prescription-drugs (accessed April 24, 2019).
37. Rasmussen, N. America's first amphetamine epidemic 1929–1971. *Am. J. Public Health* **2008**, *98*, 974–985.
 38. Glennon, R. A.; Titeler, M.; McKenney, J. D. Evidence for 5-HT₂ involvement in the mechanism of action of hallucinogenic agents. *Life Sci.* **1984**, *35*, 2505–2511.
 39. Osmond, H. A review of the clinical effects of psychotomimetic agents. *Ann. N. Y. Acad. Sci.* **1957**, *66*, 418–434.
 40. Nichols, D. E. Psychedelics. *Pharmacol. Rev.* **2016**, *68*, 264–355.
 41. Nichols, D.; Yensen, R.; Metzner, R. The great entactogen - empathogen debate. *Newsletter of the Multidisciplinary Association for Psychedelic Studies* [Online], 1993, pp 47–49. Multidisciplinary Association for Psychedelic Studies. <https://maps.org/newsletters/v04n2/04247eed.html> (accessed March 2, 2019).
 42. Vizeli, P.; Liechti, M. E. Oxytocin receptor gene variations and socio-emotional effects of MDMA: a pooled analysis of controlled studies in healthy subjects. *PLoS One* **2018**, *13*, e0199384.
 43. *Fatal Drug Overdose Quarterly Report 2nd Quarter 2018*; Virginia Department Of Health Office Of The Chief Medical Examiner: Richmond, VA, 2018.
 44. *Monitoring the Future Study: Trends in Prevalence of Various Drugs*, National Institute on Drug Abuse (NIDA) [Online] **2018**, <https://www.drugabuse.gov/trends-statistics/monitoring-future/monitoring-future-study-trends-in-prevalence-various-drugs> (Accessed April 25, 2019).
 45. *World Drug Report 2018* (United Nations publication, Sales No. E.18.XI.9).

46. Management of Substance Abuse: Amphetamine-type stimulants, World Health Organization; https://www.who.int/substance_abuse/facts/ATS/en/ (Accessed February 19th, 2019).
47. Prekupec, M. P.; Mansky, P. A.; Baumann, M. H. Misuse of novel synthetic opioids. *J. Addict. Med.* **2017**, *11*, 256–265.
48. O'Donnell, J. K.; Gladden, R. M.; Seth, P. *Trends in deaths involving heroin and synthetic opioids excluding methadone, and law enforcement drug product reports, by census region — United States, 2006–2015*. Morbidity and Mortality Weekly Report Vol. 66; Centers for Disease Control and Prevention: Atlanta, GA, 2017, 897–903.
49. *States That Schedule Pseudoephedrine*; Report for the National Alliance for Model State Drug Laws, Bureau of Justice Assistance, Santa Fe, NM, 2012.
50. *States That Schedule Ephedrine*; Report for the National Alliance for Model State Drug Laws, Bureau of Justice Assistance, Santa Fe, NM, 2012.
51. Rothman, R. B.; Baumann, M. H.; Dersch, C. M.; Romero, D. V.; Rice, K. C.; Carroll, F. I.; Partilla, J. S. Amphetamine-type central nervous system stimulants release norepinephrine more potently than they release dopamine and serotonin. *Synapse* **2001**, *39*, 32–41.
52. Biel, J. H.; Bopp, B. A. Amphetamines: structure-activity relationships. In *Handbook of Psychopharmacology: Stimulants*; Iversen, L. L., Iversen, S. D., Eds.; Springer: Boston; 1978; pp 1–39.
53. Sulzer, D.; Sonders, M. S.; Poulsen, N. W.; Galli, A. Mechanisms of neurotransmitter release by amphetamines: a review. *Prog. Neurobiol.* **2005**, *75*, 406–433.
54. Datta, D.; Kumar, S.; Uslu, H. Status of the Reactive Extraction as a Method of

- Separation. *J. Chem.* **2015**, 2015, 1–16.
55. Edeleano, L. Ueber einige Derivate der Phenylmethacrylsäure und der Phenylisobuttersäure. *Berichte der Dtsch. Chem. Gesellschaft* **1887**, 20, 616–622.
 56. Alles, G. A.; Fairchild, M. D.; Jensen, M. Chemical pharmacology of catha edulis. *J. Med. Chem.* **1961**, 3, 323–352.
 57. Al-Motarreb, A.; Baker, K.; Broadley, K. J. Khat: pharmacological and medical aspects and its social use in Yemen. *Phytother. Res.* **2002**, 16, 403–413.
 58. Forskal, P. *Flora Aegyptico-Arabica*; Niebuhr, C., Ed.; 1775.
 59. Vaughan, J. Notes upon the drugs observed at Aden, Arabia. *Pharm. J.* **1852**, 12, 268–271.
 60. Glennon, R. A.; Young, R.; Martin, B. R.; Dal Cason, T. A. Methcathinone (“cat”): an enantiomeric potency comparison. *Pharmacol. Biochem. Behav.* **1995**, 50, 601–606.
 61. Scheindindlin, S. A brief history of pharmacology. *Mod. Drug Discov.* **2001**, 4, 87–88.
 62. Lee, M. R. The history of ephedra. *J. R. Coll. Physicians Edinbg.* **2011**, 41, 78–84.
 63. Miura, K. Vorläufige Mittheilung über Ephedrin, ein neues Mydriaticum. *Berl. Klin. Wochenschr.* **1887**, 24, 707.
 64. Oliver, G.; Schäfer, F. R. The physiological effects of extracts of the suprarenal capsules. *J. Physiol.* **1895**, 18, 230–279.
 65. Barger, G.; Dale, H. H. Chemical structure and sympathomimetic action of amines. *J. Physiol.* **1910**, 41, 19–59.
 66. Kennedy, J. G.; Teague, J.; Fairbanks, L. Qat use in north Yemen and the problem of addiction: a study in medical anthropology. *Cult. Med. Psychiatry* **1980**, 4, 311–344.
 67. Rothman, R. B.; Vu, N.; Partilla, J. S.; Roth, B. L.; Hufeisen, S. J.; Compton-Toth, B. A;

- Birkes, J.; Young, R.; Glennon, R. A. In vitro characterization of ephedrine-related stereoisomers at biogenic amine transporters and the receptorome reveals selective actions as norepinephrine transporter substrates. *J. Pharmacol. Exp. Ther.* **2003**, *307*, 138–145.
68. Bonano, J. S.; Banks, M. L.; Kolanos, R.; Sakloth, F.; Barnier, M. L.; Glennon, R. A.; Cozzi, N. V.; Partilla, J. S.; Baumann, M. H.; Negus, S. S. Quantitative structure-activity relationship analysis of the pharmacology of *para*-substituted methcathinone analogues. *Br. J. Pharmacol.* **2015**, *172*, 2433–2444.
69. Sakloth, F.; Kolanos, R.; Mosier, P. D.; Bonano, J. S.; Banks, M. L.; Partilla, J. S.; Baumann, M. H.; Negus, S. S.; Glennon, R. A. Steric parameters, molecular modeling and hydrophobic interaction analysis of the pharmacology of *para*-substituted methcathinone analogues. *Br. J. Pharmacol.* **2015**, *172*, 2210–2218.
70. Roth, R. P.; Cantekin, E. I.; Bluestone, C. D.; Welch, R. M.; Cho, Y. W. Nasal decongestant activity of pseudoephedrine. *Ann. Otol. Rhinol. Laryngol.* **1977**, *86*, 235–242.
71. Wilson, S. D.; Sun, L.-H. Ephedrine: II. Some new benzyl homologs. *J. Chinese Chem. Soc.* **1934**, *2*, 243–256.
72. Hyde, J. F.; Browning, E.; Adams, R. Synthetic homologs of *d,l*-ephedrine. *J. Am. Chem. Soc.* **1928**, *50*, 2287–2292.
73. Wilson, S. D.; Chang, C. Ephedrine. III. Di-(α -hydroxyl- β -methylaminopropyl)-benzenes. *J. Am. Chem. Soc.* **1940**, *62*, 287–288.
74. Miller, H.; Piness, G. A synthetic substitute for ephedrine. *J. Am. Med. Assoc.* **1928**, *91*, 1033–1035.

75. Piness, G.; Miller, H.; Alles, G. A. Clinical observations on phenylaminoethanol sulphate. *J. Am. Med. Assoc.* **1930**, *94*, 790.
76. Rasmussen, N. Making the first anti-depressant: amphetamine in American medicine, 1929–1950. *J. Hist. Med. Allied Sci.* **2006**, *61*, 288–323.
77. Bloomberg, W. Treatment of chronic alcoholism with amphetamine (benzedrine) sulfate. *N. Engl. J. Med.* **1939**, *220*, 129–135.
78. Prinzmetal, M.; Bloomberg, W. The use of benzedrine for the treatment of narcolepsy. *J. Am. Med. Assoc.* **1935**, *105*, 2051.
79. Logan, B. K. Amphetamines: an update on forensic issues. *J. Anal. Toxicol.* **2001**, *25*, 400–404.
80. Lange, K. W.; Reichl, S.; Lange, K. M.; Tucha, L.; Tucha, O. The history of attention deficit hyperactivity disorder. *Atten. Defic. Hyperact. Disord.* **2010**, *2*, 241–255.
81. Higgs, R. A.; Glennon, R. A. Stimulus properties of ring-methyl amphetamine analogs. *Pharmacol., Biochem. Behav.* **1990**, *37*, 835–837.
82. Pentney, A. R. An exploration of the history and controversies surrounding MDMA and MDA. *J. Psychoact. Drugs* **2001**, *33*, 213–221.
83. Szigeti, B.; Winstock, A. R.; Erritzoe, D.; Maier, L. J. Are ecstasy induced serotonergic alterations overestimated for the majority of users? *J. Psychopharmacol.* **2018**, *32*, 741–748.
84. Mithoefer, M. C.; Grob, C. S.; Brewerton, T. D. Novel psychopharmacological therapies for psychiatric disorders: psilocybin and MDMA. *Lancet Psychiatry* **2016**, *3*, 481–488.
85. Bonner, R. C. Schedules of controlled substances temporary placement of methcathinone into Schedule I. Fed. Reg. 57: 18824- 18825; 1992.

86. Glennon, R. A. Bath salts, mephedrone, and methylenedioxypropylone as emerging illicit drugs that will need targeted therapeutic intervention. In *Advances in Pharmacology*; 2014; pp 581–620.
87. Spiller, H. A.; Ryan, M. L.; Weston, R. G.; Jansen, J. Clinical experience with and analytical confirmation of “bath salts” and “legal highs” (synthetic cathinones) in the United States. *Clin. Toxicol.* **2011**, *49*, 499–505.
88. Measham, F.; Moore, K.; Newcombe, R. Tweaking, bombing, dabbing and stockpiling: the emergence of mephedrone and the perversity of prohibition. *Drugs and Alcohol Today* **2010**, *10*, 14–21.
89. Cameron, K. N.; Kolanos, R.; Solis, E.; Glennon, R. A.; De Felice, L. J. Bath salts components mephedrone and methylenedioxypropylone (MDPV) act synergistically at the human dopamine transporter. *Br. J. Pharmacol.* **2013**, *168*, 1750–1757.
90. De Felice, L. J.; Glennon, R. A.; Negus, S. S. Synthetic cathinones: chemical phylogeny, physiology, and neuropharmacology. *Life Sci.* **2014**, *97*, 20–26.
91. Glennon, R. A.; Young, R. Neurobiology of 3,4-methylenedioxypropylone (MDPV) and α -pyrrolidinovalerophenone (α -PVP). *Brain Res. Bull.* **2016**, *126*, 111–126.
92. Xu, P.; Qiu, Y.; Zhang, Y.; Bai, Y.; Xu, P.; Liu, Y.; Kim, J. H.; Shen, H. W. The effects of 4-methylethcathinone on conditioned place preference, locomotor sensitization, and anxiety-like behavior: a comparison with methamphetamine. *Int. J. Neuropsychopharmacol.* **2016**, *19*, 1–7.
93. Giannotti, G.; Canazza, I.; Caffino, L.; Bilel, S.; Ossato, A.; Fumagalli, F.; Marti, M. The cathinones MDPV and α -PVP elicit different behavioral and molecular effects following acute exposure. *Neurotox. Res.* **2017**, 1–9.

94. Elsworth, J. D.; Roth, R. H. Dopamine synthesis, uptake, metabolism, and receptors: relevance to gene therapy of Parkinson's disease. *Exp. Neurol.* **1997**, *144*, 4–9.
95. Seiler, N.; Demisch, L.; Schneider, H. Biochemistry and function of biogenic amines in the central nervous system. *Angew. Chem., Int. Ed. Engl.* **1971**, *10*, 51–66.
96. Craine, J. E.; Daniels, G. H.; Kaufman, S.; Craine, E.; Daniels, H. Dopamine- β -hydroxylase. *J. Biol. Chem.* **1973**, *248*, 7838–7844.
97. De Potter, W. P.; Smith, A. D.; De Schaepdryver, A. F. Subcellular fractionation of splenic nerve: ATP, chromogranin A and dopamine β -hydroxylase in noradrenergic vesicles. *Tissue Cell* **1970**, *2*, 529–546.
98. Glennon, R. A.; Dukat, M.; Westkaemper, R. B. Serotonin receptor subtypes and ligands. In *Psychopharmacology - The Fourth Generation of Progress*; American College of Neuropsychopharmacology, 2000.
99. Young, R.; Glennon, R. A. A three-lever operant procedure differentiates the stimulus effects of *R*(-)-MDA from *S*(+)-MDA. *J. Pharmacol. Exp. Ther.* **1996**, *276*, 594–601.
100. Iversen, L. Neurotransmitter transporters and their impact on the development of psychopharmacology. *Br. J. Pharmacol.* **2006**, *147* (Suppl. 1), S82–S88.
101. Iversen, L. Neurotransmitter transporters and their impact on the development of psychopharmacology. *Br. J. Pharmacol.* **2006**, *147*, 82–88.
102. Björklund, A.; Dunnett, S. B. Dopamine neuron systems in the brain: an update. *Trends Neurosci.* **2007**, *30*, 194–202.
103. Romanelli, R. J.; Williams, J. T.; Neve, K. A. Dopamine receptor signaling: intracellular pathways to behavior. In *The Dopamine Receptors*, 2nd ed.; Neve, K. A., Ed.; Humana Press: Totowa, NJ, 2010; pp 137–173.

104. Pacholczyk, T.; Blakely, R. D.; Amara, S. G. Expression cloning of a cocaine-and antidepressant-sensitive human noradrenaline transporter. *Nature* **1991**, *350*, 350–354.
105. Guastella, J.; Nelson, N.; Nelson, H.; Czyzyk, L.; Keynan, S.; Miedel, M.; Davidson, N.; Lester, H.; Kanner, B. Cloning and expression of a rat brain GABA transporter. *Science* **1990**, *249*, 1303–1306.
106. Kilty, J. E.; Lorang, D.; Amara, S. G. Cloning and expression of a cocaine-sensitive rat dopamine transporter. *Science* **1991**, *254*, 578–579.
107. Hoffman, B. J.; Mezey, E.; Brownstein, M. J. Cloning of a serotonin transporter affected by antidepressants. *Science* **1991**, *254*, 579–580.
108. Ramamoorthy, S.; Baumant, A. L.; Mooret, K. R.; Han, H.; Yang-Feng, T.; Chang, A. S.; Ganapathy, V.; Blakely, R. D. Antidepressant-and cocaine-sensitive human serotonin transporter: molecular cloning, expression, and chromosomal localization. *Proc. Natl. Acad. Sci. U. S. A.* **1993**, *90*, 2542–2546.
109. Sitte, H. H.; Freissmuth, M. Amphetamines, new psychoactive drugs and the monoamine transporter cycle. *Trends Pharmacol. Sci.* **2015**, *36*, 41–50.
110. Penmatsa, A.; Wang, K. H.; Gouaux, E. X-ray structure of dopamine transporter elucidates antidepressant mechanism. *Nature* **2013**, *503*, 85–90.
111. Wang, K. H.; Penmatsa, A.; Gouaux, E. Neurotransmitter and psychostimulant recognition by the dopamine transporter. *Nature* **2015**, *521*, 322–327.
112. Coleman, J. A.; Green, E. M.; Gouaux, E. X-ray structures and mechanism of the human serotonin transporter. *Nature* **2016**, *532*, 334–339.
113. Shi, L.; Quick, M.; Zhao, Y.; Weinstein, H.; Javitch, J. A. The mechanism of a neurotransmitter:sodium symporter-inward release of Na⁺ and substrate is triggered by

- substrate in a second binding site. *Mol. Cell* **2008**, *30*, 667–677.
114. Koldsø, H.; Christiansen, A. B.; Sinning, S.; Schiøtt, B. Comparative modeling of the human monoamine transporters: similarities in substrate binding. *ACS Chem. Neurosci.* **2013**, *4*, 295–309.
115. Caveney, S.; Cladman, W.; Verellen, L.; Donly, C. Ancestry of neuronal monoamine transporters in the metazoa. *J. Exp. Biol.* **2006**, *209*, 4858–4868.
116. Kristensen, A. S.; Andersen, J.; Jørgensen, T. N.; Sørensen, L.; Eriksen, J.; Loland, C. J.; Strømgaard, K. SLC6 neurotransmitter transporters: structure, function, and regulation. **2011**, *63*, 585–640.
117. Grouleff, J.; Ladefoged, L. K.; Koldsø, H.; Schiøtt, B. Monoamine transporters: insights from molecular dynamics simulations. *Front. Pharmacol.* **2015**, *6*, 1–15.
118. Su, A.; Mager, S.; Mayo, S. L.; Lester, H. A. A multi-substrate single-file model for ion-coupled transporters. *Biophys. J.* **1996**, *70*, 762–777.
119. Petersen, C. I.; DeFelice, L. J. Ionic interactions in the drosophila serotonin transporter identify it as a serotonin channel. *Nat. Neurosci.* **1999**, *2*, 605–610.
120. Adams, S. V.; DeFelice, L. J. Flux coupling in the human serotonin transporter. *Biophys. J.* **2002**, *83*, 3268–3282.
121. Badiani, A.; Berridge, K. C.; Heilig, M.; Nutt, D. J.; Robinson, T. E. Addiction research and theory: a commentary on the surgeon general's report on alcohol, drugs, and health. *Addict. Biol.* **2018**, *23*, 3–5.
122. Substance-related and addictive disorders. In *Diagnostic and Statistical Manual of Mental Disorders*; American Psychiatric Association, 2013.
123. U.S. Department of Health and Human Services (HHS), Office of the Surgeon General,

- Facing Addiction in America: The Surgeon General's Report on Alcohol, Drugs, and Health. Washington, DC: HHS, November 2016.
124. Badiani, A.; Belin, D.; Epstein, D.; Calu, D.; Shaham, Y. Opiate versus psychostimulant addiction: the differences do matter. *Nat. Rev. Neurosci.* **2011**, *12*, 685–700.
 125. Leshner, A. I. Addiction is a brain disease, and it matters. *Science* **1997**, *278*, 45–47.
 126. U.S. Department of Health and Human Services (HHS), Office of the Surgeon General, Facing Addiction in America: The Surgeon General's Report on Alcohol, Drugs, and Health. Chapter 2. Washington, DC: HHS, November 2016.
 127. Koob, G. F. Drugs of abuse: anatomy, pharmacology and function of reward pathways. *Trends Pharmacol. Sci.* **1992**, *13*, 177–184.
 128. Merikangas, K. R.; McClair, V. L. Epidemiology of substance use disorders. *Hum. Genet.* **2012**, *131*, 779–789.
 129. Cantin, L.; Lenoir, M.; Augier, E.; Vanhille, N.; Dubreucq, S.; Serre, F.; Vouillac, C.; Ahmed, S. H. Cocaine is low on the value ladder of rats: possible evidence for resilience to addiction. *PLoS One* **2010**, *5*, e11592.
 130. Wise, R. A.; Hoffman, D. C. Localization of drug reward mechanisms by intracranial injections. *Synapse* **1992**, *10*, 247–263.
 131. Ellison, G.; Eison, M.; Huberman, H.; Daniel, F. Long-term changes in dopaminergic innervation of caudate nucleus after continuous amphetamine administration. *Science* **1978**, *201*, 276–278.
 132. Woolverton, W. L.; Ricaurte, G. A.; Forno, L. S.; Seiden, L. S. Long-term effects of chronic methamphetamine administration in rhesus monkeys. *Brain Res.* **1989**, *486*, 73–78.

133. Bakhit, C.; Gibb, J. W. Methamphetamine-induced depression of tryptophan hydroxylase: recovery following acute treatment. *Eur. J. Pharmacol.* **1981**, *76*, 229–233.
134. Buening, M. K.; Gibb, J. W. Influence of methamphetamine and neuroleptic drugs on tyrosine hydroxylase activity. *Eur. J. Pharmacol.* **1974**, *26*, 30–34.
135. Gibb, J. W.; Kogan, F. J. Influence of dopamine synthesis on methamphetamine-induced changes in striatal and adrenal tyrosine hydroxylase activity. *Naunyn-Schmiedeberg's Arch. Pharmacol.* **1979**, *310*, 185-187.
136. Koda, L. Y.; Gibb, J. W. Adrenal and striatal tyrosine hydroxylase activity after methamphetamine. *J. Pharmacol. Exp. Ther.* **1973**, *185*, 42–48.
137. Volkow, N. D.; Chang, L.; Wang, G.-J.; Fowler, J. S.; Leonido-Yee, M.; Franceschi, D.; Sedler, M. J.; Gatley, S. J.; Hitzemann, R.; Ding, Y.-S.; Logan, J.; Wong, C.; Miller, E. N. Association of dopamine transporter reduction with psychomotor impairment in methamphetamine abusers. *Am. J. Psychiatry* **2001**, *158*, 377–382.
138. Volkow, N. D.; Fowler, J. S.; Wang, G.-J. The addicted human brain: insights from imaging studies. *J. Clin. Invest.* **2003**, *111*, 1444–1451.
139. Kelly, J. F.; Bergman, B.; Hoepfner, B. B.; Vilsaint, C.; White, W. L. Prevalence and pathways of recovery from drug and alcohol problems in the United States population: implications for practice, research, and policy. *Drug Alcohol Depend.* **2017**, *181*, 162–169.
140. Rawson, R. A.; Gonzales, R.; Brethen, P. Treatment of methamphetamine use disorders: an update. *J. Subst. Abuse Treat.* **2002**, *23*, 145–150.
141. Winkelman, T. N. A.; Admon, L. K.; Jennings, L.; Shippee, N. D.; Richardson, C. R.; Bart, G. Evaluation of amphetamine-related hospitalizations and associated clinical

- outcomes and costs in the United States. *JAMA Netw. Open* **2018**, *1*, e183758.
142. Sandtner, W.; Stockner, T.; Hasenhuetl, P. S.; Partilla, J. S.; Seddik, A.; Zhang, Y.; Cao, J.; Holy, M.; Steinkellner, T.; Rudnick, G.; Baumann, M. H.; Ecker, G. F.; Newman, A. H.; Sitte, H. H. Binding mode selection determines the action of ecstasy homologs at monoamine transporters. *Mol. Pharmacol.* **2015**, *89*, 165-167.
143. Gregg, R. A.; Baumann, M. H.; Partilla, J. S.; Bonano, J. S.; Vouga, A.; Tallarida, C. S.; Velvadapu, V.; Smith, G. R.; Peet, M. M.; Reitz, A. B.; Negus, S. S.; Rawls, S. M. Stereochemistry of mephedrone neuropharmacology: enantiomer-specific behavioural and neurochemical effects in rats. *Br. J. Pharmacol.* **2015**, *172*, 883–894.
144. Baumann, M. H.; Partilla, J. S.; Lehner, K. R.; Thorndike, E. B.; Hoffman, A. F.; Holy, M.; Rothman, R. B.; Goldberg, S. R.; Lupica, C. R.; Sitte, H. H.; Brandt, S. D.; Tella, S. R.; Cozzi, N. V; Schindler, C. W. Powerful cocaine-like actions of 3,4-methylenedioxypyrovalerone (MDPV), a principal constituent of psychoactive “bath salts” products. *Neuropsychopharmacology* **2013**, *38*, 552–562.
145. Luethi, D.; Kaeser, P. J.; Brandt, S. D.; Krähenbühl, S.; Hoener, M. C.; Liechti, M. E. Pharmacological profile of methylphenidate-based designer drugs. *Neuropharmacology* **2018**, *134*, 133–140.
146. Shalabi, A. R.; Walther, D.; Baumann, M. H.; Glennon, R. A. Deconstructed analogues of bupropion reveal structural requirements for transporter inhibition versus substrate-induced neurotransmitter release. *ACS Chem. Neurosci.* **2017**, *8*, 1397–1403.
147. Fung, M.; Thornton, A.; Mybeck, K.; Wu, J. H.; Hornbuckle, K.; Muniz, E. Evaluation of the characteristics of safety withdrawal of prescription drugs from worldwide pharmaceutical markets-1960 to 1999. *Drug Inf. J.* **2001**, *35*, 293–317.

148. Sulzer, D.; Maidment, N. T.; Rayport, S. Amphetamine and other weak bases act to promote reverse transport of dopamine in ventral midbrain neurons. *J. Neurochem.* **1993**, *60*, 527–535.
149. Solis, E.; Partilla, J. S.; Sakloth, F.; Ruchala, I.; Schwienteck, K. L.; De Felice, L. J.; Eltit, J. M.; Glennon, R. A.; Negus, S. S.; Baumann, M. H. *N*-Alkylated analogs of 4-methylamphetamine (4-MA) differentially affect monoamine transporters and abuse liability. *Neuropsychopharmacology* **2017**, *42*, 1950–1961.
150. Steele, T. W. E.; Eltit, J. M. Using Ca²⁺-channel biosensors to profile amphetamines and cathinones at monoamine transporters: electro-engineering cells to detect potential new psychoactive substances. *Psychopharmacology* **2019**, *236*, 973–988.
151. Negus, S. S.; Miller, L. L. Intracranial self-stimulation to evaluate abuse potential of drugs. *Pharmacol. Rev.* **2014**, *66*, 869–917.
152. Gregg, R. A.; Baumann, M. H.; Partilla, J. S.; Bonano, J. S.; Vouga, A.; Tallarida, C. S.; Velvadapu, V.; Smith, G. R.; Peet, M. M.; Reitz, A. B.; Negus, S. S.; Rawls, S. M. Stereochemistry of mephedrone neuropharmacology: enantiomer-specific behavioural and neurochemical effects in rats. *Br. J. Pharmacol.* **2015**, *172*, 883–894.
153. Romanelli, F.; Smith, K. M. Clinical effects and management of methamphetamine abuse. *Pharmacotherapy* **2006**, *26*, 1148–1156.
154. Differences between Stimulants: Methamphetamine and Amphetamines
<https://methoide.fcm.arizona.edu/infocenter/index.cfm?stid=172> (accessed Apr 8, 2019).
155. Baumann, M. H.; Clark, R. D.; Woolverton, W. L.; Wee, S.; Blough, B. E.; Rothman, R. B. In vivo effects of amphetamine analogs reveal evidence for serotonergic inhibition of mesolimbic dopamine transmission in the rat. *J. Pharmacol. Exp. Ther.* **2011**, *337*, 218–

- 225.
156. Shoblock, J. R.; Sullivan, E. B.; Maisonneuve, I. M.; Glick, S. D. Neurochemical and behavioral differences between d-methamphetamine and *d*-amphetamine in rats. *Psychopharmacology* **2003**, *165*, 359–369.
157. Goodwin, J. S.; Larson, G. A.; Swant, J.; Sen, N.; Javitch, J. A.; Zahniser, N. R.; De Felice, L. J.; Khoshbouei, H. Amphetamine and methamphetamine differentially affect dopamine transporters in vitro and in vivo. *J. Biol. Chem.* **2009**, *284*, 2978–2989.
158. Balster, R. L.; Schuster, C. R. A comparison of *d*-amphetamine, *l*-amphetamine, and methamphetamine self-administration in rhesus monkeys. *Pharmacol., Biochem. Behav.* **1973**, *1*, 67-71.
159. Kuhn, D. M.; Appel, J. B.; Greenberg, I. An analysis of some discriminative properties of *d*-amphetamine. *Psychopharmacologia* **1974**, *39*, 57–66.
160. Lamb, R. J.; Henningfield, J. E. Human *d*-amphetamine drug discrimination: methamphetamine and hydromorphone. *J. Exp. Anal. Behav.* **2006**, *61*, 169-180.
161. Milesi-Hallé, A.; McMillan, D. E.; Laurenzana, E. M.; Byrnes-Blake, K. A.; Owens, S. M. Sex differences in (+)-amphetamine- and (+)-methamphetamine-induced behavioral response in male and female Sprague–Dawley rats. *Pharmacol. Biochem. Behav.* **2007**, *86*, 140–149.
162. Yokel, R. A.; Pickens, R. Self-administration of optical isomers of amphetamine and methylamphetamine by rats. *J. Pharmacol. Exp. Ther.* **1973**, *187*, 27-33.
163. Cox Jr., R. H.; Maickel, R. P. Comparison of anorexigenic and behavioral potency of phenylethylamines. *J. Pharmacol. Exp. Ther.* **1972**, *181*, 1-9.
164. Owen, J. E. The influence of *dl*-, *d*-, and *l*-amphetamine and *d*-methamphetamine on a

- fixed-ratio schedule. *J. Exp. Anal. Behav.* **1960**, *3*, 293–310.
165. Kuczenski, R.; Segal, D. S.; Cho, A. K.; Melega, W. Hippocampus norepinephrine, caudate dopamine and serotonin, and behavioral responses to the stereoisomers of amphetamine and methamphetamine. *J. Neurosci.* **1995**, *15*, 1308–1317.
166. Segal, D. S.; Kuczenski, R. Repeated binge exposures to amphetamine and methamphetamine: behavioral and neurochemical characterization. *J. Pharmacol. Exp. Ther.* **1997**, *282*, 561-573.
167. Ewing, P. L.; Moore, B. M.; Moore, W. T. The effect of amphetamine and related compounds on maze performance of white rats. *J. Pharmacol. Exp. Ther.* **1952**, *105*, 343–348.
168. Novelli, A. N.; Tainter, M. L. The stimulant power of secondary and tertiary phenylisopropyl-amines. *J. Pharmacol. Exp. Ther.* **1943**, *77*, 324–331.
169. Hall, D. A.; Stanis, J. J.; Marquez Avila, H.; Gulley, J. M. A comparison of amphetamine- and methamphetamine-induced locomotor activity in rats: evidence for qualitative differences in behavior. *Psychopharmacology* **2007**, *195*, 469–478.
170. Van der Schoot, J. Phenylisopropylamine derivatives, structure and action. *Arzneim. Forsch.* **1962**, *12*, 902–907.
171. Young, R.; Glennon, R. A. Discriminative stimulus properties of amphetamine, cathinone, and related agents. *Med. Res. Rev.* **1986**, *6*, 99–130.
172. Kolanos, R.; Partilla, J. S.; Baumann, M. H.; Hutsell, B. a; Banks, M. L.; Negus, S. S.; Glennon, R. A. Stereoselective actions of methylenedioxypyrovalerone (MDPV) to inhibit dopamine and norepinephrine transporters and facilitate intracranial self-stimulation in rats. *ACS Chem. Neurosci.* **2015**, *6*, 771–777.

173. Eshleman, A. J.; Wolfrum, K. M.; Reed, J. F.; Kim, S. O.; Swanson, T.; Johnson, R. A.; Janowsky, A. Structure-activity relationships of substituted cathinones, with transporter binding, uptake, and release. *J. Pharmacol. Exp. Ther.* **2016**, *360*, 33–47.
174. Kolanos, R.; Solis, E.; Sakloth, F.; De Felice, L. J.; Glennon, R. A. “Deconstruction” of the abused synthetic cathinone methylenedioxypropylamphetamine (MDPV) and an examination of effects at the human dopamine transporter. *ACS Chem. Neurosci.* **2013**, *4*, 1524–1529.
175. Peretz, D. I.; Smythies, J. R.; Gibson, W. C. A new hallucinogen: 3,4,5-trimethoxyphenyl- β -aminopropane. *J. Ment. Sci.* **2008**, *101*, 317–329.
176. Stimulant-induced psychotic disorder including amphetamines, methamphetamine or methcathinone; World Health Organization. In *ICD-11 for Mortality and Morbidity Statistics* [Online] <https://icd.who.int/browse11/l-m/en/#/http://id.who.int/icd/entity/199002751> (accessed Apr 13, 2019).
177. Hsieh, J. H.; Stein, D. J.; Howells, F. M. The neurobiology of methamphetamine induced psychosis. *Front. Hum. Neurosci.* **2014**, *8*, 537.
178. Smythies, J. R.; Bradley, R. J.; Johnston, V. S.; Benington, F.; Morin, R. D.; Clark Jr., L. C. Structure-activity relationship studies on mescaline. *Psychopharmacologia* **1967**, *10*, 379–387.
179. Smythies, J. R.; Johnston, V. S.; Bradley, R. J.; Benington, F.; Morin, R. D.; Clark, L. C. Some new behaviour-disrupting amphetamines and their significance. *Nature* **1967**, *216*, 128–129.
180. Beaton, J. M.; Smythies, J. R.; Benington, F.; Morin, R. D.; Clark, L. C. Behavioural effects of some 4-substituted amphetamines. *Nature* **1968**, *220*, 800–801.

181. Walther, D.; Shalabi, A. R.; Baumann, M. H.; Glennon, R. A. Systematic structure-activity studies on selected 2-, 3-, and 4-monosubstituted synthetic methcathinone analogs as monoamine transporter releasing agents. *ACS Chem. Neurosci.* **2019**, *10*, 740–745.
182. Bondarev, M. L.; Bondareva, T. S.; Young, R.; Glennon, R. A. Behavioral and biochemical investigations of bupropion metabolites. *Eur. J. Pharmacol.* **2003**, *474*, 85–93.
183. Young, R.; Glennon, R. A. Discriminative stimulus effects of *S*(–)methcathinone (CAT): a potent stimulant drug of abuse. *Psychopharmacology* **1998**, *140*, 250–256.
184. Goudie, A. J.; Atkinson, J.; West, C. R. Discriminative properties of the psychostimulant *dl*-cathinone in a two lever operant task. *Neuropharmacology* **1986**, *25*, 85–94.
185. Kalix, P.; Glennon, R. A. Further evidence for an amphetamine-like mechanism of action of the alkaloid cathinone. *Biochem. Pharmacol.* **1986**, *35*, 3015–3019.
186. Glennon, R. A.; Dukat, M. Structure-activity relationships of synthetic cathinones. In *Current Topics in Behavioral Neurosciences*; Baumann, M., Glennon, R. A., Wiley, J., Eds.; Springer: Cham, 2016; Vol. 32, pp 19–47.
187. Reith, M. E. A.; Blough, B. E.; Hong, W. C.; Jones, K. T.; Schmitt, K. C.; Baumann, M. H.; Partilla, J. S.; Rothman, R. B.; Katz, J. L. Behavioral, biological, and chemical perspectives on atypical agents targeting the dopamine transporter. *Drug Alcohol Depend.* **2015**, *147*, 1–19.
188. Portoghese, P. S.; Ronsisvalle, G.; Larson, D. L.; Yim, C. B.; Sayre, L. M.; Takemori, A. E. Opioid agonist and antagonist bivalent ligands as receptor probes. *Life Sci.* **1982**, *31*, 1283–1286.

189. Davis, S.; Blakey, K.; Rands-Trevor, K. GC-MS and GC-IRD analysis of 2-, 3- and 4-methylmethamphetamine and 2-, 3- and 4-methylamphetamine. *Forensic Sci. Int.* **2012**, *220*, 67–73.
190. Battisti, U. M.; Sitta, R.; Harris, A.; Sakloth, F.; Walther, D.; Ruchala, I.; Negus, S. S.; Baumann, M. H.; Glennon, R. A.; Eltit, J. M. Effects of *N*-alkyl-4-methylamphetamine optical isomers on plasma membrane monoamine transporters and abuse-related behavior. *ACS Chem. Neurosci.* **2018**, *9*, 1829–1839.
191. Layer, R. W.; MacGregor, I. R. Preparation of 1-indanones from α -bromoaralkyl ketones. *J. Org. Chem.* **1956**, *21*, 1120–1123.
192. Blough, B. E.; Landavazo, A.; Partilla, J. S.; Baumann, M. H.; Decker, A. M.; Page, K. M.; Rothman, R. B. Hybrid dopamine uptake blocker–serotonin releaser ligands: a new twist on transporter-focused therapeutics. *ACS Med. Chem. Lett.* **2014**, *5*, 623–627.
193. Perboni, A.; Giubellina, N. Improved process of amide formation. WO 2008/155334 A2, Dec 24, 2008.
194. Sebti, S. M.; Hamilton, A. D.; Augeri, D. J.; Barr, K. J.; Fakhoury, S. A.; Janowick, D. A.; Kalvin, D. M.; O'Connor, S. J.; Rosenberg, S. H.; Shen, W.; Swenson, R. E.; Sorensen, B. K.; Sullivan, G. M.; Tasker, A. S.; Wasicak, J. T.; Nelson, L. T. J.; Henry, K. J.; Wang, L.; Liu, G.; Gunawardana, I. W. Inhibitors of protein isoprenyl transferases, WO1998050029A1, March 20, 2001.
195. Guha, S.; Rajeshkumar, V.; Kotha, S. S.; Sekar, G. A versatile and one-pot strategy to synthesize α -amino ketones from benzylic secondary alcohols using *N*-bromosuccinimide. *Org. Lett.* **2015**, *17*, 406–409.
196. Jacob, P. I.; Tisdale, E. C.; Panganiban, K.; Cannon, D.; Zabel, K.; Mendelson, J. E.;

- Jones, R. T. Gas chromatographic determination of methamphetamine and its metabolite amphetamine in human plasma and urine following conversion to *N*-propyl derivatives. *J. Chromatogr. B: Biomed. Sci. Appl.* **1995**, *664*, 449–457.
197. Heinzelman, R. V.; Aspergren, B. D. Compounds containing the pyrrolidine ring analogs of sympathomimetic amines. *J. Am. Chem. Soc.* **1953**, *75*, 3409–3413.
198. Koremura, M.; Nagawa, M. Studies on some relationships between chemical structures and antimicrobial and insecticidal activities in organo-nitro compounds. Part IX. *J. Agric. Chem. Soc. Japan* **1962**, *36*, 629–634.
199. Carroll, F. I.; Blough, B. E.; Mascarella, S. W.; Navarro, H. A.; Lukas, R. J.; Damaj, M. I. Bupropion and bupropion analogs as treatments for CNS disorders. In *Advances in Pharmacology*; Elsevier Inc., 2014; Vol. 69, pp 177–216.
200. Sievers, F.; Wilm, A.; Dineen, D.; Gibson, T. J.; Karplus, K.; Li, W.; Lopez, R.; McWilliam, H.; Remmert, M.; Söding, J.; Thompson, J. D.; Higgins, D. G. Fast, scalable generation of high-quality protein multiple sequence alignments using Clustal Omega. *Mol. Syst. Biol.* **2011**, *7*, 1-6.
201. Šali, A. Comparative protein modeling by satisfaction of spatial restraints. *Mol. Med. Today* **1995**, *1*, 270–277.
202. Melo, F.; Sánchez, R.; Šali, A. Statistical potentials for fold assessment. *Protein Sci.* **2009**, *11*, 430–448.
203. John, B. Comparative protein structure modeling by iterative alignment, model building and model assessment. *Nucleic Acids Res.* **2003**, *31*, 3982–3992.
204. Shen, M.-Y.; Šali, A. Statistical potential for assessment and prediction of protein structures. *Protein Sci.* **2006**, *15*, 2507–2524.

205. Laskowski, R. A.; MacArthur, M. W.; Moss, D. S.; Thornton, J. M. PROCHECK: a program to check the stereochemical quality of protein structures. *J. Appl. Crystallogr.* **2002**, *26*, 283-291.
206. Gu, H.; Wall, S. C.; Rudnick, G. Stable expression of biogenic amine transporters reveals differences in inhibitor sensitivity, kinetics, and ion dependence. *J. Biol. Chem.* **1994**, *269*, 7124–7130.
207. Kellogg, G. E. ; Abraham, D. J. Hydrophobicity: is $\text{LogP}_{o/w}$ more than the sum of its parts? *Eur. J. Med. Chem.* **2000**, *35*, 651–661.
208. Stevens, C. L.; Chang, C. H. Epoxy ethers. XIX. Reaction of 1,2-epoxy-1-methoxy-2-methyl-1-phenylpropane with amines. *J. Org. Chem.* **1962**, *27*, 4392–4396.
209. De Kimpe, N. Facile synthesis of 2-alkoxy-2-aryloxiranes. *Chem. Ber.* **1983**, *58*, 3631–3636.
210. Schulz, H.; Jassmann, E.; Kowarsch, R. N-methyl- ω -phenyl-tertiary-butylamine, Ger. (East) Patent DD 50619, Nov 24, 1966.
211. Nordlander, J. E.; Payne, M. J.; Njoroge, F. G.; Balk, M. A.; Laikos, G. D.; Vishwanath, V. M. Friedel-crafts acylation with *N*-(trifluoroacetyl)- α -amino acid chlorides. application to the preparation of beta-arylalkylamines and 3-substituted 1,2,3,4-tetrahydroisoquinolines. *J. Org. Chem.* **1984**, *49*, 4107–4111.
212. Lowry, P.; Benchikh, E.; McConnell, I.; Crumlin, A.; Fitzgerald, P. Immunoassay for pyrrolidinophenones. Eur. Pat. Appl. EP 2 626 358 A1, Aug 14, 2013.
213. Rosenmund, K. W.; Karg, E.; Marcus, F. K. Über die Darstellung von β -Aryl-alkylaminen. *Ber. Dtsch. Chem. Ges. B* **1942**, *75*, 1850–1859.
214. Matsushima, K.; Nagai, T.; Kanaya, H.; Kato, Y.; Takahashi, M.; Kamiyama, S. Urinary

- output changes in racemic ethylamphetamine and optical activity discrimination in rat urine by HPLC analysis. *Jpn. J. Legal Med.* **1998**, *52*, 19–26.
215. Kondekar, N. B.; Kumar, P. Synthesis of (*R*)-selegiline via hydrolytic kinetic resolution. *Synth. Commun.* **2011**, *41*, 1301–1308.
216. Meindl, W.; Böhm, M. Antimykobakterielle β -Aminoketone. *Arch. Pharm. (Weinheim, Ger.)* **1987**, *320*, 507–514.
217. Ishikura, M.; Mori, M.; Ikeda, T.; Terashima, M.; Ban, Y. New synthesis of diazepam and the related 1,4-benzodiazepines by means of palladium-catalyzed carbonylation. *J. Org. Chem.* **1982**, *47*, 2456–2461.
218. Nishiguchi, I.; Oki, T.; Hirashima, T.; Shiokawa, J. Electroreductive acylation of benzyl chlorides with acid anhydrides. stereoselective formation of (*E*)-enol esters from benzyl alkyl ketones. *Chem. Lett.* **1991**, *20*, 2005–2008.
219. Mustanir, A., Than, S., Itoh, S., and Mishima, M. Thermodynamic stabilities of propylenebenzenium ions in the gas phase. Substituent effect of unsymmetrical phenonium ions. *Arch. Org. Chem.*, **2008**, *26*, 135–150.
220. Nakazawa, K.; Matsuura, S.; Kusuda, K. Studies on the application of polyphosphoric acid as a condensing agent. *Yakugaku Zasshi* **1954**, *74*, 495–497.
221. Lindeman, S. V.; Rathore, R.; Kochi, J. K.; Heirtzler, F. R.; Hopf, H.; Jones, P. G.; Bubenitachek, P.; Lehne, V.; Gano, J. E.; Subramaniam, G.; Birnbaum, R.; Chebny, V. J.; Abdelwahed, S. H. Duplexiphane: a polyaromatic receptor containing two adjoined Δ -shaped cavities for an efficient hopping of a single silver cation. *J. Am. Chem. Soc.* **2000**, *58*, 8012.
222. Ghosh, U.; Ganessunker, D.; Sattigeri, V. J.; Carlson, K. E.; Mortensen, D. J.;

- Katzenellenbogen, B. S.; Katzenellenbogen, J. A. Estrogenic diazenes: heterocyclic non-steroidal estrogens of unusual structure with selectivity for estrogen receptor subtypes. *Bioorg. Med. Chem.* **2003**, *11*, 629–657.
223. Cowper, R. M.; Stevens, T. S. Mechanism of the reaction between arylamines and benzoin. *J. Chem. Soc.* **1940**, 347.
224. Bess, E. N.; Bischoff, A. J.; Sigman, M. S. Designer substrate library for quantitative, predictive modeling of reaction performance. *Proc. Natl. Acad. Sci. U.S.A.* **2014**, *111*, 14698–14703.
225. Ema, T.; Nakano, Y.; Yoshida, D.; Kamata, S.; Sakai, T. Redesign of enzyme for improving catalytic activity and enantioselectivity toward poor substrates: manipulation of the transition state. *Org. Biomol. Chem.* **2012**, *10*, 6299–6308.
226. Jones, G.; Willett, P.; Glen, R. C.; Leach, A. R.; Taylor, R. Development and validation of a genetic algorithm for flexible docking. *J. Mol. Biol.* **1997**.
227. Schrödinger, L. The PyMOL molecular graphics system, version 1.8. November 2015.
228. Cameron, K. N.; Solis, E.; Ruchala, I.; De Felice, L. J.; Eltit, J. M. Amphetamine activates calcium channels through dopamine transporter-mediated depolarization. *Cell Calcium* **2015**, *58*, 457–466.
229. Ruchala, I.; Cabra, V.; Solis, E.; Glennon, R. A.; De Felice, L. J.; Eltit, J. M. Electrical coupling between the human serotonin transporter and voltage-gated Ca²⁺ channels. *Cell Calcium* **2014**, *56*, 25–33.
230. Solis, E.; Partilla, J. S.; Sakloth, F.; Ruchala, I.; Schwienteck, K. L.; De Felice, L. J.; Eltit, J. M.; Glennon, R. A.; Negus, S. S.; Baumann, M. H. *N*-alkylated analogs of 4-methylamphetamine (4-MA) differentially affect monoamine transporters and abuse

liability. *Neuropsychopharmacology* **2017**, *42*, 1950–1961.

VITA

Rachel Davies was born April 26th, 1988 in Northeast Portland, Oregon, at Providence hospital – where her mother (Ellen Mast) and father (Dr. Jack Davies) had met. She received her bachelors of science degree in biochemistry from Middle Tennessee State University in Murfreesboro, Tennessee in 2013.